INVESTIGATION OF CALCIUM SIGNALING MOLECULES IN *TOXOPLASMA GONDII*

by

ABIGAIL CALIXTO

(Under the Direction of SILVIA NJ MORENO)

ABSTRACT

T. gondii is a parasite that forms part of the apicomplexan phylum. Members of this phylum can cause a wide range of devastating diseases to humans and livestock. *T. gondii* is an excellent model organism as it can be easily cultured and is a genetically tractable organism. The hallmark of *T. gondii* pathogenesis is the lytic cycle. This cycle causes rapid lysis and ultimately destruction of the host cell. Our lab established that calcium (Ca^{2+}) stimulates all of the steps of the lytic cycle. The ability to manipulate the genome has allowed us to utilize reverse and forward genetic techniques to learn more about Ca^{2+} signaling within the parasite. This work shows a new member of the Ca^{2+} signaling toolkit, a calcium/proton exchanger TgCAXL1. TgCAXL1 has proven to be critical for parasite invasion of the host cell and regulated Ca^{2+} signaling and pH homeostasis at the Golgi apparatus and the endoplasmic reticulum (ER). We found that pH is critical for proper protein function, specifically the *T. gondii* sarco/endoplasmic Ca-ATPase, TgSERCA, a pump on the ER essential for sequestration of Ca^{2+}. To perform Ca^{2+} measurements in a high-throughput manner, we developed a dual fluorescent parasite to produce ratiometric Ca^{2+} measurements. We were able to measure cytosolic

Ca^{2+} measurements in a large number of clones. Lastly, we investigated the top hit from a CRISPR-genome wide screen, known as the ClpP protease, performed in the presence of a voltage-gated Ca^{2+} channel inhibitor, cilnidipine. To conclude, our work revealed various genes and techniques that have allowed us to learn about Ca^{2+} regulation in *T. gondii.*

INDEX WORDS: *Toxoplasma gondii*, Ca^{2+} signaling, Calcium/proton exchanger, Golgi Apparatus, Endoplasmic reticulum, High-throughput Ca^{2+} measurements, FURA2, GCaMP6

INVESTIGATION OF CALCIUM SIGNALING MOLECULES IN *TOXOPLASMA GONDII*

by

ABIGAIL CALIXTO

B.S., The College of New Jersey, 2016

A Dissertation Submitted to the Graduate Faculty of the University of Georgia in Partial Fulfillment of the Requirements of the Degree

DOCTOR OF PHILOSOPHY

ATHENS, GEORGIA

2022

INVESTIGATION OF CALCIUM SIGNALING MOLECULES IN *TOXOPLASMA GONDII*

By

ABIGAIL CALIXTO

Major Professor:	Silvia NJ Moreno
Committee:	Ronald Drew Etheridge
	Zachary A. Lewis
	Christopher West

Ron Walcottt

Vice Provost for Graduate Education and Dean of the Graduate School

The University of Georgia

August 2022

Dedication

I dedicate this dissertation to my entire family, but mainly my Mom, Dad, sister and brother. For always being there for me. Thank you for your never-ending support.

Acknowledgments

I want to begin by thanking my scientific support system in chronological order. It all began at the College of New Jersey. My mentor Dr. KT Elliot believed in me when I didn't. Without her I could not have gotten to where I am today. I want to thank Dr. Jay Brewster at Pepperdine University for providing me the opportunity to expand my scientific family and gain confidence in my scientific skills.

I want to thank everyone from my graduate school journey. Thank you all for supporting me and never tiring from my questions. The Moreno and Docampo lab have provided so much support. Specifically, Dr. Srinivasan Ramakrishnan, Dr. Briam Mantilla, Dr. Ciro Cordeiro, Dr. AJ Stasic, Dr. Stephen Vella, Dr. Karla M Nogueras, Dr. Myriam Andrea Hortua, Dr. Alejandro Pezza, Dr. Nuria Negrao, Beejan Asady, Eric Dykes and Dana Alvin. My current lab members who aren't just my colleagues but also my friends, Mayara Bertollini, Berna Baihetiya, Katie Moen, Melissa Sleda, and Dr. Anna Gioseffi thank you for making it fun to do science. In the CTEGD specifically, I would like to give a big special thanks to Dr. Drew Etheridge for always having tissues in his office for me and Dr. Christopher Rice for taking the time to give me professional, scientific and personal advice.

My friends from the microbiology department, you all have been there from the very beginning of graduate school and thank you for being such an incredible support system. I want to thank Dr. Jessica Irons, Dr. Sophia Weerth, Dr. Michael Paxhia, Dr. Huong Nguyen and Dr. Taiwo Solomon.

Lastly from the scientific community, I would like to thank my PhD mentor Dr. Silvia NJ Moreno. Thank you, Silvia for never giving up on me and giving me the chance to become an independent and rigorous scientist. Thank you also for giving me the space to learn and do incredible science and to become a fighter.

As for my family and friends outside of the scientific community I want to thank all of my cousins, aunts, uncles, and grandparents. Thank you for teaching me to be humble and to value the important things in life. Life is so beautiful with you in it. Thank you to my friends from Union Catholic, The College of New Jersey, studying abroad and Athens. I love that we can still chat today as if no time has passed. I want to thank my siblings for their honesty and making me laugh all the time. And ultimately my parents. Without them I wouldn't be here right now. They always pushed me to do my best and always ensured that I strived for more. Thank you for putting me on this path.

TABLE OF CONTENTS

Page

List of Tables

List of Figures

Chapter 1

Literature Review

Introduction to *Toxoplasma gondii*

Toxoplasma gondii (*T. gondii*) is an apicomplexan parasite originally discovered in 1908 in Southern Tunisia, Africa in the rodent *Ctenodactylus gundi (Innes, 2010)*. The apicomplexan phylum is characterized by the apical complex that consists of a group of cytoskeletal structures and associated membrane-bounded organelles, like the rhoptries and micronemes, found at the anterior end of the parasite (Fig. 1). Unique to apicomplexans, these organelles are necessary for invasion of the host cell (N. D. Levine & G. Poljansky, 1980). Several members of the apicomplexan phylum can cause serious diseases such as *Plasmodium falciparum*, the causative agent of malaria and *Cryptosporidium parvum*, the causative agent of cryptosporidiosis. *T. gondii* currently infects one third of the world's population and poses a threat not only to humans but also animals. According to the CDC, at least 11% of Americans over the age of 6 are infected with *T. gondii*. Within the last 100 years, the *Toxoplasma* research community has outlined and studied the entire life cycle, forms of transmission and pathological consequences of *T. gondii* infection. *T. gondii* begins its life cycle in the lining of the small intestine of the cat, where it undergoes several rounds of asexual replication that lead to the generation of merozoites. Merozoites can differentiate into male and female gametes and the male gamete fertilizes the female gamete, creating a zygote. A cyst wall is formed around the zygote, turning the zygote into an unsporulated oocyst. Once shed into the

environment via the cat feces, the unsporulated oocyst will undergo sporulation forming sporozoites within the oocyst which can be shed 3-20 days after infection (J. P. DUBEY, 1998; Martorelli Di Genova & Knoll, 2020).The oocyst cell wall is very resistant to environmental stresses allowing the oocyst to persist in the environment for months. The sporulated oocysts are infective to any warm-blooded animal, including humans (J. P. DUBEY, 1998; Martorelli Di Genova & Knoll, 2020).

Once sporulated oocysts are ingested, the sporozoites will differentiate into tachyzoites in the intestinal lining of the host. Tachyzoites spread within the gut and find their way to the circulatory and lymphatic system. Motile immune cells within these systems can also harbor tachyzoites, aiding in the dissemination of the parasite, due to their migratory behavior (Courret *et al.*, 2006; Da Gama *et al.*, 2004). Tachyzoites spread to various types of organs and tissues such as muscle tissue, the brain, eye, and placenta. They enter these organs either through infected cells in a Trojan horse style, or through transmigration (Harker *et al.*, 2015). The pathogenesis of tachyzoites is remarkable as it can infect any nucleated cell within the host.

The host immune response is one of the main factors for tachyzoite conversion into bradyzoites, the parasite life-stage that replicates at a significantly slower rate than tachyzoites and develops a quiescent-like infection (Sullivan & Jeffers, 2012). Bradyzoite conversion is accompanied by the upregulation of different interferons and cytokines and the formation of a cyst wall comprised of vesicles, tubules, sugars, and even dense granule proteins, a secretory organelle (Tu *et al.*, 2018). The cyst wall protects bradyzoites from stomach acids and the immune system, allowing them to persist and cause chronic infection. In an immunocompetent individual, tissue cysts can remain in the

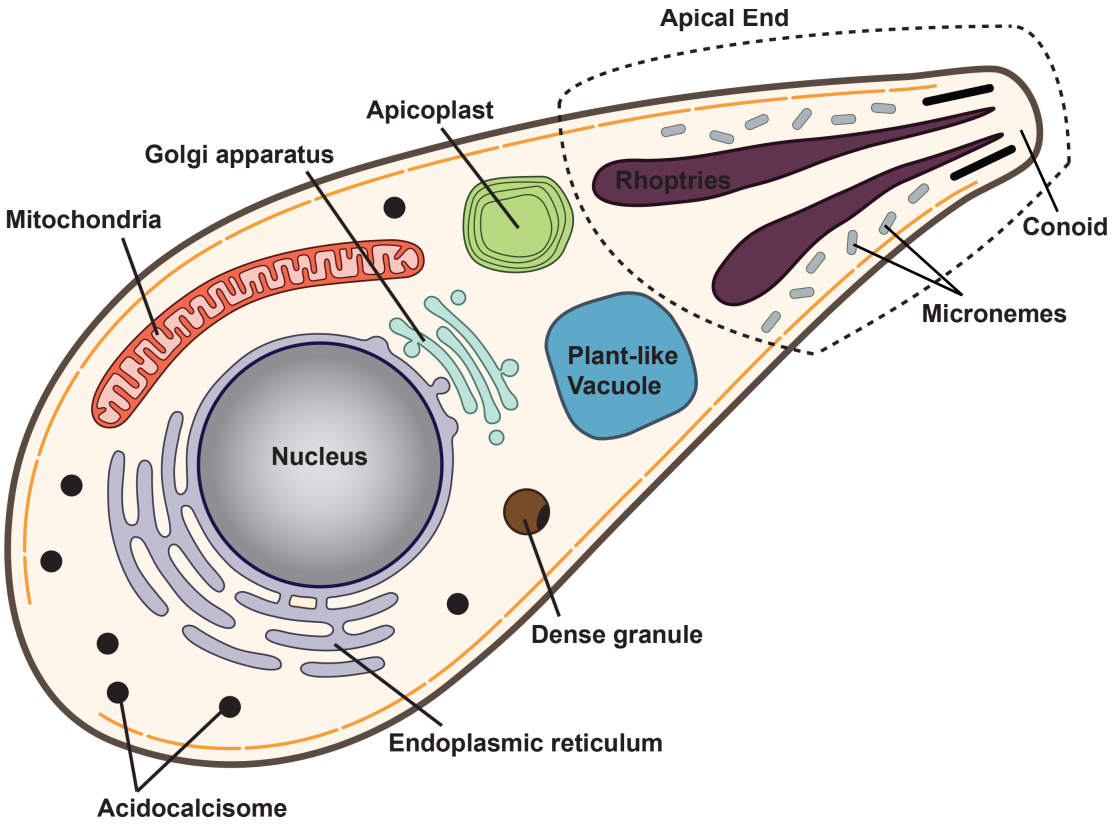

Figure 1.1 Organelles found in *T. gondii*. Schematic of organellar distribution in the cytosol of an extracellular *T. gondii* tachyzoite. Dotted lines indicate the apical end of the parasite.

host for the duration of its life, however in immunocompromised individuals, reactivation of the infection can lead to life-threatening neurological diseases like encephalitis (Dubey & Jones, 2008). Women infected with *T. gondii* during pregnancy can transmit the parasite to the fetus and transmission rate is highest in the last trimester (60-90%). The child could suffer from hydrocephalus, convulsions and retinochoroiditis, infection in the eye (Montoya & Remington, 2008).

The oocyst, tachyzoite and bradyzoite are all capable of establishing infection within the secondary host. The secondary host can be any type of warm-blooded mammal, however reports of *T. gondii* outbreak have also been discovered in marine wildlife (Dubey *et al.*, 2020). Transmission occurs through fecal-oral route, congenitally or

through consumption of contaminated meat or vegetables. In humans, seroprevalence of *T. gondii* can be anywhere as low as 10% in Iceland (Birgisdottir *et al.*, 2006) and as high as 80% in Brazil (Dubey *et al.*, 2012). Prevalence varies in different countries and is influenced by climate, culture, and socioeconomic status (Elmore *et al.*, 2010). Clinical treatment of toxoplasmosis is usually a combination drug therapy of sulfadiazine and pyrimethamine, however this treatment can lead to toxic side effects (Wei *et al.*, 2015). Furthermore, current drug treatments are not able to eliminate bradyzoite tissue cysts (Alday & Doggett, 2017) and further research is needed to learn about the basic biology of the parasite and find targets for therapeutic intervention.

Ca^{2+} in the tachyzoite lytic cycle

Dissemination of *T. gondii* within the host mainly occurs in the tachyzoite life stage, where rapid cell lysis occurs via the highly regulated process, the lytic cycle. The lytic cycle is comprised of invasion of the host cell, replication within a parasitophorous vacuole, egress from the host cell and motility to identify a new host to repeat the cycle. The ubiquitous signaling ion, Ca^{2+}, is important for the different steps of the lytic cycle and is involved with various signaling cascades necessary for proper cell function. A steep concentration gradient (~20,000-fold difference) exists between the extracellular and intracellular environment of the cell and Ca^{2+} entry can stimulate various signaling cascades and initiate different cellular events (Fig. 2). Returning to basal/resting levels of Ca^{2+} (70-100 nM) is essential as high concentrations of Ca^{2+} prove to be detrimental for the cell (Zhong, 1996). *T. gondii* utilizes Ca^{2+}-ATPases, channels, kinases and Ca^{2+} binding proteins to ensure Ca^{2+} homeostasis throughout the lytic cycle.

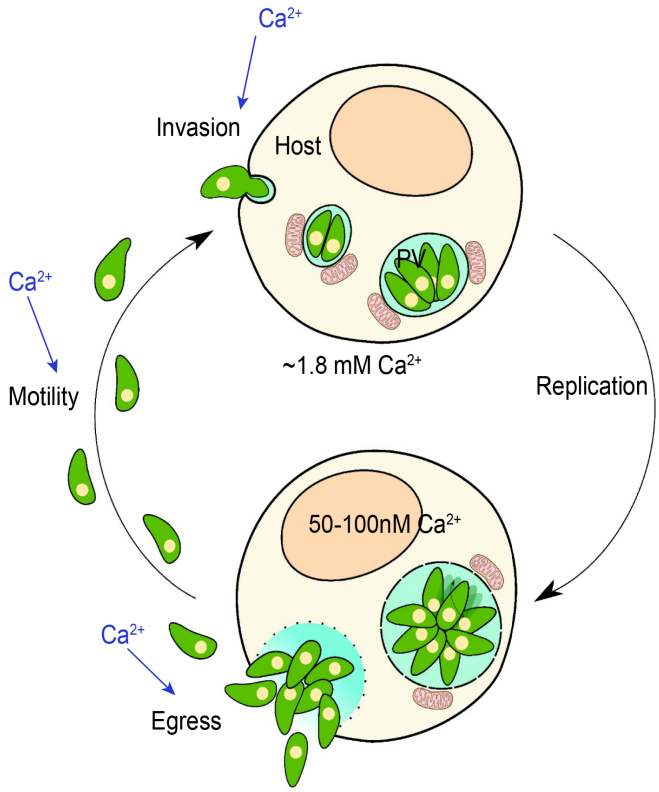

Figure 1.2 Role of Ca^{2+} in the *T. gondii* lytic cycle. The lytic cycle consists of the tachyzoite undergoing motility, invasion, replication and egress. The extracellular milieu is 1.8 mM of Ca^{2+} and the intracellular environment is between 50-100 nM Ca^{2+}. Ca^{2+} stimulates each step of the lytic cycle.

For the lytic cycle to progress, the tachyzoite needs to identify its host target by engaging in movement known as gliding motility. Movement is largely facilitated by the glideosome, a complex comprised of the myosin A (MyoA) molecular motor in association with glideosome associated proteins (GAP 40, 45 and 50) (Angelika Herm-Gotz *et al.*, 2002; Frenal *et al.*, 2010; Gaskins *et al.*, 2004). The GAP proteins tether the MyoA motor in the inner membrane complex (IMC) to the plasma membrane. Myosin light chain (MLC) and essential light chains (ELC1 and 2) form a lever arm to connect the GAP proteins to MyoA (Angelika Herm-Gotz *et al.*, 2002; Williams *et al.*, 2015). ELC1 and 2 are Ca^{2+} binding domain containing proteins proven to bind Ca^{2+} and necessary for proper assembly and function of the glideosome. Using its gliding machinery, the parasite identifies a host to invade. The parasite will extrude its conoid, a cone-shaped structure at the apical end comprised of an organized arrangement of tubulin polymers and attach to the host cell. A tight moving junction is formed between the parasite and the host, facilitated by the secretion of microneme proteins and rhoptry neck proteins. After the

completion of invasion, rhoptry bulb proteins are secreted into the host cytosol followed by dense granule proteins. Conoid extrusion and secretion of micronemes have been shown to be triggered by Ca^{2+} ionophores (Borges-Pereira *et al.*, 2015; Sibley, 1999) and a higher percentage of parasite invasion/attachment is observed under high Ca^{2+} conditions (Borges-Pereira *et al.*, 2015; Pace *et al.*, 2014).

Within the host, the parasite will form a parasitophorous vacuole (PV) and undergo replication via endodyogeny, where two daughter cells are assembled within the mother cell. The parasite cell cycle consists of G1 (gap phase 1), S (DNA replication occurs), a very brief G2 (gap phase 2), and M (mitosis) phases. After the G1 phase, centriole-containing centrosomes divide and mark the genesis of daughter cells. Mitosis follows where the mitotic spindle attaches to the kinetochore found at the centromere of the chromosomes and migrate to the apical end of the mother cell. Cytokinesis, known as budding, occurs simultaneously as mitosis, leading to the formation of early daughter cells (Blader *et al.*, 2015; Francia & Striepen, 2014). Cell division culminates with the assembly of the secretory organelles, the micronemes and rhoptries (Ke Hu, 2002). Ca^{2+} dependent protein kinase 7 (CDPK7) is an essential kinase for replication and affects parasite division. CDPK7 knockdown mutants divide in an asynchronous matter resulting in mislocalization and aggregation of secretory organelles. Furthermore, mutants resulted in disruption of centrosome formation as well as the kinetochore and centrocone, an extension of the nucleus that appears during mitosis and is housed in the mitotic spindle (Morlon-Guyot *et al.*, 2014).

After various rounds of replication within the PV, the parasite will egress from the host cell and destroy it. Egress can be triggered by the immune system where T-cells

induce cell death in *T. gondii*-infected host cells (Persson *et al.*, 2007). Egress has also been shown to be activated by a rise in abscisic acid, a decrease in pH and potassium and an increase in cytosolic calcium (Nagamune *et al.*, 2008; Roiko *et al.*, 2014). Increase of cytosolic Ca^{2+} stimulated by Ca^{2+} itself or other stimulants leads to egress from the PV (Arrizabalaga *et al.*, 2004; Borges-Pereira *et al.*, 2015; Elijah W. Stommel, 1997; Lourido *et al.*, 2012). The implementation of genetically encoded Ca^{2+} indicators (GECI) led to the discovery of two stark and pronounced increases of Ca^{2+} before an egress event (Vella *et al.*, 2021). The first increase is believed to originate from both the host's and parasite's intracellular stores and the second from the extracellular environment (Vella *et al.*, 2021). In combination with PV pore formation perforin like protein 1 (PLP1) (Björn F. C. Kafsack, 2009), enhanced secretion of microneme proteins and motility, egress from the host cell is achieved.

Tying two ions together: H^+ and Ca^{2+}

The endoplasmic reticulum (ER) serves as one of the largest and best studied reservoirs of Ca^{2+} in the cell. *T. gondii* expresses a Ca^{2+}-ATPase, known as the sarcoplasmic/endoplasmic Ca^{2+}-ATPase (SERCA), responsible for pumping Ca^{2+} against the gradient into the ER. Release of Ca^{2+} from the ER can occur through transient receptor channels 1 and 2 (Borges-Pereira *et al.*, 2015; Marquez-Nogueras *et al.*, 2021), however additional modes of release remain unknown. Inhibition of SERCA by thapsigargin, a known SERCA inhibitor, leads to an increase in cytosolic Ca^{2+} through an unknown leak mechanism. Ca^{2+} can also be stored in acidic organelles in *T. gondii*. The acidocalcisome is an electron dense organelle containing high amounts of polyphosphate and pyrophosphate. X-ray microanalysis of acidocalcisome enriched fractions revealed

the presence of Ca^{2+} as well (Rodrigues *et al.*, 2002). Discovery of the plant-like vacuole (PLV) by Miranda *et al* showed Ca^{2+}/proton exchange activity in PLV enriched fractions suggesting the presence of Ca^{2+} in this organelle as well (Miranda *et al.*, 2010). The PLV is similar in structure to the plant vacuole, which also houses Ca^{2+}, and expresses similar proteins such as aquaporin channel (TgAQP1) and the vacuolar H^+ pyrophosphatase (TgVP1). The PLV also exhibits lysosomal like features and contains cathepsin proteases L and B. Ca^{2+} entry into these organelles most likely occurs through the Ca^{2+}-ATPase TgA1 and potentially an unidentified Ca^{2+}/proton exchanger. Storage of Ca^{2+} in acidic organelles opens the door to investigating the relationship between Ca^{2+} and pH.

Carruthers *et al* established that a low pH environment can activate egress by enhancing microneme secretion and motility (Roiko *et al.*, 2014). pH levels of 5.4 led to a higher percentage of motile parasites as well as higher secretion of microneme proteins MIC2, 4 and PLP1. Interestingly, chelating Ca^{2+} in the buffer with Ca^{2+} chelator, 1,2-bis(*o*-aminophenoxy)ethane-*N*,*N*,*N′*,*N′*-tetraacetic acid), or BAPTA, under acidic conditions prevented secretion of these proteins. Recombinant PLP1 activity, processing and binding peaked at pH 5.4 as well. Inducing egress with Ca^{2+} ionophores in the presence of the weak base, NH_4Cl, to alkalynize the environment, reduced the percentage of egress (Roiko *et al.*, 2014). Recent findings imply that the Ca^{2+} dependent acidification can be explained through players involved in glycolysis (Huynh & Carruthers, 2021), however the exact mechanism remains unknown. For the first time, pH is shown to induce egress in a Ca^{2+} dependent manner, supporting the interrelation between pH and Ca^{2+}.

The pH and Ca^{2+} relationship were further assessed in TgVHa1 mutants. TgVHa1 encodes a subunit of the vacuolar proton ATPase in *T. gondii*, which is involved in

pumping protons into the PLV and out of the cytosol into the extracellular environment to maintain a neutral cytosolic pH (Stasic *et al.*, 2019). TgVHa1 drives cytosolic pH recovery after exposing the parasite to acidic stress and downregulation of this protein causes defects in microneme and rhoptry maturation. It is possible that deficient proton pumping in TgVHa1 mutants is what causes unregulated Ca^{2+} entry into the cytosol, which is toxic for the parasite (Stasic *et al.*, 2021). Storage of Ca^{2+} in acidic organelles and leakage of Ca^{2+} from the ER was also disrupted in the mutants. This work demonstrates that TgVHa1 is a proton ATPase that also controls Ca^{2+} homeostasis in *T. gondii*.

pH and Ca^{2+} are clearly interrelated in *T. gondii*, however the mechanism behind this relationship is not fully understood. A major aspect of Ca^{2+} homeostasis regulation is sequestration of Ca^{2+} into the organelles to ensure low levels of Ca^{2+} in the cytosol. Transport of the Ca^{2+} ions across different membranes is carried out by pumps, channels and exchangers. Pumps need to use the energy from ATP to transport ions against a concentration gradient. Ions can pass through channels however, due to their concentration or electrochemical gradient. Ion flow creates currents, that can lead to changes in membrane potential and act as signals. Secondary pumps are co-transporters and exchangers. Two major families of proteins that drive Ca^{2+} transport into the organelles are Ca^{2+}-ATPases and Ca^{2+} /H^{+} exchangers. Several works have shown the significance of these proteins in pH regulation. We attempt to assess the relationship between pH and Ca^{2+} by dissecting the function of these two families of Ca^{2+} signaling proteins and their role in pH homeostasis.

Type II Ca^{2+} ATPases

P-type ATPases were first identified in 1956 by Danish scientist, Skou, who studied the nerves of crab legs and discovered a Na^+/K^+ ATPase pump (Skou, 1957). Over time, proteins with similar qualities were discovered in different tissues and organisms. These integral proteins are characterized by containing 10 transmembrane domains and actively translocating a variety of ions and lipids across a lipid bilayer. The name P-type comes from the formation of a **p**hosphorylated asparagine intermediate during the catalytic cycle. P-type ATPases can be further divided into 5 subfamilies (I-V) (Palmgren, 1998). In this section, we will focus on type II P-type ATPases, known to mainly transport Ca^{2+}.

Sarcoplasmic/endoplasic Ca^{2+} ATPase (SERCA)

The sarco/endoplasmic reticulum (SR/ER) is known for storing the highest amount of Ca^{2+} within the cell. The primary mechanism of Ca^{2+} uptake is by the SERCA, which uses the energy from ATP hydrolysis to pump Ca^{2+} into the ER against the Ca^{2+} concentration gradient (Lipmann, 1962). SERCA adopts two conformations, E1 and E2 (Chikashi Toyoshima, 2000; Mizutani, 2004). In the E1 phase, the two Ca^{2+} binding sites are facing the cytoplasmic side and prepared to bind to ATP. The E2 phase occurs when the Ca^{2+} binding sites are facing the ER lumen and Ca^{2+} is released into the ER (Jesper V. Moller, 1996). The Ca^{2+} binding sites in the E1 phase are in a high Ca^{2+} affinity state, as opposed to the E2 phase where they are in a low Ca^{2+} affinity state. The uptake of Ca^{2+} is counterbalanced by the release of other ions, such as H^+, to maintain the membrane potential of the SR/ER at zero (Espinoza-Fonseca, 2017). Biophysical assays showed that after Ca^{2+} is released into the lumen from the SERCA Ca^{2+} binding sites, two protons will take their place and are countertransported to the cytosol (Yu *et al.*, 1994).

In mammals, pH homeostasis is essential for SERCA function, as an alkaline pH can inhibit SERCA activity. Using the Ca^{2+} indicator, Fluo-3, in the cytosol and extracellular space of permeabilized HeLa cells, Li *et al.* showed fluorescence decay from Fluo-3 in the cytosol was associated with Ca^{2+} uptake into the ER (Li *et al.*, 2012). The decay was completely inhibited by thapsigargin, ensuring the fluorescence decay was mediated by SERCA. However, a reduced amount of decay (or Ca^{2+} uptake into the ER by SERCA) was observed in the presence of a pH 8 buffer, as compared to pH 6 and 7. It is hypothesized that protonation of SERCA residues involved in 1) ATP dephosphorylation in the E1 phase and 2) in the release of Ca^{2+} in the E2 phase could be affected in alkaline environments.

Phylogenetic analysis of SERCA-like proteins in apicomplexans revealed that *T. gondii* only expresses one SERCA isoform (TgSERCA) (Nagamune & Sibley, 2006). TgSERCA displayed about 50% similarity with the mammalian isoform. Antibodies against TgSERCA resulted in ER specific localization. Yeast complementation mutants of TgSERCA were generated in a yeast triple mutant strain lacking the Golgi and vacuolar Ca^{2+}-ATPases (Pmr1 and Pmc1 respectively) and the vacuolar Ca^{2+} binding protein, calcineurin. The mutants displayed a growth phenotype under low Ca^{2+} concentrations which is restored by complementing with TgSERCA. Growth of the mutant complemented with TgSERCA was affected by thapsigargin, and no effect was seen in the vector control, supporting its specific function as a SERCA pump (Nagamune *et al.*, 2007). The depletion of Ca^{2+} from the ER in *T. gondii* is possible through addition of thapsigargin, the SERCA inhibitor. In *T. gondii*, thapsigargin has been implemented to study ER Ca^{2+} signaling,

Ca^{2+}-activated Ca^{2+} entry, and the role of ER Ca^{2+} throughout the lytic cycle (Marquez-Nogueras *et al.*, 2021; Sidik, Hortua Triana*, et al.*, 2016; Stasic *et al.*, 2021).

ATP4-type ATPases

Lehane *et al.* identified a novel subgroup of type II apicomplexan specific P-type ATPases, that consist of TgATP4, a homolog of the apicomplexan parasite, *Plasmodium falciparum* (*P. falciparum*), PfATP4 (Lehane *et al.*, 2019). PfATP4 was characterized first and due to its sequence similarity to other type II P-type ATPases, it was originally annotated as a Ca^{2+}-ATPase (Krishna *et al.*, 2001). Studies however showed that PfATP4 regulates and transports sodium rather than Ca^{2+}. PfATP4 is a potential target of ciparmagine, a drug that is a part of a novel class of antimalarials called spiroindolones. In *T. gondii* wildtype (WT) parasites, ciparmagine lead to an increase in cytosolic sodium, similar to what was observed in *P. falciparum*. However, parasites lacking TgATP4 had a higher level of resting cytosolic sodium and displayed a decreased magnitude in ciparmargine induced sodium influx. TgATP4 is hypothesized to extrude sodium out of the cytosol in exchange for hydrogen into the cytosol, causing an acid influx. Cytosolic pH measurements demonstrated that cipargmagine leads to alkalinization of the cytosol, probably due to inhibition of pH import activity conducted by TgATP4. Ciparmagine however had no effect on pH in TgATP4 knockdown mutants. Ciparmagin displayed no effects on Ca^{2+} homeostasis and TgATP4 mutants did not have any Ca^{2+} related phenotype. The inability to regulate sodium and proton homeostasis in the mutants disrupted the viability of extracellular parasites and resulted in parasites being less virulent in mice. These data suggest that TgATP4 regulates sodium and protons and not

Ca^{2+}. However more studies related to Ca^{2+} signaling would have to be done to rule out any Ca^{2+} related activity (Lehane *et al.*, 2019).

Plasma membrane Ca^{2+} ATPase

The plasma membrane Ca^{2+}-ATPase (PMCA) is also a type II P-type ATPase that uses ATP to pump Ca^{2+} in exchange for one proton across the plasma membrane against the Ca^{2+} gradient. Unique to PMCA, this pump contains a much longer c-terminal tail than other Type II Ca^{2+}-ATPases. This long extension is known to bind to a number of different proteins such as calmodulin, phospholipids and kinases (DeMarco & Strehler, 2001; James *et al.*, 1988; Peter Brodin, 1992). While the main mechanistic role of PMCA is to translocate Ca^{2+} across the membrane, it's regulatory characteristics and function provide evidence for its role in local Ca^{2+} signaling events.

The role of PMCA in pH regulation has been explored in rat neuroendocrine cells, PC12 cell (Boczek *et al.*, 2014). Knockdown mutants of different PMCA isoforms in PC12 cells resulted in higher resting cytosolic and mitochondrial pH. Mutants showed defects in Ca^{2+} recovery after KCl induced Ca^{2+} entry. A higher amount of Ca^{2+} was able to enter in the mutants, while acidification of the mitochondria and the cytosol was of a decreased magnitude in the knockdowns. In these cells, KCl-induced cellular acidification was mainly attributed to the PMCA proteins. An alkaline response has been demonstrated in the extracellular milieu of neurons (Makani & Chesler, 2010). Depolarization of voltage-clamped CA1 pyramidial neurons demonstrated that this "proton sink" arises because of PMCA proteins. Extracellular alkalinization is dependent on Ca^{2+} in the buffer and inhibitors specific to the extracellular and cytosolic side of PMCA drastically diminished this response.

T. gondii expresses a homolog of PMCA known as TgA1 (Luo, S. *et al.*, 2005). Antibodies specific to A1 detected expression of TgA1 in both tachyzoite and bradyzoites through western blot analysis. Immunofluorescence experiments revealed it's localization to both the plasma membrane and the acidocalcisomes. Yeast complementation with TgA1 was performed in a Pmc1 and Vcx1 (vacuolar Ca^{2+}/H^{+} exchanger) double mutant cell line. TgA1 complemented yeasts were able to tolerate high Ca^{2+} concentrations, while the double mutant without TgA1 could not, supporting TgA1's function as a Ca^{2+}-ATPase. Luo *et al* established that resting Ca^{2+} cytosolic levels were significantly higher in TgA1 deletion mutants and release of Ca^{2+} from acidic stores, most likely the acidocalcisome, and the ER was unregulated. The absence of TgA1 resulted in higher intracellular Ca^{2+} after incubation with 1 mM of Ca^{2+} indicating the inability of the cells to properly extrude Ca^{2+} from the cytosol. Secretion of MIC2 occurred spontaneously and when stimulated by the Ca^{2+} ionophore, A23187, was secreted at low levels. This work further revealed that TgA1 affects levels of polyphosphate and pyrophosphate, which are mainly stored in the acidocalcisome. These mutants were unable to properly invade the host cells, suggesting that proper regulation of intracellular Ca^{2+} and acidocalcisome function is important for the parasite. Localization of TgA1 at the acidocalcisome and discovery of Ca^{2+} in this organelle supports the interdependence of Ca^{2+} and protons in *T. gondii*.

Calcium/proton exchangers

Cation/Ca^{2+} exchangers fall under one superfamily divided into 5 subfamilies: the H^{+}/Ca^{2+} exchanger (CAX), Na^{+}/Ca^{2+} exchanger (NCX), K^{+}-dependent Na^{+}/Ca^{2+} exchanger (NCKX), Cation/Ca^{2+} exchanger CCX, and bacterial YRBG family (Cai & Lytton, 2004; Shigaki *et al.*, 2006). Members of this superfamily contain anywhere from

9-11 transmembrane domains and two clusters of conserved alpha helices split by a hydrophilic stretch comprised of acidic amino acid residues. Direction of the flow of ions depends on 1) charge, 2) magnitude of the concentration gradient and 3) the electrochemical gradient (Gadsby, 2009). Animals use Na^+ as the driving force for coupled ion force, but plants and yeast often use H^+ instead. The NCKX and NCX subfamily is mainly found in human brain tissue. YRBG proteins contain homology to NCKX/NCX proteins and are exclusive to bacteria and archaea. Members of the CCX family are found in fungi, plants, invertebrates, one protozoan (*Tetrahymena thermophila*), and two mammalian organisms (humans and mouse). Finally, CAX proteins are found in prokaryotes and eukaryotes, except humans (Gadsby, 2009). Homologs in mammals were found in two mammalian organisms, the platypus and the Tasmanian devil (Melchionda *et al.*, 2016).

CAX proteins

CAX proteins have demonstrated a significant role in Ca^{2+} storage in acidic organelles. Family members contain two canonical GNxxE motifs not found in other cation/Ca^{2+} exchangers subfamilies (Cai & Lytton, 2004). The CAX prototype is the yeast CAX protein known as the vacuolar proton/Ca^{2+} exchanger (Vcx1) (Fink, 1996). Vcx1 is responsible for the majority of Ca^{2+} uptake into the vacuole, an organelle that stores up to 90% of the Ca^{2+} content in the yeast cell (Cunningham, 2011). The yeast vacuole maintains its proton gradient through the vacuolar H^+ ATPase, which pumps protons into the vacuole, thus creating this proton gradient between the vacuole and the cytosol. The proton gradient allows for Ca^{2+}/proton exchange activity to occur, where protons are exchanged to the cytosol for Ca^{2+} into the vacuole by Vcx1. Vcx1 deletion mutants are

unable to take up Ca^{2+} into the vacuole and exposure to concanamycin B, a vacuolar H^+-ATPase inhibitor, blocked Ca^{2+} uptake activity due to the inability to establish the proton gradient (Fink, 1996).

In apicomplexans, the *P. falciparum* gene PfCAX encodes for the Ca^{2+}/proton exchanger homolog of Vcx1 (Rotmann *et al.*, 2010). Characterization of PfCHA was assessed by heterologous expression on the plasma membrane of *Xenopus* oocytes. Levels of radiolabeled $^{45}Ca^{2+}$ in the oocyst cytosol were higher in PfCHA expressing oocysts than oocysts transformed with an empty vector. To test for Ca^{2+}/proton exchange activity, the pH of the extracellular space was monitored under varying conditions. Oocysts expressing PfCHA placed in a weak buffer resulted in an acidified external medium after 4 hours, establishing the role of PfCHA in proton transport activity. Translocation of protons proved to be Ca^{2+} dependent, as in Ca^{2+} free and Ca^{2+}/Mg^{2+} free buffer, very little change in the acidification of the extracellular medium was observed. Ca^{2+} uptake was measured under different external pHs, and the more basic the external media was, the more Ca^{2+} uptake occurred demonstrating that the establishment of a proton gradient across the plasma membrane is necessary for Ca^{2+} transport across the membrane. Ca^{2+} uptake activity was sensitive to known Na^+/H^+ exchanger inhibitors, amiloride, 5-[*N*-ethyl-*N*-isopropyl]amiloride (EIPA), and KB-R7943. In *P. falciparum*, localization experiments revealed that PfCHA localized to the mitochondrium, promoting the investigation of mitochondrial Ca^{2+} homeostasis. Wildtype parasites were loaded with the Ca^{2+} cytosolic indicator, Fluo4, and mitochondrial Ca^{2+} indicator, Rod2. Addition of the SERCA inhibitor, cyclopiazonic acid, lead to an increase in both the cytosolic and

mitochondrial Ca^{2+}. Interestingly, exposure to KB-R7943 lead to a reduction in CPA-induced Ca^{2+} increase.

PfCHA was further functionally characterized in the double Vcx1 and Pmc1 yeast mutant (Guttery *et al.*, 2013). Mutants were complemented with full length PfCAX cDNA (PfCAX) and N-terminally truncated PfCAX cDNA (sPfCAX). Vcx1 and Pmc1 double knockout mutant are sensitive to high Ca^{2+} concentrations and display a growth phenotype in these conditions. PfCAX and sPfCAX were able to complement growth at high Ca^{2+} concentrations, but the sPfCAX was significantly more efficient in complementing growth, indicating the N-terminus is disturbing function in yeast. Ca^{2+}/proton exchange activity was measured in vacuolar membrane vesicles extracted from yeast complemented cell lines. Radiolabeled Ca^{2+} uptake activity was measured after activation of the vacuolar H^{+}-ATPase with Mg-ATP to establish a proton gradient. These data showed that sPfCAX and PfCAX were both able to mediate Ca^{2+}/proton activity and sPfCAX uptake occurred more efficiently. The CAX protein homolog in *P. berghei* (PbCAX) was also tested for its role in the life cycle of the parasite. PbCAX mutants were severely defective in conversion to the sexual stage and were not able to establish a mosquito midgut infection. The inability of PbCAX mutants to convert to ookinetes was restored by chelating extracellular Ca^{2+}.

In the same study, the CAX homolog found in *T. gondii*, TgCAX, was used to complement the yeast mutants and TgCAX was also able to restore growth at high Ca^{2+} concentrations. Determining the localization of TgCAX in *T. gondii*, however, proved to be challenging. Attempts to determine localization using a TgCAX specific antibody or an exogenous TgCAX copy containing a C-terminal tag demonstrated vesicular localization

that did not colocalize with the PLV, acidocalcisome or mitochondria markers. More so, no signal could be detected in intracellular parasites with the antibody nor with parasites expressing an endogenous TgCAX C-terminal 3-ty tag. TgCAX knockout mutants did not have a growth, replication, or Ca^{2+} related egress phenotype. There are several explanations as to why TgCAX localization could not be determined. Perhaps the N and C-terminal sequences of the gene are crucial for function or even processing and placing a tag in the middle of the gene could help with detection. Since TgCAX appears to be lowly expressed, it might be useful to use a higher affinity tag, like spaghetti monster HA (smHA) (Hortua Triana, Marquez-Nogueras, Chang*, et al.*, 2018), which has been used to study lowly expressed channels. Lastly, it is possible that TgCAX is less expressed throughout the cell cycle, and performing localization experiments at different timepoints post invasion could reveal TgCAX is only expressed at specific time points. Dispensability of TgCAX is not entirely unexpected in *T. gondii*. The cell has multiple mechanisms to regulate Ca^{2+} and although there was not a Ca^{2+} related egress phenotype, we cannot discard that TgCAX might be involved in other aspects of Ca^{2+} homeostasis and pH regulation because they were not tested. Taken together, these studies reveal that apicomplexans possess mechanisms to regulate Ca^{2+} and protons.

A novel family of CAX proteins

Almost ten years ago, a novel family of CAX proteins was discovered in humans by Foulquier *et al* (Foulquier *et al.*, 2012). Genome sequencing of individuals suffering from congenital disorder of glycosylation (CDG) lead to the discovery of mutations in the protein TMEM165, a protein part of the unidentified protein family 0016 (UPF0016). The patients with mutated TMEM165 all suffered from CDG and symptoms included

osteoporosis, muscle weakness, and various types of severe bone deformities(Foulquier *et al.*, 2012). TMEM165 was found to localize to the Golgi apparatus and mutations resulted in several Golgi glycosylation defects. Patch clamp analysis of HeLA cells expressing TMEM165 demonstrated Ca^{2+} dependent ionic currents. Heterologous expression of TMEM165 on *Lactococcus lactis* (*L. lactis*) revealed an increase in cytosolic Ca^{2+}, detected by the ratiometric calcium indicator, Fura2 (Stribny *et al.*, 2020). This supports that TMEM165 is selective to Ca^{2+}. TMEM165 knockdown mutants in HeLA cells had a more acidic lysosome, indicating that TMEM165 affects proton homeostasis in the lysosome. If TMEM165 mediates proton transport out of the Golgi, then the absence of TMEM165 could lead to deficiencies in removing protons from the Golgi. This could cause increased acidification of the endosomes and downstream organelles. Since the discovery of TMEM165 in humans, homologs have been characterized in plants, fungi and protozoans.

The UPF0016 family encodes for a unique CAX protein because unlike the canonical CAX subfamily, there is a human homolog. The UPF0016 forms a novel family of CAX proteins found across all species of life (Demaegd *et al.*, 2013). The evolutionary question stands: why is *this* CAX family so highly conserved? These proteins contain between 5-7 transmembrane domains and the hallmark of these proteins is the presence of one or two EXGD-K/R-T/S motifs. The yeast homolog, ScGDT1, has been one of the best studied members. ScGDT1 localizes to the cis and medial Golgi and is essential for tolerance of very high concentrations of Ca^{2+}. Results showed an increase in cytosolic Ca^{2+} in *L. lactis* expressing Gdt1, whereas none was observed with expression of the empty vector, confirming that Gdt1 can also mediate Ca^{2+} transport across the plasma

membrane of *L. lactis* (Stribny *et al.*, 2020). Ca^{2+} influx was higher at pH 8 versus pH 7 due to the pH gradient generated at higher pH (Colinet *et al.*, 2016). These conditions are more energetically favorable for hydrogen efflux and in turn Ca^{2+} influx controlled by Gdt1 is pH dependent.

The interaction between GDT1 and Pmr1 has been largely investigated. Pmr1 is the SPCA-like Ca^{2+}-ATPase that localizes to the Golgi in yeast. Double mutants of Pmr1 and Gdt1 have mild growth phenotypes under homeostatic conditions but are significantly less tolerant to high concentrations of Ca^{2+} than single mutants of either gene. Using the genetically encoded Ca^{2+} indicator, aequorin, experiments showed that the resting level of Ca^{2+} in the double mutants was much higher and the amount of Ca^{2+} entry was significantly less than that of wildtype. Western blot analysis showed that higher expression of GDT1 in the Pmr1 knockout mutant (Demaegd *et al.*, 2013). Ca^{2+} entry in yeast can be activated by exposure to salts, which can also cause saline stress (RA Bressan, 1998). No difference was shown in saline induced Ca^{2+} entry between the GDT1 deletion mutant and WT. In the double knockout however, there was a drastically higher amount of Ca^{2+} entry, and an even higher increase in Pmr1 single knockouts. These data could support that GDT1 has a Ca^{2+} export mechanism while indicating Pmr1 function in importing Ca^{2+} into the Golgi.

The *Arabidopsis thaliana* UPF0016 ortholog, AtCCHA1, was identified as contributing to Ca^{2+}, manganese and proton homeostasis in the thylakoid membranes of the chloroplast (Wang *et al.*, 2016). AtCCHA1 mutants are grow slower than WT plants, and mutants displayed even greater deficiencies in plant development at higher Ca^{2+} and manganese conditions. Stomata cells, which are found on the epidermis of leaves and

contain chloroplast, were found to contain more Ca^{2+} in the cytosol than in the wildtype cells. Germination of seeds was also impacted at an acidic and alkaline pH (pH 4 and pH8, respectively) and the pH of stomata cells was more acidic in the absence of AtCCHA1. The inability to properly regulate these ions lead to defects in photosynthetic activity. Interestingly, AtCCHA1 was not able to rescue the growth phenotype of GDT1 yeast deletion mutants at high Ca^{2+} concentrations. This result could be attributed to the difference in localization of AtCCHA1 at the thylakoid, as opposed to the Golgi and in turn a divergence in function.

TMEM165 in glycosylation

Studies have also shown that TMEM165 homologs affect Golgi glycosylation in a manganese specific manner (Colinet *et al.*, 2016). The glycosylation of the vacuolar carboxypeptidase (CPY) and the glucanosyltransferase (Gas1p) was analyzed in the Gdt1 deletion mutant. Under homeostatic conditions, no defect in glycosylation was observed, but in media supplemented with 500 mM Ca^{2+} there was a defect in these proteins' maturation whereas no difference was observed in WT. Interestingly, mutants did not exhibit any glycosylation defects when manganese was added in media supplemented with Ca^{2+}, indicating that manganese has a rescuing effect. Fura2-AM experiments showed that TMEM165 and GDT1 can also transport manganese (Stribny *et al.*, 2020; Thines *et al.*, 2018). Characterization of the zebrafish ortholog, Tmem165, resulted in decreased amounts of N-linked glycosylated proteins found in the knockdown mutant that most likely led to the defects in improper formation of cartilage and bone tissue (Bammens *et al.*, 2015).

The kinetoplastid protist *Trypanasoma cruzi* (*T. cruzi*) encodes for *TcGDT1*, a UPF0016 gene member (Ramakrishnan *et al.*, 2021). *TcGDT1* was able to functionally complement the sensitivity of ScGDT1 mutants at high Ca^{2+} concentrations. However, TcGDT1 seemed to possess a larger role in manganese dependent glycosylation in the Golgi rather than regulating Ca^{2+}. Lectins are carbohydrate binding proteins that can be used to test glycosylation efficiency. Lectin-probed western blot analysis demonstrated a defect in glycan conjugation to proteins in TcGDT1 mutants. Furthermore, glycosylation of flagellum glycoprotein GP72 was disrupted in the absence of TcGDT1, and was rescued by manganese, but not by other cations such as Ca^{2+}, zinc or magnesium. The inability to properly regulate glycosylation impacted infectivity and replication of both the human and insect stage of *T. cruzi*.

Conclusion

Analysis of the Ca^{2+} signaling molecules in this review provides evidence that type II Ca^{2+} ATPases and calcium/proton exchangers are multifunctional and can mechanistically regulate more than just Ca^{2+}. This topic has not been dissected enough, but two well written reviews have discussed the interplay between Ca^{2+} and pH. The first is by Molinari and Nervo, who discuss how protons are not just regulatory ions, but also stimulants of Ca^{2+} related processes (Molinari & Nervo, 2021). The second, by Patel and Docampo, explains the significance of Ca^{2+} in acidic organelles (Patel & Docampo, 2010). We've learned that these Ca^{2+} pumps and exchangers can influence multiple aspects of the cell such as development, signaling, protein processing and maturation, and viability. It is essential to have proteins that can simultaneously monitor and control Ca^{2+} and pH homeostasis and signaling. Assessment of Ca^{2+} signaling molecules like membrane

channels and Ca^{2+} binding proteins, and the impact of protons on their function, might shed more light on the relationship between Ca^{2+} and protons. It is valuable to think about these ions outside of the context that we are most familiar with. Development of an ER pH indicator or a Golgi specific chemical Ca^{2+} indicator should allow us to learn even more. The exact mechanism of the relationship between calcium and protons has not been unraveled and we will most likely discover that there is an extensive network of molecules involved. In this dissertation, we aim to fill some of the gaps pertaining to the Ca^{2+} signaling toolkit in *T. gondii*. We provide findings on a novel calcium/proton exchanger, an apicoplast ClpP protease and advancements on measuring intracellular calcium using a high throughput method. Ultimately, these results can contribute to the community's understanding about host-pathogen interaction, specifically, *T. gondii* and its disease.

Chapter 2

A *Toxoplasma gondii* calcium/proton exchanger that regulates TgSERCA Ca^{2+} uptake and pH homeostasis[1]

[1]Calixto, Abigail and Silvia NJ Moreno. To be submitted in *Cell Calcium.*

Abstract

Calcium (Ca^{2+}) signaling is a universally conserved process among eukaryotes In *Toxoplasma gondii (T. gondii)*, an obligate intracellular parasite, a rise in intracellular Ca^{2+} stimulates each step of the lytic cycle. The lytic cycle causes rapid and constant tissue disruption, supporting a role for Ca^{2+} signaling in pathogenesis. These lytic cycle facets are essential for tissue disruption and spread of *T. gondii*, supporting a role for Ca^{2+} signaling in pathogenesis. We characterized a putative calcium proton exchanger, Tggt1_319550 (TgCAXL1), which belongs to a conserved family of transmembrane proteins predicted to be Ca^{2+}/proton exchangers that localize to the Golgi apparatus. We introduced a 10-HA tag at the C-terminus of TgCAXL1 and found that it localizes to the ER and Golgi apparatus. We used CRISPR-Cas9 to generate a clonal knockout mutant and found that TgCAXL1 is important for Ca^{2+} release from the ER and acidic stores, most likely the Golgi, causing for the mutant to be defective in invasion of host cells. We demonstrate that TgCAXL1 impacts the SERCA-Ca2+ uptake activity, suggesting a physiological interaction between both proteins. Yeast complementation validated the functional role of TgCAXL1 as a Ca^{2+}/proton exchanger, so we studied its role in pH regulation and discovered that TgCAXL1 controls the cytosolic recovery from acidic stress. We hypothesize that the deregulated pH in the Golgi and ER that results from the absence of TgCAXL1, can affect Ca^{2+} homeostasis in these organelles. For the first time, we reveal the significance of the Golgi in modulating Ca^{2+} signaling in *T. gondii*.

Graphical Abstract

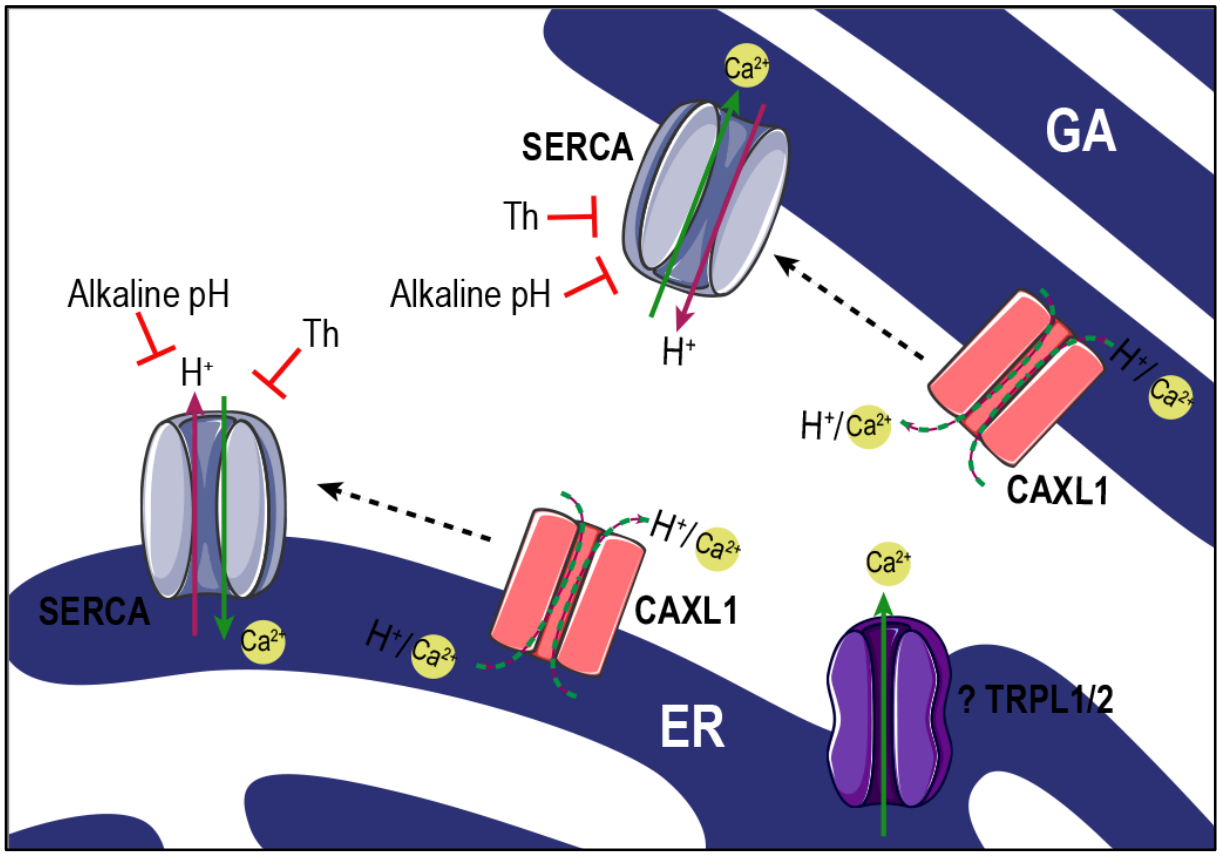

2.1 Introduction

Toxoplasma gondii is a protozoan parasite that infects approximately one third of the world's population (Dubey, 2004). In most individuals, *T. gondii* infection leads to flu like symptoms, but in immunocompromised individuals and pregnant women, a severe neurological defect can occur to the patients and fetus, respectively (Dubey, 2004). The parasite exists in two forms in the intermediate host: the bradyzoite, which causes chronic infection and can persist in tissues undetected by the host immune system and the tachyzoite, which is the fast-replicating stage and causes acute infection (Dubey, 2004). The tachyzoite undergoes the lytic cycle, which consists of attaching and invading host cells, replicating inside a parasitophorous vacuole, egressing, and moving to search for another host cell and repeat the cycle again. Calcium (Ca^{2+}) is a ubiquitous signaling molecule that plays a major role throughout the tachyzoite lytic cycle (Hortua Triana, Marquez-Nogueras, Vella*, et al.*, 2018). Ca^{2+} entry through the plasma membrane and release from intracellular stores can stimulate key lytic cycle steps including egress, invasion, and motility (Borges-Pereira *et al.*, 2015; Pace *et al.*, 2014; Vella *et al.*, 2021). The steep difference in the concentration gradient between the extracellular and intracellular environment has led the parasite to evolve various mechanisms to ensure that cytosolic Ca^{2+} is maintained at non-toxic low levels (around 100nM) (Pace *et al.*, 2014). In *T. gondii*, many of these mechanisms that contribute to regulating cytosolic levels of Ca^{2+} remain unknown. Due to the significance of Ca^{2+} for tachyzoite pathogenesis, it is important to continue to investigate and discover additional members of the Ca^{2+} signaling toolbox.

To prevent high concentrations of Ca^{2+} from harming the cell, organelles can store Ca^{2+} through various Ca^{2+} transporters, ATPases, and Ca^{2+}/ion exchangers (Clapham, 2007). In *T. gondii*, the endoplasmic reticulum (ER) serves as a major Ca^{2+} storage organelle and pumps Ca^{2+} via the canonical thapsigargin sensitive **S**arco/**E**ndoplasmic **R**eticulum **C**a^{2+} **A**TPase (TgSERCA) (Nagamune & Sibley, 2006). Within the last 20 years, Ca^{2+} has also been found in the acidic organelles, such as the electron dense, acidocalcisome, and the plant-like vacuole (PLV) (Miranda *et al.*, 2010). Mobilization of Ca^{2+} into the acidocalcisome occurs by the **C**a^{2+} **A**TPase TgA1, which is also found on the plasma membrane (Shuhong Luo, 2001). The presence of Ca^{2+} has also been detected in the PLV, where transport most likely occurs through a Ca^{2+}/H^{+} exchanger, although the exact mechanism and player through which this occurs remains unknown (Miranda *et al.*, 2010; Stasic *et al.*, 2021). Ca^{2+}/H^{+} exchanger proteins (CAX) are one of five families that form part of the Ca^{2+}/cation superfamily (Shigaki *et al.*, 2006). CAX is an essential mechanism of Ca^{2+} organellar uptake, mainly into acidic stores, however there are reports in plants of localization to the plasma membrane (Luo, G. Z. *et al.*, 2005). These proteins use a proton gradient created by the vacuolar H^{+}-ATPase or vacuolar H^{+}-pyrophosphatase to transport Ca^{2+} into the organelles. Members of CAX are present in fungi, plants, protozoans, lower vertebrates, and bacteria, but interestingly, not in mammals (Melchionda *et al.*, 2016). A homolog of CAX from the malaria parasite *Plasmodium falciparum* (*P. falciparum*) PfCAX was functionally characterized in 2010. Found on the mitochondria, Ca^{2+} and proton transport activity was characterized by heterologously expressing PfCAX in *Xenopus* oocysts. Uptake of radiolabeled Ca^{2+} into the oocyst cytosol by PfCAX was proton dependent and proton efflux into the extracellular

medium was Ca^{2+} dependent (Rotmann *et al.*, 2010). The *T. gondii* ortholog, TgCAX, appeared to localize to the PLV, but results were inconclusive due to low levels of expression (Guttery *et al.*, 2013). In a functional yeast analysis, PfCAX and TgCAX demonstrated less hypersensitivity to high Ca^{2+} concentrations suggesting a role in tolerating stressful Ca^{2+} conditions. In the same study, the *P. berghei* ortholog PbCAX was important in tolerating extracellular Ca^{2+} in the parasite's sexual stage (Guttery *et al.*, 2013). The role of Ca^{2+}/H^{+} exchangers in the *T. gondii* Ca^{2+} signaling network is largely unexplored and opens up the door to investigate the role of acidic organelles and protons in regulating Ca^{2+}.

To study Ca^{2+}/H^{+} exchange activities in *T. gondii*, we characterized a putative Ca^{2+}/H^{+} exchanger, TgCAXL1 (TgGT1_319550). To date, TgCAXL1 is part of a novel family of Ca^{2+} antiporters, UPF0016 proteins, that were first described in mammalians (Foulquier *et al.*, 2012). Foulquier and colleagues observed that the human ortholog, HsTMEM165, is a Golgi specific protein and mutations in HsTMEM165 caused congenital disorders of glycosylation. UPF0016 proteins form a conserved family of Ca^{2+} transporters that contain six transmembrane domains and two unique consensus motifs (EXGD-K/R-T/S) (Demaegd *et al.*, 2014). The yeast ortholog, ScGDT1, was characterized and localized to Golgi bodies as well (Demaegd *et al.*, 2013). Ca^{2+} transport has been observed in both HsTMEM165 and ScGDT1. Whole cell patch clamp experiments in HeLa cells expressing HsTMEM165 cells displayed ionic currents in response to Ca^{2+} (Demaegd *et al.*, 2013). Experiments with the chemical calcium indicator, FURA2, in *Lactococcus lactis* expressing HsTMEM165 or ScGDT1, demonstrated the ability of the proteins to mobilize Ca^{2+} across a plasma membrane

(Colinet *et al.*, 2016; Stribny *et al.*, 2020). HsTMEM165 and ScGDT1 are important for tolerating high concentrations of Ca^{2+}, indicating a role in Ca^{2+} homeostasis (Demaegd *et al.*, 2013). Ca^{2+} transport mediated by GDT1 was dependent on pH, and lysosomes of HeLa cells deficient in TMEM165 were more acidic than wildtype (Colinet *et al.*, 2016; Demaegd *et al.*, 2013). Ca^{2+} dependent phenotypes are all exacerbated in double mutants of ScGDT1 and the Golgi specific Ca^{2+}-ATPase, ScPmr1, suggesting interaction between ScGDT1 and ScPmr1 (Colinet *et al.*, 2016; Demaegd *et al.*, 2013; Dulary *et al.*, 2018).

In this work, we show that the **Ca**$^{2+}$/proton e**x**changer-**l**ike protein **1** (TgCAXL1) has dual localization in the Golgi apparatus and the ER and is important for invasion. We investigate TgCAXL1's function in Ca^{2+} signaling, pH homeostasis and its relationship with TgSERCA. This work is novel as it raises the significance of the relationship between Ca^{2+} and pH and the role of Ca^{2+}/H^{+} exchanger proteins in ion homeostasis.

2.2 Methodology and Materials

Cell culturing

For this study *T. gondii* RH type I and TATiΔKu80 (Sheiner *et al.*, 2011) tachyzoites were utilized. Parasites were grown in human telomerase reverse transcriptase (hTERT) confluent monolayers in Dulbecco's Modified Eagle Medium with high glucose (DMEM-HG) supplemented with 1% bovine calf serum (BCS) (GemCell™ GeminiBio). For replication and invasion experiments, parasites were grown in human foreskin fibroblasts (HFF) in DMEM-HG + 1% BCS.

Epitope tagging and mutant generation

Development of cell lines was achieved using CRISPR/Cas9 mediated gene disruption (Shen *et al.*, 2014; Sidik *et al.*, 2014). For C-terminal epitope tagging, the

CRISPR/Cas9 plasmid consisted of a 20 bp sgRNA homologous to the C-terminal end of the TgCAXL1 (TgGT1 319550) locus (amplified with AC107 and AC119). The repair template, consisting of ten copies of a human influenza hemagglutinin (HA) tag (smHA) and a chloramphenicol (CAT) drug cassette (Hortua Triana, Marquez-Nogueras, Chang*, et al.*, 2018) was amplified from the smHA-pLIC-CAT(Huynh & Carruthers, 2009) plasmid with primers, AC105 and AC106, that contain 35 to 40 bp of homologous DNA to TgCAXL1. TATiΔKu80 parasites were transfected with the tagging construct alongside the CRISPR/Cas9 plasmid. Parasites were selected with 34 µg chloramphenicol and serially diluted to select for a clonal population. Parasites were validated with PCR, immunofluorescence assay (IFA), and western blotting. To create the ΔCAXL1 mutant, 1 kb of homologous DNA to the 5' and 3' UTR of TgCAXL1 were placed upstream and downstream of the dihydrofolate reductase (DHFR) cassette, respectively. The insert for transfection was amplified from this newly made plasmid using primers AC178 and AC179. To increase the chance of obtaining a clean deletion mutant, two CRISPR/Cas9 plasmids were created, one consisting of sgRNA specific for the 5' end (using primers AC163 and AC119) and one for the 3' end (using primers AC164 and AC119). The repair template and both plasmids were transfected in RH type I parasites in hTERT cells and selected with 1 µM pyrimethamine for two passages. The mixed population was serially diluted to select for clonal populations for further analysis. Clones were validated via PCR and then quantitative real time-PCR.

Construction of Phylogenetic tree

The phylogenetic tree constructed by Demaeged *et al*. was often referenced for annotated UPF0016 proteins from eukaryotes to prokaryotes. Updated protein

sequences and names were obtained from the National Center for Biotechnology Information protein (NCBI) database. Apicomplexan sequences were found on ToxoDB by Orthomcl.org. Kinetoplastid sequences were acquired using the Basic local alignment search tool for proteins (BlastP) tool on TriTrypDB. Sequences were aligned using phylogeney.fr (Dereeper *et al.*, 2008) by selecting the ClustalW program (Goujon *et al.*, 2010; Sievers *et al.*, 2011). Using MEGA, a maximum likelihood tree was constructed with the LG substitution model and a discrete gamma distribution (G) with a bootstrap of 1000 (Tamura *et al.*, 2021).

Immunofluorescence assay

Parasites that were 70% egressed were filtered with a 5 µM filter and washed once with buffer A with glucose (BAG) (116 mM NaCl, 5.4 mM KCl, 0.8 mM $MgSO_4 \bullet 7H2O$, 50 mM HEPES, 5.5 mM Glucose, pH adjusted to 7.3) (Pace *et al.*, 2014). Parasites were adhered to glass slides using poly-L-lysine, fixed with 3% paraformaldehyde, permeabilized with 0.3% triton-X-100, and blocked with 3% bovine serum albumin (BSA) made in 1x PBS pH 8. Parasites were then incubated in primary antibody for 1 hr at room temperature and washed with PBS (pH 8) 3x and then incubated with secondary antibody for 1 hr in the dark. Slides were washed 4x with PBS (pH 8). Coverslips with parasites were mounted on slides using Fluoromount-G and 1% DAPI. Intracellular parasites were stained in the same way, however host cells were prepared on sterile coverslips and allowed to grow for 24 hrs and then infected with parasites and allowed to grow for another 24 hrs. To stain for the Golgi-apparatus, GRASP-55 (Brydges *et al.*, 2008) plasmid was used. Parasites were transfected with 50 µg of GRASP55-RFP plasmid and seeded onto a coverslip containing host cells made in advance. Rabbit anti-RFP was used at a 1:1000

dilution to detect GRASP55. To stain for the ER, we used anti-Calumenin at 1:1000. Mouse anti-HA was used at 1:1000 and Rat anti-HA was used at 1:100. Secondary antibodies consisted of Invitrogen Alexa Fluor 488 Goat anti-Mouse and Goat anti-Rat, 546 Goat Anti-Rat and Goat Anti-Rabbit all at 1:1000 dilutions. Slides were visualized with the Olympus IX71 inverted microscope using the DeltaVision imaging system. Images were deconvolved and analyzed with softWoRx software.

qRT-PCR

RNA was extracted from parasites using TRIzol™ Reagent (Ambion-Life Technologies) as directed by the product manual and treated with 1 µL of DNase I (NEB) for 10 min at 37 °C. cDNA creation was performed using the Superscript® III First Strand System from Invitrogen and diluted to a working stock of 100 ng/µl. Transcript levels were detected by iQ™ Syber® Green supermix with primers AC214 and AC215 targeting the first exon of TgCAXL1. 100 ng of cDNA were used for each assay reaction. Samples were run in a CFX96 Real Time PCR System (Bio-Rad). All values were analyzed using BioRad CFX manager program to determine the relative expression level of TgCAXL1 in all cell lines. TgCAXL1 expression level in RH was set to 1 and actin (TgGT1_209030) and tubulin (TgGT1_316400B) were used as housekeeping genes (Tubulin amplified with primers AC327 and AC328 and actin amplified with primers AC329 and AC330).

Yeast growth assays

GDT1Δ+EV, GDT1Δ+GDT1, and GDT1Δ yeast strains and the pRS416 plasmid were a gift from Dr. Roberto Docampo, who obtained them from Dr. Pierre Morsomme at the Université catholique de Louvain in Belgium (Demaegd *et al.*, 2013). The pRS416 plasmid (Demaegd *et al.*, 2013), consisting of the TP1 (triose phosphate isomerase 1)

promoter and a URA3 metabolic marker, was used as the complementation vector. TgCAXL1 cDNA was fused to 69 bp of the GDT1 signal peptide by Twist Bioscience and cloned into the pRS416 plasmid downstream the TP1 promoter using Restriction Enzymes XhoI and EcoRI (NEB). The pRS416-CAXL1 plasmid was then transformed into GDT1Δ and selected on synthetic defined (SD) medium supplemented with all amino acids except uracil (0.7% Yeast Nitrogen Base without amino acids, 2% glucose and 0.77% complete supplement mixture without uracil- pH 6). For Ca^{2+} growth experiments, the media consisted of 0.2% Yeast Nitrogen Base without amino acids and ammonium sulfate, 76 mM NH_4Cl, 2% glucose, and 0.77% complete supplement mixture (CSM) without uracil, pH 6 and 550 mM of Ca^{2+}. Ca^{2+} was added after autoclaving the media to avoid precipitation. Solid media was made by adding 2% agar (BD Bacto™Agar, Fisher Scientific). For plate growth assays, yeast was grown overnight in SD medium without uracil at 30°C. Yeast was diluted to an OD_{600} of 1 and three 1:10 serial dilutions were made. 10 µL of each dilution were plated on solid media with and without 550 mM Ca^{2+} and allowed to grow for 4-6 days at 30°C. For the liquid growth assay, yeast was grown overnight at 30°C. After 24 hrs of incubation, yeast was diluted to a 0.1 OD in SD media with and without 550 mM of Ca^{2+}. 200 µL was added to each well of a 96 well plate and the OD_{600} was measured every 30 minutes for 48 hrs.

Plaque and Plaquing efficiency assay

Parasites were filtered with a 5 µM Nucleopore membrane to remove host cell debris. 200 parasites from a clonal population were seeded on a confluent hTERT host cell monolayer in a 6 well plate and allowed to grow for 7 days at 37°C. The monolayer was then fixed with 70% ethanol and stained with crystal violet. Plaque sizes were

analyzed with ImageJ (Schneider *et al.*, 2012). Plaquing efficiency was assayed using 1000 parasites that were allowed to infect a confluent host cell monolayer for 30 min at 37°C before being washed twice with sterile PBS. Parasites were left to growth for 4 days and then fixed with 70% ethanol and stained with crystal violet. Number of plaques were counted using ImageJ.

Replication Assay

Replication assays were performed with parasites expressing RFP td-tomato. HFF cells were seeded on coverslips 24 hrs in advance in DMEM-HG + 15% fetal bovine serum. After 24 hrs, HFF cells were infected with 5 x 10^5 RFP expressing parasites and allowed to grow for another 24 hrs in DMEM-HG + 1% bovine calf serum. After 24 hrs, the media was aspirated, and the coverslip was placed on a glass slide with 10 µL of 1X phosphate buffered saline (PBS). 100 parasitophorous vacuoles (PVs), performed in duplicate per cell line, were quantified for each cell line.

T. gondii growth assay

Growth assays were done with parasites expressing RFP td-tomato. Parasites that were 70% egressed were filtered through a 5 µM Nucleopore membrane, and serially diluted in clear DMEM-HG media supplemented in 1% BCS. 4000 parasites were seeded in a confluent 96 well plate and fluorescence was measured every day for 6 days using a SpectraMax M2 plate reader (Molecular Devices) with 544/590 nm emission/excitation wavelengths.

Egress assay

Egress assays were done in 35 mm MatTek dishes. hTERT cells were seeded and allowed to grow for 24 hrs to reach about 75-90% confluency. 24 hrs later, 5 x 10^5

parasites were infected and allowed to grow for another 20-24 hrs. The media was then changed to consist of Ringer's buffer, also known as extracellular buffer (155 mM NaCl, 3 mM KCl, 1 mM $MgCl_2$, 3 mM NaH_2PO_4, 10 mM HEPES, 5 mM glucose. Buffer was adjusted to pH 7.3.) (Pace *et al.*, 2014) + 1.8 mM of Ca^{2+}. Dishes were placed on the microscope in a 37°C chamber. After one minute of recording, 0.01 % saponin was added and the video was recorded until all parasites in the field of view egressed.

Invasion assay

Invasion was assayed as previously described by Kafsack *et al* (Kafsack *et al.*, 2004). Briefly, HFF cells were prepared on coverslips 24 hrs in advance. The following day, freshly lysed parasites were collected from a T-25 flask, spun down at 1800 RPM and resuspended in 2 mL of freshly made invasion media (DMEM-HG supplemented with 3% FBS, 10 mM HEPES, pH at 7.4). 2 x 10^7 parasites were resuspended in a final volume of 2 mL and added to HFF cells incubated on ice for 20 min. The plate was placed at 37°C for 5 min and immediately placed back on ice. Slides were fixed with 3% paraformaldehyde and blocked in 10% FBS. For antibody incubation, slides were first placed in Rabbit anti-SAG1 at 1:1000, exposed to 1% triton X-100, and then incubated in Mouse anti-SAG 1:200. Secondary antibodies used were Alexa Fluor 488 Goat anti-Mouse and Alexa Fluor 546 Goat-anti Rabbit. Slides were also stained with DAPI. 100 parasites were analyzed for each slide (two slides per cell line).

Indicator incubation and fluorometric protocol

All experiments were carried out in the Hitachi F-7100 fluorescence spectrophotometer. A small magnetic spinner was placed in the cuvette to ensure that the parasites were evenly distributed the entire time. Reagents were added with a needle

at indicated times. To harvest parasites for fluorometry experiments, parasites from a fully lysed T-25 flask were used to infect 3-4 fully confluent hTERT T-75s. The media was changed 24 hrs later, and the following day parasites were collected when 70-80% egressed. The host cell monolayer was gently scraped off and parasites were gently resuspended in BAG. The suspension was pipetted up and down to break the host cell monolayer to gently release intracellular parasites and passed through an 8 µM Nucleopore membrane to remove host cell debris.

For FURA2 experiments, the following steps including, centrifugation, FURA2-AM loading and fluorometric measurements (including calibration) were all done using a previously published protocol to measure FURA2 fluorescence in extracellular tachyzoites (Pace *et al.*, 2014). Final parasite resuspension and all experiments were done in Ca^{2+} free Ringer's Buffer. All experiments were done in a Ca^{2+} free environment by adding 100 µM EGTA to chelate extracellular Ca^{2+}, unless otherwise mentioned. Fluorescence was detected by using 340/380 nm excitation wavelengths and a 510 nm emission wavelength.

For BCECF experiments, parasite harvest, centrifugation, BCECF loading and fluorescence experiments were done following the previously published protocol to measure cytosolic pH in extracellular tachyzoites (Stasic *et al.*, 2019). After parasite collection and centrifugation, 6 µM of BCECF-AM was added to parasites resuspension and incubated in a 30°C shaking water bath for 20 min. Parasites were resuspended in BAG for experiments and fluorescence measurements (including calibration) were done in Ca^{2+} free Standard buffer (135 mM NaCl, 5 mM KCl, 1 mM $MgSO_4$-H_2O, and 5 mM

Glucose) with 100 µM of EGTA unless otherwise indicated. BCECF fluorescence signal was detected with a 440/505 nm excitation wavelength and 530 nm emission wavelength.

For MagFluo4 experiments, purified parasites were centrifuged at 1800 rpm for 10 min. The pellet was washed in 10 mL of BAG and then centrifuged again at 1800 rpm for 10 min. Parasites were then washed in 1 mL of BAG and centrifuged at 5000 rpm for 2 min. The pellet was then resuspended in HBS buffer (135 mM NaCl, 5.9 mM KCl, 11.6 mM HEPES, 1.5 mM $CaCl_2$, 11.5 mM Dextrose, 1.2 mM $MgCl_2$, using 1 M NaOH to pH to a final pH 7.3) containing 20 µM MagFluo4-AM, 1 mg/mL bovine serum albumin, and 0.2 mg/mL Pluronic F127. Parasites with indicator were incubated for 20°C shaking for 1 hr as well as inverting tube every 10-15 min to avoid parasites from settling. After incubation, parasites were washed twice with Cytosol Like Media (CLM) (140 mM KCl, 20 mM NaCL, PIPES 20 mM, 1 mM EGTA, buffered with 10 M KOH to a final pH 7.0). The entire resuspension was then transferred to a cuvette in a final volume of 1.8 mL of CLM and placed in the fluorometer with a stir bar. MagFluo4 signal is detected with 485 nm emission wavelength and 520 nm emission wavelength. After 100 sec, 48.6 µM digitonin was added for 300 sec to allow for permeabilization. Permeabilized cells were centrifuged at 5000 rpm for 2 min twice and washed with CLM and then resuspended at a final concentration of 1 x 10^9 parasites/mL. 2 x 10^7 parasites were placed in a final volume of 1.95 CLM+Ca^{2+} (CLM + 375 µM Ca^{2+}) in a cuvette. All experiments were carried out in CLM + 375 µM Ca^{2+} unless otherwise indicated.

For LysoSensor experiments, parasites were collected between 80-90% out, filtered through an 8 µm Nucleopore membrane, washed in BAG and centrifuged at 1900 rpm for 5 min twice. Parasites were resuspended in a final concentration 1 x 10^8

parasites/mL in BAG. Parasites were separated in 1 mL quantities and mixed with 1 µM of LysoSensor Green DND-189 (Thermo-Fischer) for 1 hr at 30 °C. Afterwards, parasites were washed twice with BAG and centrifuged for 2 min at 5000 RPM each time and then resuspended to a final concentration of 1 x 10^8 parasites/mL in BAG for experiments. Experimenters were carried out using flow cytometry (see below).

ImageStream Flow Cytometry Analysis

Measurement of LysoSensor fluorescence was carried out in the ImageStream X MK II (Luminex Corporation, Seattle, Washington). 200 µL of parasites resuspended at concentration of 1 x 10^8 parasites/mL were used for analysis. Parasites were excited at 405 nm using channel 7 and the bright field using channel 1. 10,000 events were sampled for each run. We used the IDEAS software to gate and mask the intensity of fluorescent single parasites in focus. IDEAS used this data to calculate for the median fluorescence intensity for each run.

Co-immunoprecipitation protocol

Immunoprecipitation experiments were done with Thermo Scientific Anti-HA Magnetic beads (Cat # P188836). Freshly egressed parasites from 1 T75 were filtered with an 8 µm Nucleopore membrane, washed and spun down twice with BAG at 1800 rpm for 10 min. 2 x 10^8 parasites were collected for further analysis. Parasites were mixed gently with lysis buffer (50 mM Tris-HCl, 150 mM KCl, 1 mM EDTA, 0.4% NP-40, 1 tablet of complete protease inhibitor cocktail) for 30 min at 4°C. Parasites were then centrifuged at 15,000 x g for 20 min at 4°C and the supernatant was collected for incubation with the beads. Magnetic beads were prepped by rinsing 12.5 µL magnetic beads with 50 µL wash buffer (25mM Tris-HCl, 150 mM KCl, 1 mM EDTA, 0.1% NP-40) 3x. Beads were collected

using a DynaMag2 magnetic rack. Parasite supernatant was gently mixed with prepped magnetic beads for 1 hr at 4°C. After, the supernatant was separated from the beads (this is the flow through). At this point the bait protein should be attached to the beads. Beads were gently washed 3x with 100 µL of wash buffer for 5 min at 4°C. Beads were collected on the magnetic rack and incubated with 20 µL of 1x Laemmli buffer for 10 min at 65°C. After heating, beads were separated from the Laemmli buffer. The bait protein and it's interacting proteins will be in the buffer (this is the elution). Samples were stored at -20°C.

3.3 Results

CAXL1 is part of a novel family of Ca^{2+} antiporters

Phylogenetic analysis revealed that HsTMEM165 and ScGDT1 belong to a family of Ca^{2+} antiporters distinct from the canonical five, now named Unknown Protein Family (UPF) 0016. Members of the UPF0016 proteins not only lack homology with other CAX subfamily proteins, but also contain between 5-7 transmembrane domains and two canonical motifs, EXGD-K/R-T/S (Demaegd *et al.*, 2014). Through bioinformatic analyses we found that TgCAXL1 is also part of the UPF0016. TgCAXL1 contains six transmembrane domains according to the Protter prediction (Omasits *et al.*, 2014) and contains both of the canonical motifs (Fig 1. A+B). We generated a maximum likelihood tree to look at the relationship of TgCAXL1 with other orthologs and saw that there is a clear divergence between prokaryotic and eukaryotic orthologs (Fig. 1C). Additionally, the tree showed that coccidian apicomplexans cluster with one another indicating conservation of TgCAXL1 among coccidians. These data indicate that TgCAXL1 is part of UPF0016, apicomplexan CAXL1s are phylogenetically different than other eukaryotes and there is a common function and relationship amongst protozoans.

CAXL1 localizes to the endoplasmic reticulum and Golgi apparatus

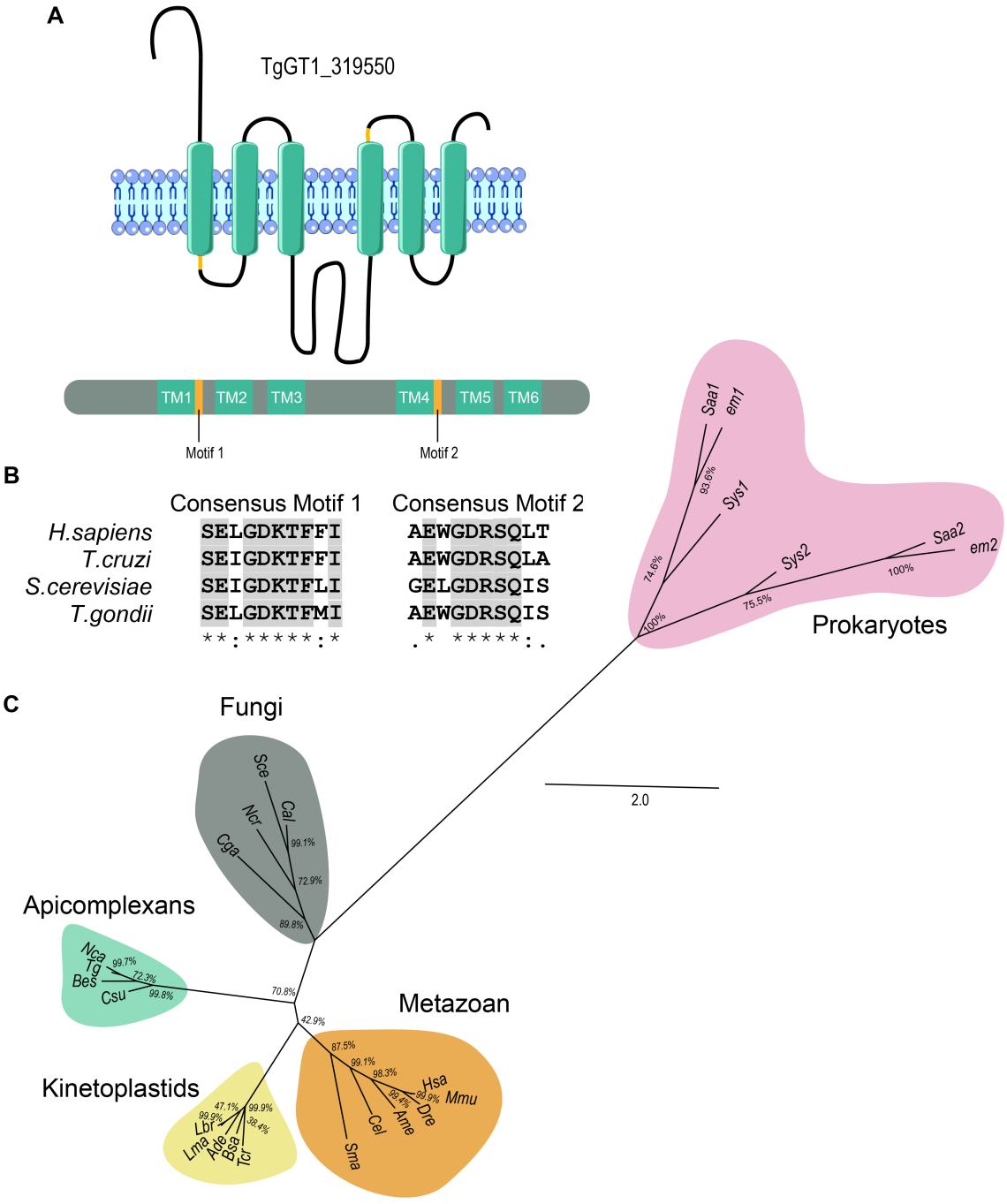

Figure 2.1 Curation of TgGT1_319550. A) Protter prediction and gene annotation of TgGT1_319550. TM= transmembrane domain. B) Multiple sequence alignment of conserved motifs in TgGT1_319550 orthologs using ClustalW multiple sequence alignment. Gray highlight indicates fully conserved amino acids. C) Phylogenetic analysis of UPF0016 family orthologs. Accession numbers and full length names for each organism is listed in Supplementary table 1. Scale indicates branch length as a number of substitutions per site.

Using a previously described strategy, we started by endogenously tagging the C-terminal end of TgCAXL1 with a 3-copy hemagglutinin tag (3xHA) using a CRISPR/Cas9 (Shen *et al.*, 2014; Sidik *et al.*, 2014) approach in the RH-TATiΔKu80 (TATiΔKu80) background to favor homologous recombination. Clonal cell lines were initially screened by PCR, western blotting and immunofluorescence analysis. However, detection was not ideal as shown through a weak signal in the western blot and inconclusive localization (data not shown). Identification of integral membrane proteins has been known to be difficult due to their low expression levels, therefore we decided to use a previously described strategy and endogenously tagged the C-terminal end with a 10-copy hemagglutinin tag (smHA) instead (Hortua Triana, Marquez-Nogueras, Chang*, et al.*, 2018) (Fig. 2A). Clonal cell lines of TgCAXL1-smHA were first analyzed via PCR and western blotting. To further overcome difficulty in detection of TgCAXL1, we enriched for TgCAXL1-smHA by performing an integral membrane protein extraction. This protocol consisted of a freeze/thaw method for parasite lysis and a refrigerated high centrifugation for isolation of membrane specific proteins in the pellet. Membrane protein extract (pellet) and non-membrane proteins extract (supernatant) of TgCAXL1-smHA clone and negative control, TATiΔKu80, were analyzed with HA antibodies. Western blot analysis revealed a desired band at the expected size, around 76 kDa, in the TgCAXL1-smHA pellet and not in the negative control indicating that the gene of interest was correctly tagged. Some signal is detected in the supernatant that could have been contamination from the pellet. Several bands at smaller sizes were detected in the pellet suggesting potential protein degradation (Fig. 2B).

To determine localization of TgCAXL1, we performed intracellular and extracellular immunofluorescence analysis of TgCAXL1-smHA with HA antibody. Due to previous studies demonstrating that TgCAXL1 orthologs localize to the Golgi apparatus, we first colocalized TgCAXL1-smHA with the *T. gondii* Golgi apparatus transient marker, GRASP55 and saw colocalization between intracellular TgCAXL1 and GRASP55 (Fig.

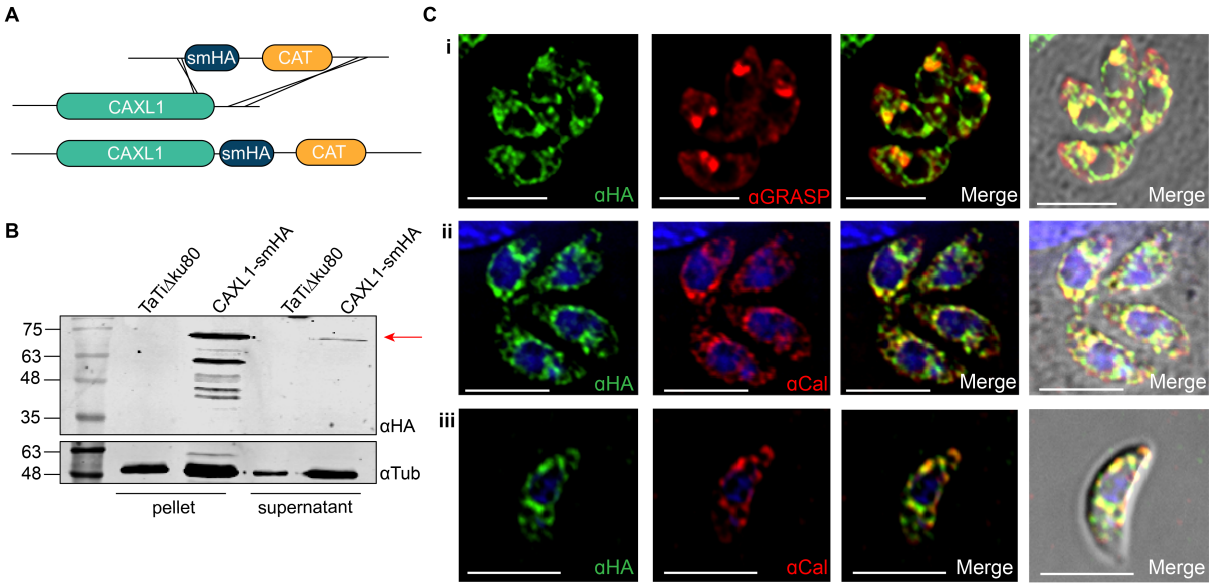

Figure 2.2 TgCAXL1 localizes to the Golgi apparatus and the endoplasmic reticulum. A) Schematic of endogenous tagging of 3'-terminus of TgCAXL1 with spaghetti monster hemagglutinin tag (smHA). B) Western blot of lysate following integral protein enrichment with anti-HA antibody (αHA) and anti-tubulin (αTub) as a loading control. Pellet contains insoluble protein and supernatant contains soluble protein. Arrow indicates expected band size. C) Intracellular immunofluorescence assays (IFAs) showing colocalization between CAXL1-SMHA and the Golgi marker GRASP55 (i) and intracellular (ii) and extracellular (iii) IFAs showing co-localization ER marker calumenin (αCal). Bar is 5 μm.

2Ci). We noticed additional signal surrounding the nucleus and hypothesized potential ER localization. To validate this, we also colocalized TgCAXL1-smHA with the ER marker ER resident Ca^{2+} binding protein, calumenin (αCal), and saw co-localization (Fig. 2Cii, iii). Ultimately, we successfully tagged TgCAXL1 with an endogenous epitope tag and determined localization to the Golgi apparatus and the ER.

Generation of CAXL1 knockout mutant

To investigate the biological significance of TgCAXL1 in the parasites, we began by generating TgCAXL1 knockout mutants (Sup. Fig. 1A, B). TgCAXL1 is predicted to be dispensable in the CRIPSR phenotypic score (Sidik, Huet*, et al.*, 2016) so we decided to create a clean deletion knockout in RH type I parasites (wildtype) using a CRISPR/Cas9 approach. A DHFR drug cassette was constructed and flanked with 1 kb homology arms corresponding to the 5' and 3' UTR of CAXL1 (Fig. 3A). Additionally, two sgRNAs were designed, one specific to the 5' end and one specific to the 3' end to increase the chances of generating a clean deletion. Both sgRNAs were transfected simultaneously with the drug cassette and drug resistant clones were selected. Relative expression of TgCAXL1 was measured in one of the clones (Fig. 3G). The data showed almost no transcription of TgCAXL1 compared to that of wildtype RH, indicating that we had successfully constructed a TgCAXL1 knockout mutant (*ΔCAXL1*) (Fig. 3G). To complement TgCAXL1 expression in *ΔCAXL1*, we transfected *ΔCAXL1* by randomly integrating TgCAXL1 cDNA fused with 3xHA at the C-terminal end and used chloramphenicol to select for resistant parasites (Supp. Fig. 1C). We selected for a clonal population and validated the complement *(ΔCAXL1-comp*) with western blotting using an HA antibody as well as with qRT-PCR where we saw restoration of TgCAXL1 transcripts (Fig. 3D+G). To conclude, we successfully generated both *ΔCAXL1* and *ΔCAXL1-comp* cell lines for further biochemical and cellular characterization of TgCAXL1.

CAXL1 is important for invasion

To assess the significance of TgCAXL1 for the tachyzoite lytic cycle, we began by performing plaque assays. Plaque assays consisted of allowing parasites to grow on a confluent host cell monolayer for 7 days, and then quantifying the sizes of the zone of

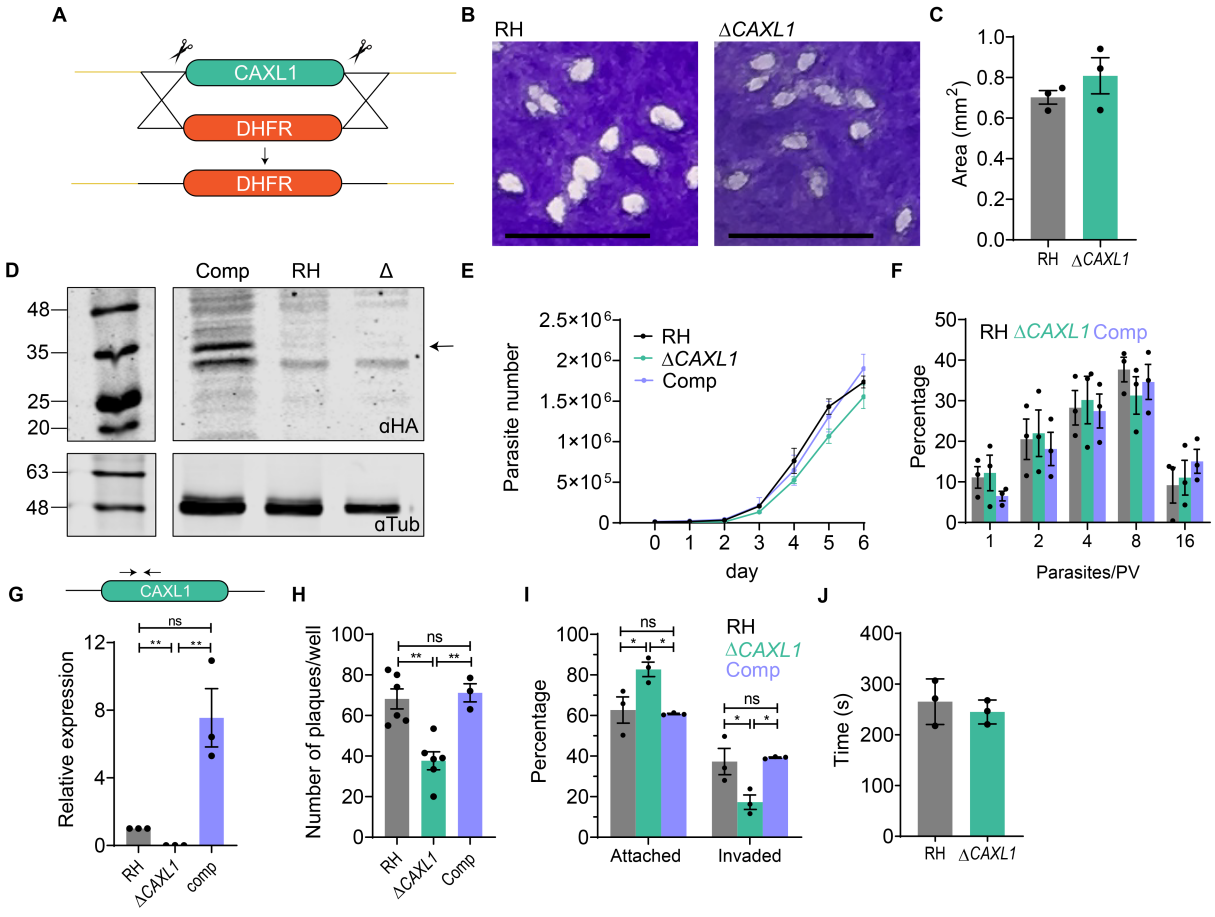

Figure 2.3 Parasite invasion of the host cell is impacted by the absence TgCAXL1. A) Schematic of repair template used to create KO in RH wildtype strain. B) Plaque assays of RH and Δ*CAXL1* after 7 days. Scale bar = 5 mm. C) Quantification of average plaque areas from D. D) Western blot of Δ*CAXL1-comp*-3xHA (comp), RH, and Δ*CAXL1* (Δ) lysates with anti-HA (αHA) antibody and anti-tubulin (αTub) as loading controls. Expected band location of CAXL1-3xHA is denoted with an arrow. E) RH, Δ*CAXL1*, and Δ*CAXL1-comp* td-tomato expressing clones were used for plate reader growth assays. Fluorescence was measured every day for 6 days and normalized to parasite number. F) Replication of RH, Δ*CAXL1*, and Δ*CAXL1-comp* td-tomato expressing clones after 24 hrs of infecting HFFs. At least 100 PVs were quantified. G) Quantification of gene expression by method of real time PCR. Expression values are from three independent biological replicates done in triplicate. Arrows indicate location of primers in TgCAXL1 used for RT-PCR. H) Number of plaques formed from plaquing efficiency assay. I) Percentage of parasites invaded and attached from red-green assay. At least 100 parasites were analyzed for each cell line. J) Time in seconds (s) it takes for parasites to egress from host cells after addition of 0.01% saponin at 1 min in Ringer's buffer media containing 1.8 mM of Ca^{2+}. C, E, F, G, H, I and J mean values ± SEM are from three independent biological replicates. E and G were done in triplicates and F, H, I and J were done in duplicates. C, G, H and I were all analyzed using one-way ANOVA. E was analyzed using Student t-test. * = p< 0.5, ** = p<0.01.

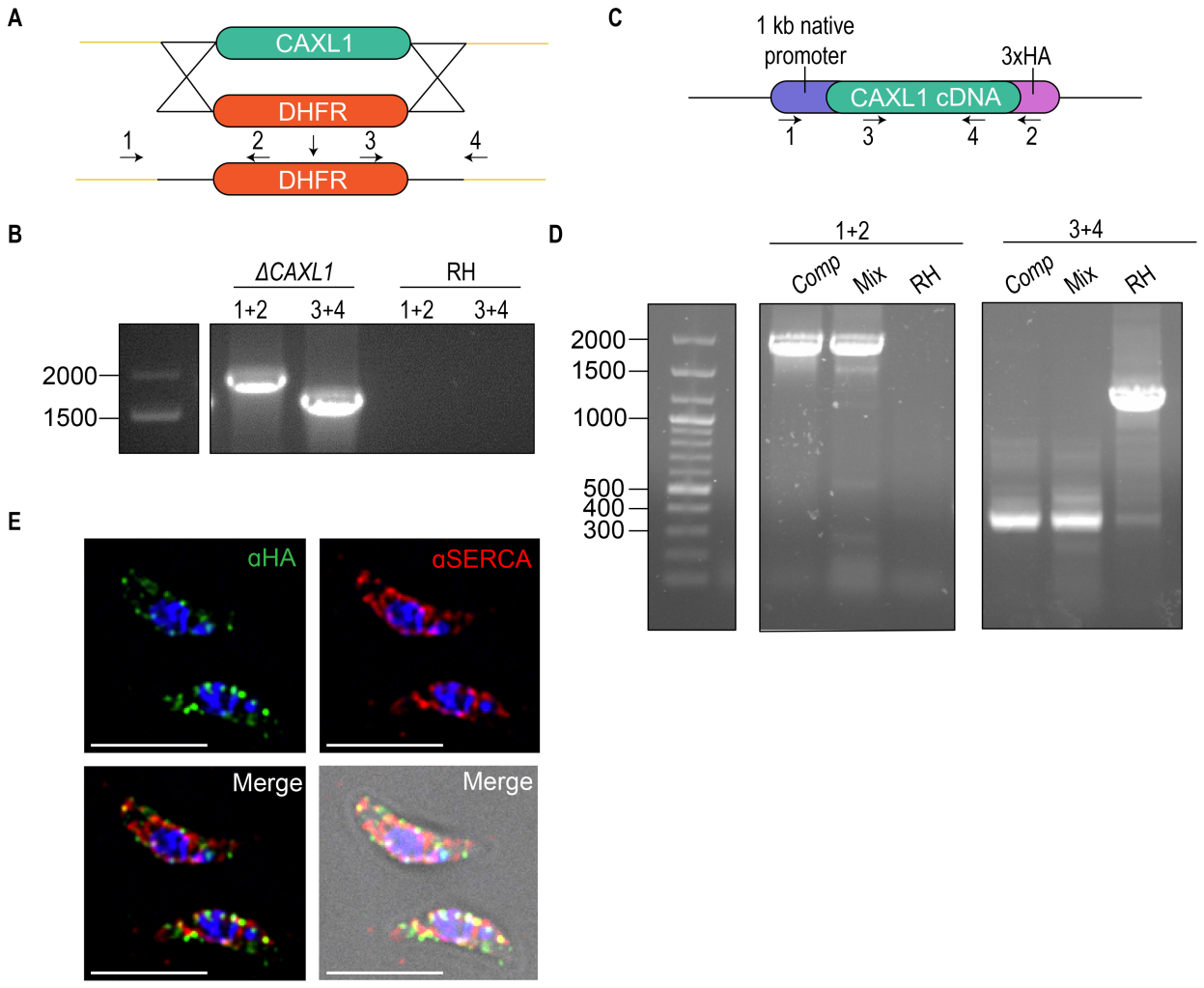

Supplemental Figure 2.1 Validation of *ΔCAXL1* and *ΔCAXL1-comp*. A) Schematic of generation of knockout of TgCAXL1 in RH Type I parasites. Numbers indicate primers used in PCR validation in B. B) Genomic validation of *ΔCAXL1* using primer pair 1+2 and 3+4 as shown in A. Expected size of primer pair 1+2 in *ΔCAXL1* is 1.9 kb and of primer pair 3+4 in *ΔCAXL1* is 1.6 kb. C) Schematic of plasmid used to generate *ΔCAXL1-comp* in *ΔCAXL1* parasites. Numbers indicate primers used in PCR validation in D). D) Genomic validation of *ΔCAXL1-comp* (denoted as *Comp*) using primer pair 1+2 and 3+4 as shown in C. Mix is mixed population used as a control. Expected size of primer pair 1+2 in *ΔCAXL1-comp* is 2 kb. Expected size of primer pair 3+4 in *ΔCAXL1-comp* is 441 bp and in RH wildtype parasites is 1.3 kb. E) Extracellular immunofluorescence assay showing co-localization between *ΔCAXL1-comp* and ER marker SERCA.

clearance or plaques in the host cell monolayer created by the parasites. Plaque sizes between *ΔCAXL1* and RH showed no significant difference (Fig. 3B+C), which is expected due to the dispensable CRISPR score of TgCAXL1. These data were supported

by the kinetic analysis of *ΔCAXL1* growth. *ΔCAXL1* and RH were transfected with the red fluorescent protein, tdTomato (RFP) and enriched for tdTomato expressing parasites using fluorescence activated flow cytometry sorting and then isolated clonal populations. *ΔCAXL1-RFP* and RH-RFP growth were analyzed via fluorescence for 6 days in a 96-well plate format in a plate reader. Fluorescence values of *ΔCAXL1-RFP* and RH-RFP showed no difference in the growth rate between *ΔCAXL1-RFP* and RH-RFP (Fig. 3E). While overall growth did not appear to be affected, we investigated the potential effects of *ΔCAXL1* for specific steps of the lytic cycle and observed that TgCAXL1 was not important for replication or egress (Fig. 3F+J). Next, we investigated the role of TgCAXL1 in the invasion step of the lytic cycle. Plaquing efficiency assays were done by growing confluent host cell monolayers and infecting them with 1000 parasites for 30 minutes (Fig. 3H). Parasites were washed off and allowed to grow for four days. Host cell monolayers were fixed and stained. We quantified the number of plaques providing an indication of the number of parasites that were able to attach and invade to the host cells. The number of plaques formed by *ΔCAXL1* were significantly less than those made by RH, indicating that *ΔCAXL1* may have a defect in attachment and invasion. To further support the invasion and/or attachment phenotype, we performed red-green assays where differential staining is used to distinguish attached parasites from invaded parasites (Fig. 3I). Our data showed that approximately 50% less of *ΔCAXL1* parasites were capable of invading the host cell monolayer and attached to the monolayer instead, as compared to the wildtype strain. Invasion was restored by complementation. While the defect doesn't completely abolish the ability for the parasite to invade, it does suggest that TgCAXL1 is important for invasion of the host cell monolayer.

Yeast complementation studies

It has been previously shown that the absence of the yeast ortholog, GDT1, does not confer any yeast growth defects under homeostatic growth conditions (Demaegd *et al.*, 2013). However, under high Ca^{2+} concentrations (550 mM), GDT1Δ mutants grow at a slower rate. This suggests that GDT1 is important for regulating Ca^{2+} homeostasis after extreme Ca^{2+} conditions. To study the function of TgCAXL1, yeast complementation experiments with TgCAXL1 were performed. The full-length TgCAXL1 was fused to the first 69 bps of the GDT1 reading frame, which consists of the ScGDT1 signal peptide for translocation to Golgi bodies. This construct was placed into a plasmid containing the URA3 metabolic marker (URA) that allows for growth on plates lacking uracil (Fig. 4A). We successfully obtained GDT1Δ + TgCAXL1 transformants on this selective media.

Plate growth assays supported previous data demonstrating no growth defect of GDT1Δ (GDT1Δ + empty vector (EV)) (Demaegd *et al.*, 2013) under homeostatic conditions (CSM-ura). However, once a high concentration of Ca^{2+} was added, in this case 550 mM Ca^{2+} (CSM-ura + 550mM Ca^{2+}), growth of GDT1Δ + EV was partially inhibited. Expression of the ScGDT1 restored growth under high Ca^{2+} concentrations, and even more, we discovered that, GDT1Δ inhibition was rescued by the expression of *TgCAXL1* gene (Fig. 4B). Liquid growth assays further supported this finding where over 48 hrs, GDT1Δ growth was not affected in CSM-ura liquid media, but when cultivated in high Ca^{2+} concentrations (550 mM), a clear growth defect was observed (Fig. 4C). The

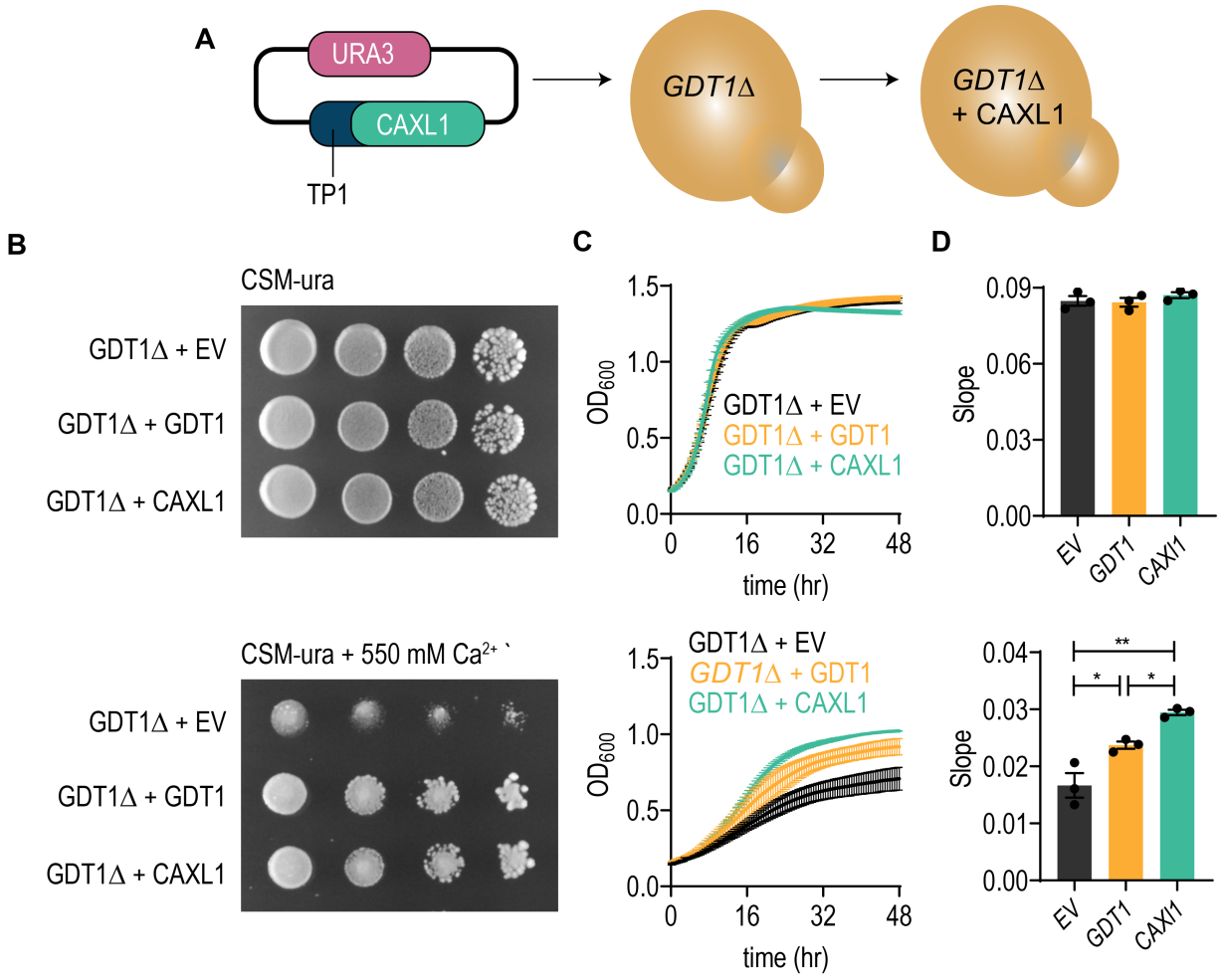

Figure 2.4 TgCAXL1 aids in tolerating a high calcium environment in yeast. A) Schematic of CAXL1 complementation in GDT1Δ. B) Plate growth assay of GDT1Δ complemented with the empty vector (EV), GDT1 and CAXL1. All strains were grown overnight and diluted to a final OD of 1 and serially diluted at 1:10, 1:100 and 1:1000 dilution. 10 µL of each dilution was plated on synthetic defined medium without uracil (SD-ura) supplemented with and without 550 mM Ca^{2+}. C) Liquid growth assay in SD-ura medium with (bottom graph) and without (top graph) 550 mM Ca^{2+}. All strains were precultured to an OD600 of 0.1. Graph represents three independent biological replicates done in triplicate. Error bars represent mean ± SEM. D) Slope of exponentially growth phases for all strains (4-16 h in media without Ca^{2+} and 8-32 h in media with Ca^{2+}) from C. Values indicate mean ± SEM and analyzed using one-way ANOVA. *= p< 0.5, ** = p<0.01.

decrease in the growth rate during the exponential growth phase was complemented by ScGDT1 and TgCAXL1 (Fig. 4D). These results indicate TgCAXL1 can complement growth and functions in tolerating high Ca^{2+} concentrations in yeast.

∆*CAXL1* impacts release of Ca^{2+} from intracellular stores

To study the role of TgCAXL1 on intracellular Ca^{2+} signaling, we loaded parasites with the Ca^{2+} indicator FURA2. We began by testing whether TgCAXL1 functions Ca^{2+} influx. In ∆*CAXL1* , the basal level of Ca^{2+} was around 60 nM and no different than wildtype and previously published known basal levels (Pace *et al.*, 2014) (Fig. 5D). Addition of 1.8 mM extracellular Ca^{2+} did not show a difference in the amount of Ca^{2+} entry into the cytosol between ∆*CAXL1* and wildtype (Fig. 5D). TgCAXL's localization in the ER led us to assess the effect of TgCAXL1 on ER Ca^{2+} signaling. We used thapsigargin, an inhibitor of SERCA that blocks Ca^{2+} uptake into the ER (S. Brogger Christensen, 1982), causing leakage from the ER into the cytosol (Pace *et al.*, 2014; Sidik, Hortua Triana*, et al.*, 2016). We observed that after blocking SERCA with thapsigargin the leakage was significantly reduced in ∆*CAXL1* (Fig. H+I). Ca^{2+} influx at the plasma membrane is stimulated by Ca^{2+} in a Ca^{2+}-activated Ca^{2+} entry (CACE) mechanism (Pace *et al.*, 2014). Addition of extracellular Ca^{2+} after addition of thapsigargin, elevates cytosolic calcium, resulting in a higher extent of Ca^{2+} influx (Marquez-Nogueras *et al.*, 2021; Pace *et al.*, 2014). This process was also monitored in this work. After addition of thapsigargin, 1.8 mM of Ca^{2+} was added at 400 sec (Fig. 5H). Due to a smaller elevation in cytosolic Ca^{2+} induced by thapsigargin in the mutants, CACE was affected by ~50% (Fig. 5I). To further test Ca^{2+} release from the ER, we exposed the parasites to the phosphodiesterase inhibitor, zaprinast, a Ca^{2+} agonist that can be used to deplete Ca^{2+} from intracellular stores (Howard *et al.*, 2015; Lourido *et al.*, 2012). Zaprinast targets a PDE that is responsible for activating protein kinase G, leading to an increase in cyclic guanosine monophosphate, which ultimately causes an increase in cytosolic Ca^{2+}. This dramatic

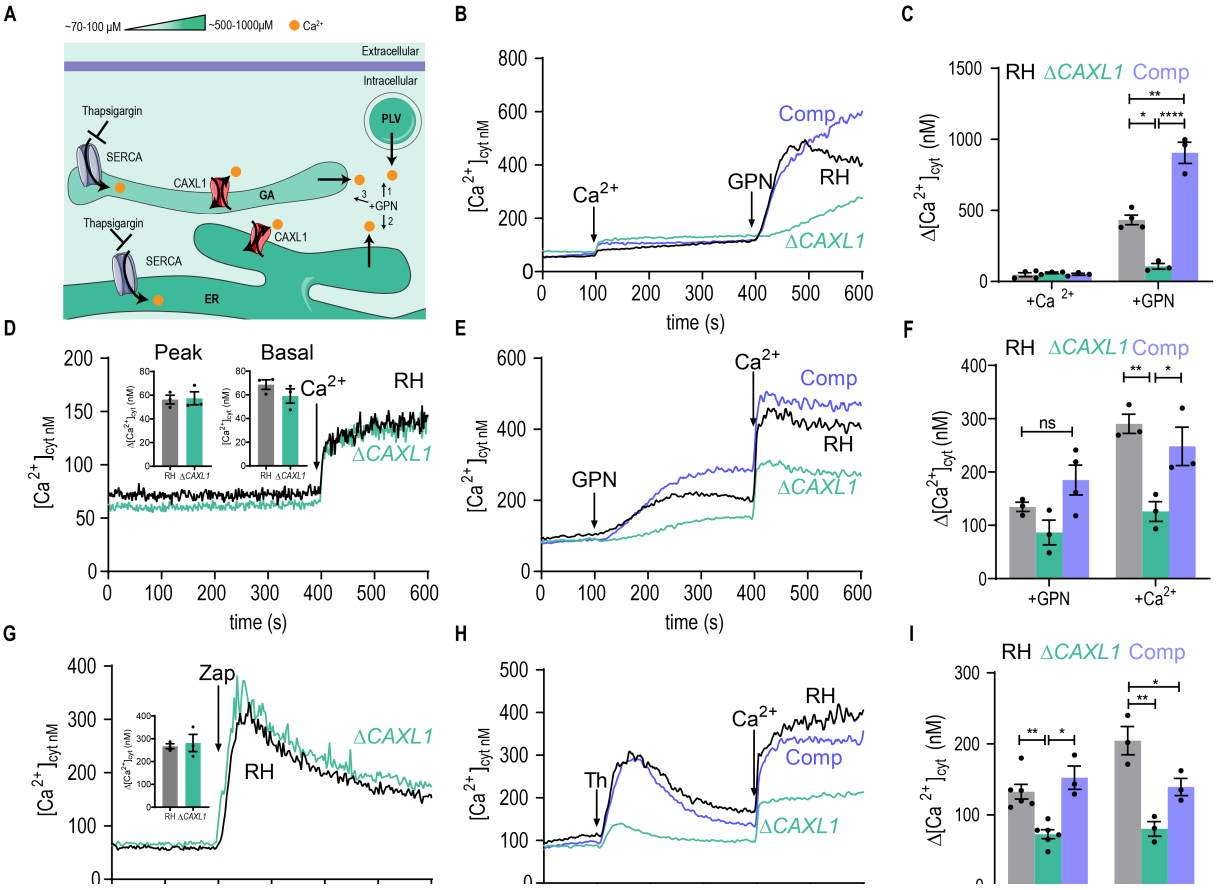

Figure 2.5 CAXL1 affects release of Ca^{2+} from intracellular stores and Ca^{2+}-activated Ca^{2+} entry. A) Model establishing Ca^{2+} transport into the ER and Golgi after addition of thapsigargin and GPN. B) Intracellular levels of calcium in RH, Δ*CAXL1* and Δ*CAXL1-comp* cell lines loaded with FURA2-AM. Experiments were done in Ringer's buffer with 100 µM EGTA. 1.8mM of Ca^{2+} was added at 100 sec, followed by GPN at 400 sec. C) Quantification of difference in cytosolic Ca^{2+} after addition of Ca^{2+} or GPN. Differences were calculated by measuring the difference between peak Ca^{2+} and the average Ca^{2+} 20 sec prior to addition of Ca^{2+} or GPN. D) Intracellular levels of Ca^{2+} after addition of 1.8 mM Ca^{2+} at 400 sec. Inset graphs represent the basal level of cytosolic Ca^{2+} and the peak Ca^{2+} after addition of 1.8 mM of Ca^{2+}. E) Intracellular levels of Ca^{2+} in all cell lines after addition of GPN at 100 s followed by 1.8 mM Ca^{2+} at 400 sec. F) Quantification of difference in cytosolic Ca^{2+} after addition of Ca^{2+} or GPN. Differences were calculated by measuring the difference between peak Ca^{2+} and the average Ca^{2+} 20 sec prior to addition of Ca^{2+} or GPN. G) Response to 100 µM zaprinast at 100 sec in RH and Δ*CAXL1*. Inset graphs represent peak Ca^{2+} after addition of zaprinast. H) Cytosolic Ca^{2+} leakage after the addition of 1 µM thapsigargin at 100 sec followed by 1.8 mM Ca^{2+} at 400 sec. I) Quantification of difference in cytosolic Ca^{2+} after addition of Ca^{2+} or thapsigargin. Δ[Ca^{2+}] was calculated by measuring the difference between peak Ca^{2+} and the average Ca^{2+} 20 sec prior to addition of Ca^{2+} or thapsigargin. Three independent biological replicates were done for all experiments, and each experiment was done in duplicate. For quantification of ΔCa^{2+}, mean values ± SEM were analyzed using one-way ANOVA.* = p< 0.5, ** = p<0.01, *** = p<0.005, **** = p<0.001.

increase in cytosolic Ca^{2+} can stimulate egress as well. The exact stores which zaprinast targets is unclear, but it is hypothesized that it releases Ca^{2+} from neutral stores, potentially the ER (Sidik, Hortua Triana*, et al.*, 2016). We observed no difference between Δ*CAXL1* and wildtype in the amount of Ca^{2+} released after addition of zaprinast, suggesting that TgCAXL1 does not affect the PKG signaling pathway and specifically affects calcium leakage from the ER after exposure to thapsigargin (Fig. 5G).

It was reported that downregulation of the human TMEM165 affected lysosomal pH, thus we wanted to validate whether TgCAXL1 affected storage of Ca^{2+} in acidic stores. We have previously shown that glycyl-L-phenylalanine-2-naphthylamide (GPN) can lead to Ca^{2+} release from acidic stores in *T. gondii* (Miranda *et al.*, 2010; Sidik, Hortua Triana*, et al.*, 2016). To test whether TgCAXL1 is involved in Ca^{2+} release from GPN targeted stores, the stores were filled by addition of Ca^{2+} at 100 sec, and then at 300 sec, GPN was added (Fig. 5B). Ca^{2+} release into the cytosol occurred in both the wildtype and in Δ*CAXL1*, however in Δ*CAXL1* a significantly lesser amount of Ca^{2+} was released (Fig. 5C). Either the Δ*CAXL1* mutant is not able to uptake Ca^{2+} into the stores, or GPN targeted release is affected in Δ*CAXL1*. To further investigate this, we tested whether we would see the same defect in parasites with resting levels of Ca^{2+} and 100 µM EGTA in the buffer. Under these conditions, there was no difference in the amount of GPN-induced Ca^{2+} release (Fig. 5E+F), suggesting that Ca^{2+} uptake into these organelles is not affected. CACE was also monitored under the conditions, and we observed that it is impacted in Δ*CAXL1* mutants. These data not only support that TgCAXL1 modulates CACE but also affects Ca^{2+} release from the ER and the acidic stores, potentially through the Golgi apparatus.

Absence of TgCAXL1 disrupts TgSERCA Ca^{2+} pumping

In yeast, a relationship has been inferred between the Golgi secretory pathway Ca^{2+}/Mn^{2+} ATPase, Pmr1, and GDT1 (Colinet *et al.*, 2016; Demaegd *et al.*, 2013). Single deletion mutants of each one are not lethal to the cell under high Ca^{2+} concentrations, but double deletion mutants lead to a phenotype in Ca^{2+} homeostasis and Ca^{2+} signaling (Demaegd *et al.*, 2013). We decided to study the interaction between TgSERCA and TgCAXL1 using the ER Ca^{2+} indicator MagFluo4. Cells loaded with the permeable form of MagFluo4-AM were permeabilized, resulting in MagFluo4 fluorescence from organelles that incorporated and trapped the indicator through cleavage of the AM group (Fig. 6A+B). To measure TgSERCA Ca^{2+} uptake, we activated SERCA with it's subrate, MgATP, that corresponded with an increase in fluorescence at 100 sec. After uptake plateaus, thapsigargin, the SERCA inhibitor was added, and a decrease in fluorescence occurred due to the blockage in Ca^{2+} uptake and leakage from the ER (Fig. 6A+B). Comparison of SERCA activity in RH, ∆*CAXL1* and ∆*CAXL1-comp* in buffer containing 211 nM Ca^{2+} demonstrated a reduced rate of Ca^{2+} uptake in ∆*CAXL1* (Fig. 6B). The absence of TgCAXL1 significantly decreased SERCA Ca^{2+} uptake activity at various Ca^{2+} concentrations (Fig. 6C), except at 50 nM Ca^{2+}. The rate of Ca^{2+} leakage at various concentrations was not affected after addition of thapsigargin (Fig. 6D), suggesing that TgCAXL1 affects Ca^{2+} uptake into the ER. These phenotypes were recovered in the ∆*CAXL1-comp*. The Ca^{2+} ionophore, ionomycin, removes Ca^{2+} across neutral stores, including the ER, into the cytosol. Exposure to ionomycin evoked a decrease in fluorescence in parasites with Ca^{2+} filled stores, indicating ionomycin can deplete the ER and transport Ca^{2+} across its membrane (Fig. 6E-G). No difference in the Ca^{2+} content

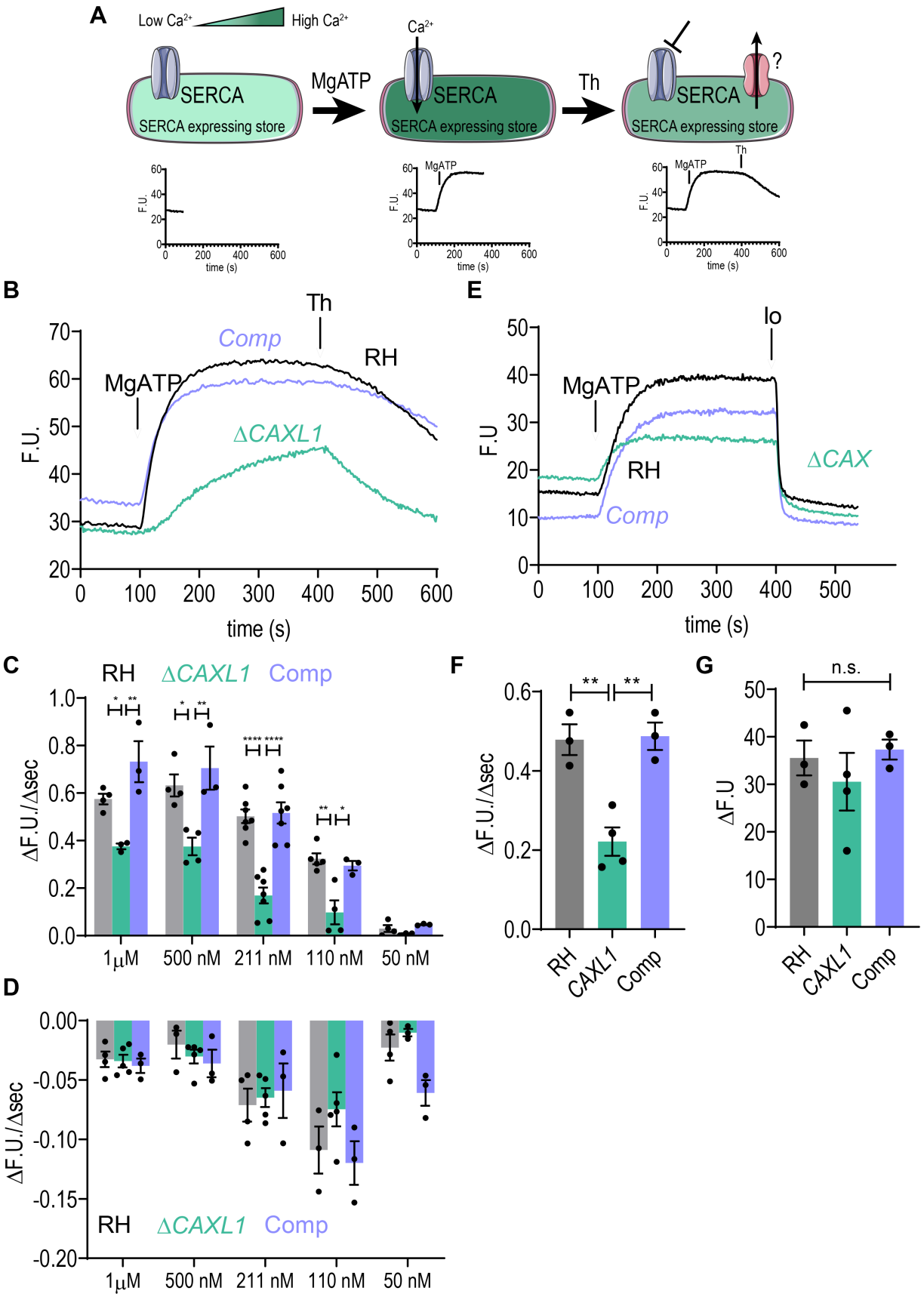
A
Low Ca2+
High Ca2+
SERCA
SERCA expressing store
MgATP
Ca2+
Th
?
F.U.
time (s)
B
Th
Comp
RH
MgATP
ΔCAXL1
F.U.
time (s)
E
Io
MgATP
RH
Comp
ΔCAX
F.U
time (s)
C
RH
ΔCAXL1
Comp
ΔF.U./Δsec
1μM
500 nM
211 nM
110 nM
50 nM
D
ΔF.U./Δsec
RH
ΔCAXL1
Comp
F
ΔF.U./Δsec
RH
CAXL1
Comp
G
n.s.
ΔF.U
RH
CAXL1
Comp

Figure 2.6 TgCAXL1 is important for Ca^{2+} pumping by SERCA. A) Model of MagFluo4 fluorometric assays in permeabilized parasites. B) Representative tracings of the fluorescence from MagFluo4 loaded cells. Parasites were resuspended in CLM buffer + 211 nM Ca^{2+} unbound. 250 µM MgATP was added at 100 sec and 1.5 µM thapsigargin at 400 sec. C) Quantification of the slope after addition of MgATP at different calcium concentrations in the CLM buffer. The slope was calculated between 100 and 140 sec. D) Quantification of the slope after addition of 1.5 µM Thapsigargin at different calcium concentrations in the CLM buffer. The slope was calculated between 400-600 sec. E) Representative tracing of the fluorescence from Mag-Fluo loaded cells after addition of 250 µM MgATP at 100 sec and 1 µM ionomycin at 400 sec in CLM buffer + 211 Ca^{2+}. F) Quantification of the slope after addition of MgATP. The slope was calculated from 100-140 sec. G) Quantification of the change in fluorescence after addition of 1 µM ionomycin. Th= Thapsigargin. Values from C, D, F and G indicate mean ± SEM and analyzed using one-way ANOVA. *= p< 0.5, ** = p<0.01, ***= p<0.01, ****=p,0.0001.

release in response to ionomycin was observed between the wildtype strain and Δ*CAXL1* mutants. These results show that TgCAXL1 mediates SERCA uptake Ca^{2+} activity and does not affect Ca^{2+} release from the ER.

TgCAXL1 affects recovery after pH stress

SERCA Ca^{2+} pumping into the ER is counterbalanced with transport of potassium, sodium or protons out of the ER to maintain a neutral electrochemical gradient at the ER membrane (Espinoza-Fonseca, 2017). Proton regulation at the ER membrane may impact SERCA activity as it is negatively impacted by alkaline pH (Li *et al.*, 2012). At neutral pH 7, the SERCA Ca^{2+} uptake of RH parasites occurs at a rate of 0.4 fluorescence units/sec (F.U./sec). Interestingly, when the pH of the environement is alkaline (pH 7.5), the rate of SERCA Ca^{2+} uptake diminshes to approximately, 0.1 F.U./sec, a 75% decrease in activity. Furthermore, activity is almost undectable under pH 8 conditions. Under acidic environements (pH6.5), SERCA Ca^{2+} uptake rates were the same as physiological conditions (pH 7). SERCA activity did not differ in Δ*CAXL1* mutants from RH parasites under an alkaline environment. However, at a neutral and acidic pH, it was significantly lower than RH parasites. These data established for the first time, the role that pH plays in the function of TgSERCA.

It has been previously shown that TgCAXL1 orthologs in yeast and in humans regulate pH homeostasis (Colinet *et al.*, 2016; Demaegd *et al.*, 2013). Downregulation of TMEM165, the human TgCAXL1 orthologue, in HeLa cells lead to a more acidic lysosome. If the cell is unable to transport protons out of the Golgi apparatus, then it might lead to an increased accumulation of protons in endosomal and lysosomal organelles. In yeast, Ca^{2+} entry increased at higher pH due to proton extrusion being more energetically favorable (Colinet *et al.*, 2016). To investigate the role of TgCAXL1 in pH regulation, we used the pH chemical indicator BCECF. Intracellular pH of the parasite is strictly controlled (Stasic *et al.*, 2019) through transport of H^+ across different membranes. The intracellulr pH under homeostatic conditions did not different between RH and the Δ*CAXL1* mutant cell line (Fig. 7A). We exposed parasites to acidic stress using propionic acid, a weak acid (Fig. 7A). After acidication of the cytosol, RH parasites were able to recover back to a neutral pH (Fig. 7B) due to various H^+ pumps, such as the V-H^+ ATPase and the V-H^+ pyrophosphatase. Δ*CAXL1* mutants displayed a significantly slower rate of recovery between 110 and 200 sec, where there was a 50% reduction in the rate of recovery (Fig. 7C+D), however they were ultimately able to reach a neutral pH. After the addition of propionic acid, we added Ca^{2+} to the parasites, and we observed a drop in pH, suggesting that the addition of calcium leads to an increase in the amount of protons in the cytosol, most likely from acidic stores. This phenomena has been previously observed, but the exact mechanism as to how Ca^{2+} can cause cytosolic acidification remains unclear (Huynh & Carruthers, 2022; Roiko *et al.*, 2014; Zhong, 1996). There was no difference in the extent of acidification between Δ*CAXL1* and WT after addition of extracellular Ca^{2+}. After assessing the role of

TgCAXL1 in acidic stress recovery, we also wanted to investigate the ability of TgCAXL1 to mediate cytosolic alkalinization. First, we exposed the parasites to GPN, a substrate of Cathepsin C, that perturbs the lysosome by causing osmotic stress and leads to an increase in pH in the lysosomes and in the cytosol (Atakpa *et al.*, 2019). No change in alkalinization of the cytosol was detected between WT and Δ*CAXL1* (Supp. Fig. 2A-C, D-F). An acidic pH in the lysosomal lumen is essential for proper function of lysosomal proteins, and dissipation of this pH gradient can disrupt their activity. We dissipated the lysosomal pH membrane using NH_4Cl, a weak base. An increase in cytosolic pH was also observed and was not different than that of Δ*CAXL1*. To determine whether TgCAXL1 regulated pH in the acidic stores, or PLV, we used the acidotropic pH indicator, LysoSensor, where a decrease in fluorescence is synonymous with an increase in proton levels and an increase in fluorescence indicates a decrease in proton levels within lysosomes or lysosomal-like organelles. LysoSensor incubated parasites were analyzed with microscopy flow cytometry (ImageStream) and we were able to predict the pH of acidic organelles in *T. gondii* (Supp. Fig. 2 G + H). Under a neutral pH, there appears to be no difference in pH levels of the acidic organelles (Supp. Fig. 2I). Addition of GPN, caused a decrease in fluorescence, indicating that GPN alkalinizes the acidic organelles, an expected result, however there was no difference between RH and Δ*CAXL1*. Bafilomycin A (Baf A), a Vacuolar H^+-ATPase inhibitor, inhibits recovery after acidic stress and most likely will lead to inhibition of acidification of the PLV. Baf A did not alter the pH levels of acidic compartments in RH (Supp. Fig. 2I). However, there was a detectable difference in the pH of acidic stores between Δ*CAXL1* treated and not treated with Baf A, indicating that

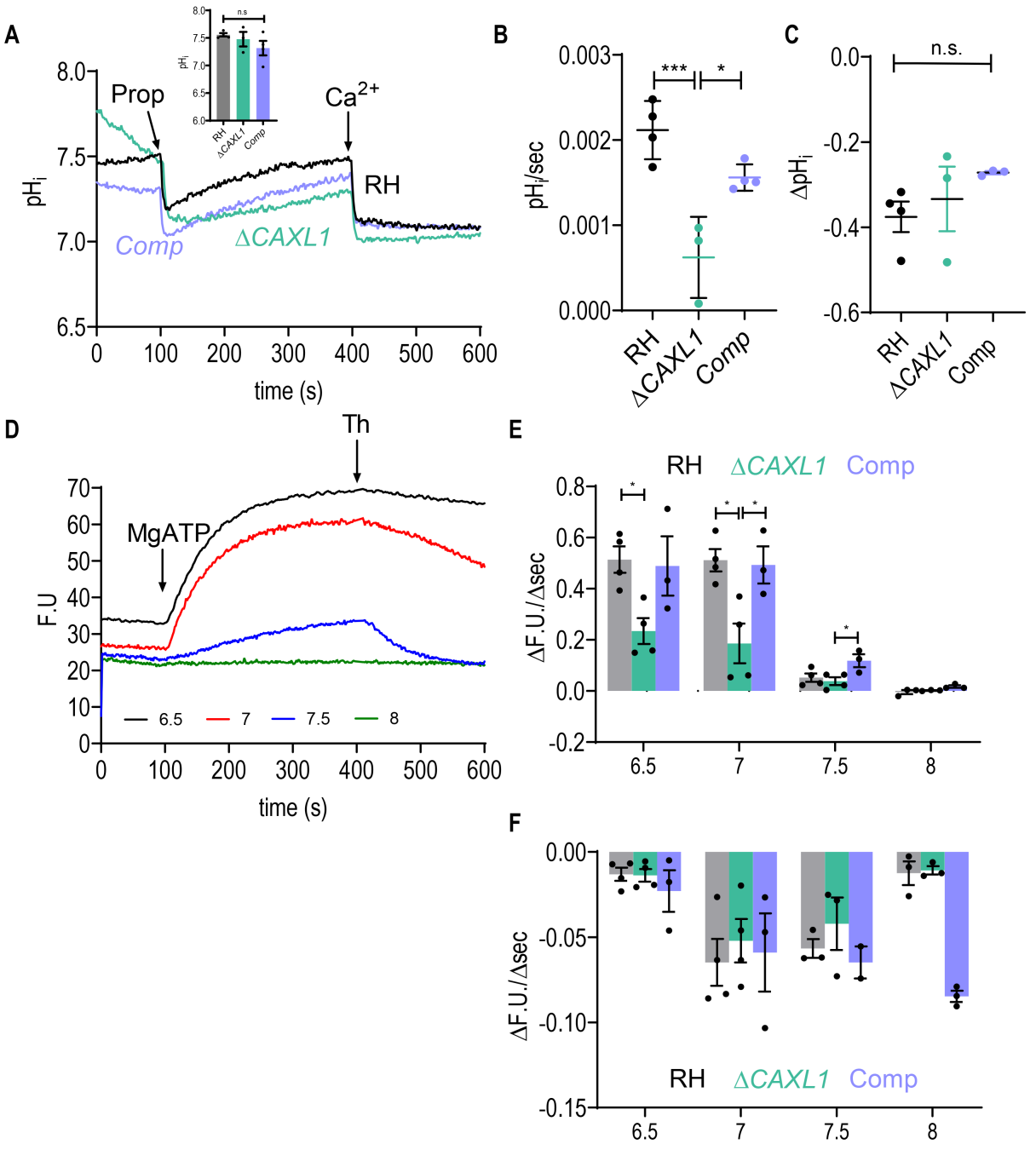

Figure 2.7 Modulating intraellular pH levels is critical for protein function. A) Intracellular pH levels in RH, Δ*CAXL1* and Δ*CAXL1-comp* cell lines loaded with BCECF-AM. Experiments were done in calcium free Standard buffer with 100 µM EGTA. At 100 sec, 3 mM of sodium propionate was added, followed by addition of 1.8 mM Ca^{2+} at 400 sec. Inset: average of basal pH levels before addition of prop. B) Quantification of the slope after addition of propionic acid. The slope was calculated between 100 and 120 sec. C) Change in pH after addition of Ca^{2+} at 400 sec. D) Representative tracings of fluorescence from MagFluo4 in permeabilized RH parasites resuspended in CLM buffers

at different pHs + 211 nM Ca^{2+}. 250 µM MgATP was added at 100 sec and 1.5 µM thapsigargin at 400 sec. E) Quantification of the slope after addition of MgATP in parasites resuspended in CLM buffers with varying pHs. Slopes were analyzed for RH, Δ*CAXL1* and Δ*CAXL1-comp*. The slope was calculated between 100 and 140 sec. F) Quantification of the slope after addition of 1.5 µM Thapsigargin in parasites resuspended in CLM buffers with varying pHs. The slope was calculated between 400-600 sec. Slopes were analyzed for RH, Δ*CAXL1* and Δ*CAXL1-comp*. Values indicate mean ± SEM and analyzed using one-way ANOVA. *= p< 0.5, *** = p<0.001. Prop=propionic acid, Th=thapsigargin.

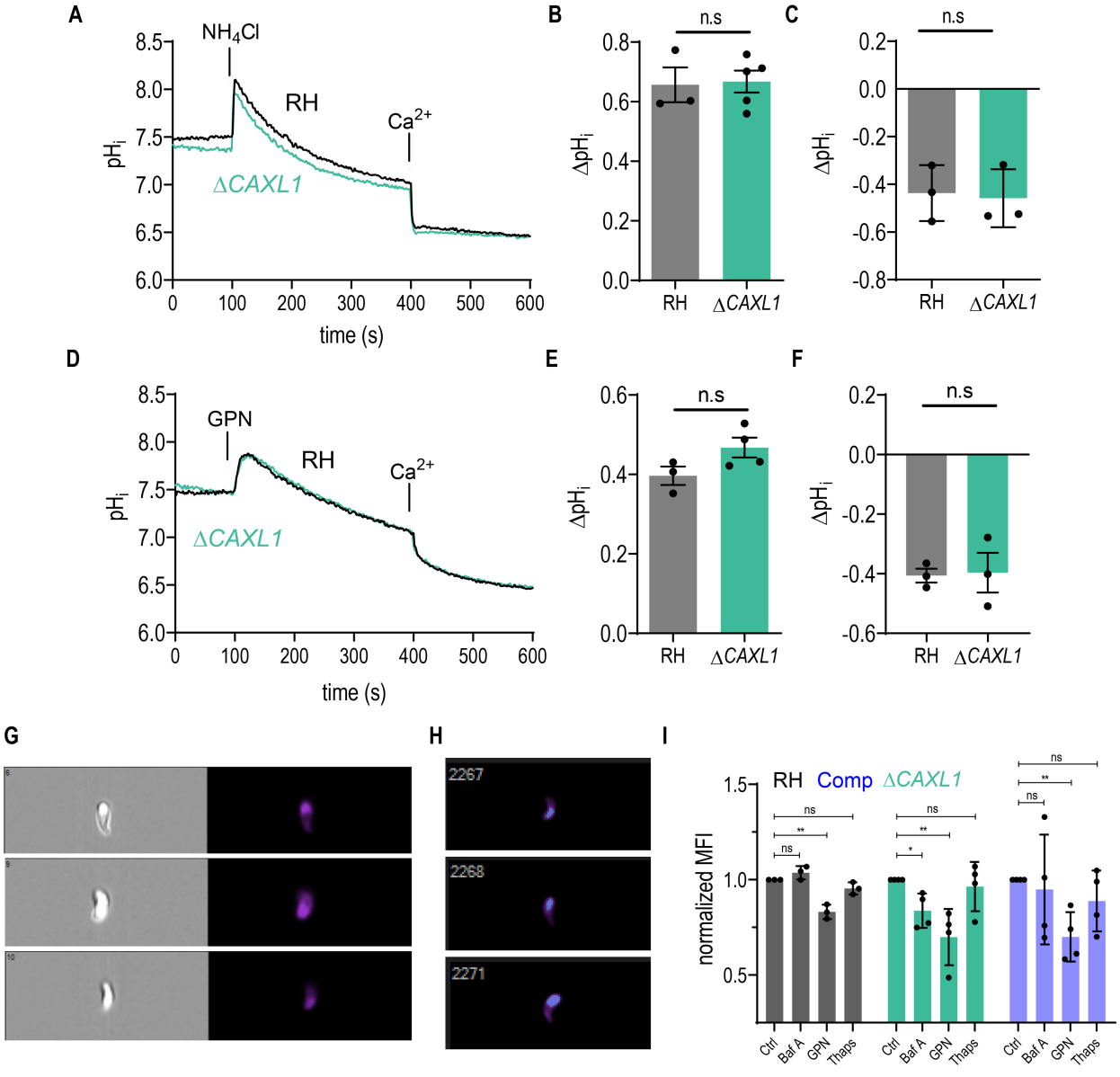

Supplemental Figure 2.2 TgCAXL1 and acidic stores. A) Intracellular pH levels in RH, Δ*CAXL1* and Δ*CAXL1-comp* cell lines loaded with BCECF-AM. Experiments were done in calcium free Standard buffer with 100 µM EGTA. At 100 sec, 20 mM NH_4Cl was added followed by 1.8 mM of Ca^{2+} at 400 sec. B) Quantification of change in pH after addition of 20 mM NH_4Cl from A. C) Quantification of change in pH after addition of Ca^{2+} from A. D) Intracellular pH levels in RH, Δ*CAXL1* and Δ*CAXL1-comp* cell lines loaded with BCECF-AM. Experiments were done in calcium free Standard buffer with 100 µM EGTA. At 100s, 40 µM GPN was added followed by 1.8 mM of Ca^{2+} at 400 sec. E) Quantification of change in pH after addition of 40 µM GPN from D. F) Quantification of change in pH after addition of Ca^{2+} D. G) The pH of acidic stores was detected using Lysosensor DND 189 in RH, Δ*CAXL1* and Δ*CAXL1-comp* cell lines. Representative image of parasites loaded with Lysosensor. H) Representative image of parasites loaded with Lysosensor and the blue is the fluorescence of the area measured for analysis. I) Values indicate the average of the median fluorescence intensity (MFI) from a minimum of 4-5 biological replicates. For each trial, the fluorescence of a minimum of 100 parasites for each cell line was analyzed. For BCECF experiments, at least three independent biological replicates were done for all experiments, and each experiment was done in duplicate. For quantification of ΔpH_i and MFI, mean values ± SEM were analyzed using one-way ANOVA.

TgCAXL1 contributes to proper acidification of the lysosomal-like organelles in *T. gondii*, most likely the PLV (Supp. Fig. 2I). Thapsigargin was tested as a control, since it targets the ER, and did not affect acidification of the acidic stores (Supp. Fig. 2I).

4. Discussion

In this work, we report that TgCAXL1 is a member of a novel family of cation/proton exchangers. TgCAXL1 is a Golgi and ER specific protein that mediates Ca^{2+} leakage from the ER and Ca^{2+} release from acidic organelles. We demonstrate that TgCAXL1 affects TgSERCA Ca^{2+} uptake activity into the ER. Lasltly, we show that TgCAXL1 affects the ability of *T. gondii* to regulate pH stress.

The unpredicted protein family 0016 (UPF0016) CAX protein family largely differs from previously characterized calcium/proton exchangers. Canonical CAX proteins of the Ca^{2+}/cation superfamily contain between 10-12 transmembrane domains, tend to localize to vacuoles and are divergent from the UPF0016 subfamily (Cai & Lytton, 2004). An in depth phylogenetic analysis of UPF0016 members from various groups of life including

metazoans, fungi, plants, bacteria and one protist, *Paramecium tetraurelia* (*P. tetraurelia*) (Demaegd *et al.*, 2014), grouped into 4 different subfamilies. The *P. tetraurelia* encodes 4 UPF0016 paralogs that all cluster together and create their own subfamily. *P. tetraurelia* was the only protist and is an alveolate, like *T. gondii*.

We demonstrate that TgCAXL1 is part of the UPF0016 new family of CAX proteins and our results show that TgCAXL1 localization is similar to the localization of known UPF0016 proteins. UPF0016 family members characterized in humans (Foulquier *et al.*, 2012), yeast (Demaegd *et al.*, 2013) and the kinetoplastid *Trypanosoma cruzi* (Ramakrishnan *et al.*, 2021) localize to Golgi and it's different compartments. The Golgi possesses the capacity to store Ca^{2+} (Paolo Pinton, 1998) and can impact proper sorting, processing and glycosylation of target proteins (Dolman & Tepikin, 2006). The Golgi Ca^{2+} signaling toolkit is comprised of different Ca^{2+} pumping ATPases and Ca^{2+} binding proteins. Expression of these molecules is not homogoneous. The Golgi consists of different stacks, divided into the cis, medial and trans golgi and is polarized in composition and function. In mammalian cells, the Golgi shares expression of specific proteins with the ER such as the SERCA (Vanoevelen *et al.*, 2004), IP_3 (Paolo Pinton, 1998) and Ryanodine receptor (Fredy Cifuentesa, 2001), Ca^{2+} release channels and several Ca^{2+} binding proteins. However, it is unique in the expression of the secretory protein Ca^{2+} ATPase (SPCA) (Ann-Marie Gunteski-Hamblin, 1992; Ton *et al.*, 2002), TMEM165, and Ca^{2+} binding proteins Calnuc (Ping Lin, 1998) and Cab45 (Phillip E. Scherer, 1996). Unlike the mammalian Golgi, the *T. gondii* Golgi is only composed of one stack (Laurence Pelletier, 2002). The *T. gondii* Golgi consists of various proteins involved in protein trafficking and maturation, shuttling and apical organelle biogenesis (Hammoudi *et al.*,

2015; Jackson *et al.*, 2013; Sloves *et al.*, 2012). TgCAXL1 distribution suggests that there is potential overlap in Golgi and ER functions.

Complementation of the yeast ortholog, ScGdt1, with TgCAXL1 further supported the function of TgCAXL1 as a member of the UPF0016 subfamily. The only other calcium/proton exchanger described in yeast is the vacuolar calcium/proton exchanger Vcx1 and deletion of Vcx1 does not cause sensitivity to high Ca^{2+} concentrations (Demaegd *et al.*, 2013), indicating that this phenotype is specific to the absence of ScGDT1. ScGDT1 modulates Ca^{2+} and manganese homeostasis at the Golgi. These ions are imperative for Golgi-dependent processing and glycosylation of proteins. ScGDT1 mutants displays a glycosylation defect of glucanosyltransferase, a marker of N and O-linked glycosylation, when grown at high Ca^{2+} concentrations (Stribny *et al.*, 2020).

TgCAXL1 plays a critical role in mediating ER calcium signaling through interaction with TgSERCA. In extracellular intact parasites, we observed a defect in the Ca^{2+} leakage induced by thapsigargin inhibition of TgSERCA. A similar phenotype was seen in FURA2 experiments with HELA cells expressing the human orthologue, TMEM165. We confirmed that TgCAXL1 affects SERCA Ca^{2+} uptake using MagFluo4 loaded permeabilized parasites. By using MgATP we could activate Ca^{2+} influx into SERCA expressing stores. SERCA driven Ca^{2+} influx was not as efficient in Δ*CAXL1*, indicating that TgSERCA requires TgCAXL1 to function properly. The dependence of Ca^{2+}-ATPase on a UPF0016 calcium/proton exchanger has also been established in yeast. ScPmr1, the TypeII Golgi-localized Ca^{2+}-ATPase, interacts and co-localizes with the TgCAXL1 yeast orthologue, ScGDT1 (Colinet *et al.*, 2016; Demaegd *et al.*, 2013). Aqueroin was used to measure cytosolic levels of Ca^{2+} in yeast, and Pmr1Δ mutants have higher resting levels of Ca^{2+}

due to the inability of the cell to properly store Ca^{2+} in the Golgi. In the double Pmr1Δ/GDT1Δ mutant, an even higher resting cytosolic Ca^{2+} level was observed indicating the GDT1 contributes to Ca^{2+} influx into the Golgi. This interaction is further supported in yeast growth assays at high Ca^{2+} concentrations. While both single mutants of ScGdt1 and ScPmr1 display a defect in growth at high Ca^{2+} concentrations, the double mutant grows at an even slower rate than the single mutants. Whether TgCAXL1 directly or indirectly controls TgSERCA function remains uncertain. TgCAXL1 could be modulating the activity of other ER specific proteins important for ER Ca^{2+} influx, however none have been identified. Until now, no additional interactors of UPF0016 members have been biochemically identified.

For the first time in *T. gondii*, we report that pH can impact SERCA activity. SERCA is part of the TypeII family of Ca^{2+} ATPases, which primarily transport Ca^{2+}. SERCA is responsible for pumping Ca^{2+} into the ER lumen, however, it has also been reported that for the ER to maintain a neutral electrochemical membrane, potassium, magnesium or hydrogen need to be countertransported across the ER membrane (Espinoza-Fonseca, 2017). SERCA undergoes a pumping cycle, transitioning from the E1 phase, where SERCA is facing the cytosol and is at it's highest affinity for Ca^{2+}, to the E2 phase, where it is facing the ER and changes to a low Ca^{2+} affinity state (Espinoza-Fonseca, 2017; F. Wuytack, 2002). At this low Ca^{2+} affinity state, SERCA will bind to two hydrogen ions and will translocate them from the ER lumen to the cytosol. Because of this activity, the SERCA has been described as possesing calcium proton exchange-like activity (Inesi & Tadini-Buoninsegni, 2014). Alkaline pH was first shown to impact SERCA Ca^{2+} uptake by Yu *et al.* in reconstituted proteoliposomes (Yu *et al.*, 1994). Ca^{2+}/proton countertransport

activity was also assessed by measuring the amount of protons ejected into the cytosol by SERCA when proteoliposome lumens were maintained at pH 6, 7, and 8. Proton ejection was highest at pH 6 and lowest at pH 8. The Ca^{2+} binding sites on SERCA are partly comprised of acidic acid residues, glutamic and aspartic acid (Chikashi Toyoshima, 2000). It is hypothesized, that when facing the lumen, a certain concentration of protons are required to faciliate Ca^{2+} dissociation and proton replacement at the Ca^{2+} binding site (Inesi & Tadini-Buoninsegni, 2014; Tadini-Buoninsegni *et al.*, 2006). An alkaline pH could potentially inhibit this from occurring and ultimatley prevent the transition from the E2 to the E1 phase. Our results showed that SERCA activity is drastically affected by the pH of the medium. It is possible that amino acid residues directly or indirectly involved in Ca^{2+} binding must be sufficiently protonated to bind to Ca^{2+} and/or transport Ca^{2+} to the ER lumen of *T. gondii*. It is also possible that an alkaline pH in the ER lumen can prevent the SERCA from transitioning from the E2 phase (lumen side) into the E1 phase (cytoplasm side), since it needs to bind to protons to ensure this transition. TgCAXL1 potentially plays a role in maintaining the ideal proton and Ca^{2+} concentrations at the membrane and lumen of the ER and Golgi. The defect in Ca^{2+} uptake at pH 6.5 and 7 could be because the proper amount of protons are not being distributed around TgSERCA.

TgCAXL1 mediates pH regulation in *T. gondii*. The exact function of UPF0016 proteins in proton exchange and pH modulation is not entirely known. When examining the lysosomes of patients with CDG caused by mutations in TMEM165, the lysosomes appeared to be more acidic (Demaegd *et al.*, 2013). The same result was detected in *in vitro* experiments with TMEM165 deficient HeLa cells. Experiments with GDT1 heterologously expressed on the plasma membrane of *L. lactis* showed that a higher pH

facilitated higher Ca^{2+} influx due to the establishment of a proton gradient. This supports ScGDT1's activity as a Ca^{2+}/proton exchanger. Modulation of pH was also tested in *A. thaliana* CCHA1 mutants, CCHA1 being a UPF0016 homolog (Wang *et al.*, 2016). *A. thaliana* CCHA1 mutant growth was significantly defective at alkaline and acidic pHs when compared to WT. These studies also showed that CCHA1 affects the pH of stomata cells, a type of cell that faciliates gas and liquid transport into plants. Our studies demonstrate that TgCAXL1 faciliates pH regulation in *T. gondii* as well. BCECF loaded Δ*CAXL1* parasites were impaired in their ability to recover from pH acidic stress. Acidification of the cytosol is quickly recovered largely due to the vacuolar H^+-ATPase on the acidic stores and plasma membrane (Stasic *et al.*, 2019). TgCAXL1 is either an additional mechanim of proton import into the Golgi and/or ER or it impacts activity of the vacuolar H^+-ATPase.

The release of Ca^{2+} from GPN targeted organelles is affected in Δ*CAXL1*. Cathepsin C protease is found in lysosomes and lysosomal-like organelles and cleavage of GPN by Cathepsin C leads to accumalation of the dipeptide causing osmotic stress and release of Ca^{2+} (Trond Olav BERG, 1994). In *T. gondii*, GPN is hypothesized to release Ca^{2+} from acidic stores most likely the PLV (Miranda *et al.*, 2010). Here we show that after filling the stores with Ca^{2+}, the Ca^{2+} release induced by adding GPN is signficantly impaired in the Δ*CAXL1* mutants, indicating that TgCAXL1 mediates Ca^{2+} uptake into the acidic organelles. One explanation for this phenotype is that improper modulation of Ca^{2+} and protons at the ER and the Golgi is affecting Ca^{2+} and proton homeostasis at the PLV. Another explanation contemplates the widley accepted mechanism of GPN. Recent work by Atakpa *et al* (Atakpa *et al.*, 2019), provides evidence

that GPN induced Ca^{2+} release might actually occur through a Cathepsin C independent manner. They propose that the Ca^{2+} released might actually come from the ER instead and that the Ca^{2+} from the ER might be transported to the lysosome. Cathepsin C is found in the dense granules and not the PLV (Que *et al.*, 2007). Recently, another study refuted this claim and reported that GPN targets Ca^{2+} release from the lysosomes (Yuan *et al.*, 2021). More studies would need to be done to determine the role of TgCAXL1 on acidic organelles.

TgCAXL1 is a calcium/proton exchanger that possesses dual localization properties in the ER and in the Golgi apparatus and for the first time, we show that the Golgi apparatus is involved in mediating Ca^{2+} in *T. gondii*. Regulating pH levels in the cytosol and in intracellular stores is critical for protein activity, specifically TgSERCA at the ER membrane. Disrupting the tight regulation of protons and Ca^{2+} impacted the parasite's ability to invade the host cell, an imperative step of the lytic cycle. This work contributes to understanding the overall pathogenesis of *T. gondii* and the different mechanisms that impact it's lytic cycle.

Table 1. Primers used in this study

Primer name	Sequence
C-terminal tagging	
AC105	TTCGTCCTCTTCGCGATCTTTGGCGCCGTCCTAGATCT GTACCCGTACGACGTCCCGGA
AC106	GGCCGAGGTGGACTCGCAGATGTGCTCTGTGCCATTG AATTAAGCCCCGCCCTGCC
AC107	TGATCTTCTCTCGCCTCCGAGTTTTAGAGCTAGAAATAG CAAG
KO	
AC119	AACTTGACATCCCCATTTAC
AC178	GCAGCTTCTGCTCATTTTACGAAGTAGAC
AC179	AGAGAGCACAAGACATGCATCCAGAG
RT-PCR	
AC 214	AGGCGTTCTGCTTCCTGC
AC 215	AGAAAAGCCTTCCACGAGCAT
AC 327 (Tubulin For)	GACGACGCCTTCAACACCTTCTTT
AC 328 (Tubulin Rev)	AGTTGTTCGCAGCATCCTCTTTCC
AC 329 (Actin For)	TCCACCATGAAGATCAAGGTCGTT
AC 330 (Actin Rev)	ACATCTGCTGGAAGGTGGAG

Table 2. Accession number of organisms used in phylogenetic analysis.

Abbreviation	**Accession Number**	**Organism**
Ncr	XP_964855.2	*Neurospora crassa*
Sce	AAS56893.1	*Saccharomyces cerevisiae*
Cal	EEQ45872.1	*Candida albicans*
Cga	XP_003194471.1	*Cryptococcus gattii*
Dre	NP_997848.1	*Danio rerio*
Sma	XP_002580560.1	*Schistosoma mansoni*
Ame	XP_623837.2	*Apis mellifera*
Hsa	NP_060945.2	*Homo sapiens*
Mmu	NP_035756.2	*Mus Musculus*
Cel	NP_497567.1	*Caenorhabditis elegans*
Tg*	XP_002369832.2	*Toxoplasma gondii*
Nca	XP_003880625.1	*Neospora caninum*
Bes	XP_029220247.1	*Besnoitia besnoiti*
Csu	PHJ21771.1	*Cytoisospora suis*
Tcr	XP_819449.1	*Trypanosoma_cruzi_CLB*
Ade	EPY40435.1	*Angomonas_deanei*
Bsa	CUI14131.1	*Bodo saltans*
Lma	XP_001682608.1	*Leishmania major strain Friedlin*
Lbr	XP_001564159.1	*Leishmania braziliensis*
Saa1	AFZ34620.1	*Stanieria cyanosphaera*
Scy2b	WP_015192292.1	*Stanieria cyanosphaera*
Sys1	WP_011619239.1	*Synechococcus*
Sys2	WP_011619238.1	*Synechococcus*
Tem1	ABG51526.1	*Trichodesmium erythraeum*
Tem2	WP_011611892.1	*Trichodesmium erythraeum*

Chapter 3

A forward genetic approach to identify mechanisms of ER Ca^{2+} release in *Toxoplasma gondii*

Introduction

To remain viable, the tachyzoite undergoes the lytic cycle consisting of invading the host cell, replicating, and ultimately egressing and invading another host cell (Blader *et al.*, 2015). Due to the rapid and constant tissue disruption, the lytic cycle has been linked to pathogenesis (Borges-Pereira *et al.*, 2015; Pace *et al.*, 2014). Our group and several others have shown that an increase in cytosolic Ca^{2+} stimulates each step of the lytic cycle, supporting a role for Ca^{2+} signaling in pathogenesis. Upon host cell egress, *T. gondii* is exposed to the extracellular environment containing <10,000 times higher concentration of Ca^{2+} than inside the parasitophorous vacuole (PV). An increase in cytosolic Ca^{2+} has been shown to stimulate all steps of the lytic cycle, indicating that Ca^{2+} entry from the extracellular environment and/or release of Ca^{2+} from intracellular organelles are responsible for regulating the steps in the parasite life cycle. In mammalian cells, several channels, receptors and sensory molecules are responsible for modulating the influx of intracellular calcium, however many of the homologue genes are missing in *T. gondii* (Prole & Taylor, 2011). Recent studies in our lab showed that a transient receptor channel (TgTRPL-2) localizes to the plasma and ER membrane, can conduct Ca^{2+} and facilitates Ca^{2+} influx (Marquez-Nogueras *et al.*, 2021). An increase in cytosolic Ca^{2+} can occur through release of Ca^{2+} from neutral intracellular stores, which has been

demonstrated using several different agonists such as the Ca^{2+} ionophores, ionomycin or A2137 (Arrizabalaga *et al.*, 2004; Sibley, 1999), the phosphodiesterase inhibitor zaprinast (Lourido *et al.*, 2012) and the sarco/endoplasmic Ca^{2+}-ATPase (SERCA) inhibitor thapsigargin (Pace *et al.*, 2014). However, the mechanism and molecule responsible for the release from these stores has not been identified.

Zaprinast is a cGMP phosphodisesterase inhibitor in *T. gondii (Lourido et al., 2012)*. Inhibition of phosphodiesterases leads to an increase in secondary messengers, cyclic-GMP (cGMP) and cyclic-AMP (cAMP), causing increased activation of Protein Kinase G (PKG) and Protein Kinase A (PKA), respectively (Howard *et al.*, 2015). PKG has been shown to play a role in Ca^{2+} signaling, by potentially interacting with Ca^{2+}-dependent protein kinase 3 (CDPK3) (Lourido *et al.*, 2012). This study was the first to show that zaprinast alone could induce egress in *T. gondii*. Sidik *et al* demonstrated that zaprinast-induced egress occurs due to an increase in cytosolic Ca^{2+} using the calcium chemical indicator, Fura2 (Sidik, Hortua Triana*, et al.*, 2016). These studies supported that the rise in cytosolic Ca^{2+} occurs in a PKG-dependent manner. Ionomycin is a Ca^{2+} ionophore that releases Ca^{2+} from organelles with a neutral pH (Fasolato *et al.*, 1991). Addition of ionomycin in Fura2 loaded parasites results in a large increase in cytosolic Ca^{2+}. Addition of zaprinast immediately after addition of ionomycin produces no change in cytosolic Ca^{2+}, indicating that zaprinast must target neutral stores as well. Our lab has been using zaprinast as a tool to study the players involved in releasing Ca^{2+} from neutral stores, potentially including the ER. Regulating Ca^{2+} is essential for the physiology of *T. gondii* and identification of any of these players could lead to discovering novel drug targets.

Our lab has established a unique and accurate method to measure intracellular Ca^{2+} levels and signaling in *T. gondii* (Pace *et al.*, 2014). Using the ratiometric indicator, Fura2, we have pharmacologically demonstrated the presence of voltage-gated Ca^{2+} channels and a SERCA-like ATPase. Additionally, we showed that Ca^{2+} is stored in the ER and in the acidic store, the PLV (Miranda *et al.*, 2010) and acidocalcisome (Zhong, 1996). To extend our understanding of mechanisms of Ca^{2+} signaling in the parasite, our goal was to develop a high throughput (HTP) method to simultaneously study Ca^{2+} entry and release from a large number of parasites. Using chemical indicators is a time-consuming process. Incubating cells with the chemical dye and performing each experimental trace results in a 3-to-4-hour experiment. Additionally, it is only feasible and advisable to perform experiments with a single cell line at a time. A method for detecting changes in Ca^{2+} cytosolic levels in a more time efficient manner is in demand. In this work, we used parasites expressing GCaMP6, a genetically encoded Ca^{2+} indicator (GECI) to develop a high throughput assay. GCaMP6 is composed of an M13 peptide, a circularly permuted enhanced green fluorescent protein (cpEGFP) and a calmodulin domain (Ding *et al.*, 2014). Upon Ca^{2+} binding to calmodulin, a Ca^{2+} binding protein, it will interact with the M13 peptide. The resulting conformational change in the cpEGFP leads to an increase in fluorescence (Junichi Nakai, 2001). Originally designed to measure neuronal Ca^{2+} dynamics, GCaMP reporters have been useful in studying Ca^{2+} dynamics in *T. gondii*. Specifically, we have been able to learn more about the role of Ca^{2+} during invasion, egress and motility (Borges-Pereira *et al.*, 2015; Uboldi *et al.*, 2018; Vella *et al.*, 2021). We can visualize Ca^{2+} oscillations in individual parasites and discern whether differences exist in the Ca^{2+} distribution across the cytosol after exposure to different pharmacological

agents or extracellular Ca^{2+}. Furthermore, it provides the opportunity to do HTP measurements of Ca^{2+} influx in *T. gondii*.

Using chemical mutagenesis as a forward genetic approach, we isolated mutants that were deficient in zaprinast-induced egress. We developed an assay to measure *T. gondii* cytosolic Ca^{2+} in a HTP way with GCaMP6f expressing parasites. Isolated mutants were ultimately analyzed for zaprinast resistance.

Methods

Cell culture and parasite transfection

For this study, hTERT cells were cultured in Dulbecco's modified Eagle medium with high glucose and 10% FBS and parasites were cultured in DMEM-HG and 1% FBS at 37°C at 5% CO_2 (Marquez-Nogueras *et al.*, 2021; Stasic *et al.*, 2019). For parasite transfection, RH parasites were harvested when 60-80% egressed from the host cell monolayer (Marquez-Nogueras *et al.*, 2021; Stasic *et al.*, 2019). Parasites were passed through a 3 µM filter and centrifuged at 1700 rpm for 10 min. Parasites were then resuspended in cytomix at a concentration of 3 $x10^7$ parasites/mL. 300 µL was transferred to a 0.4 cm cuvette and mixed with 40 µg of the GCaMP6-mScarlet plasmid. Parasite mixture was electroporated with plasmid and transferred to a confluent host cell monolayer and the media was changed the following day.

FACS sorting

Once parasites egressed from the host cell monolayer after initial transfection with the GCaMP6-mScarlet plasmid, they were passed through a 3 µM filter, centrifuged at 1700 rpm for 10 min, and resuspended in 1 mL of Ringer's buffer (155 mM NaCl, 3mM KCl, 1mM $MgCl_2$, 3mM NaH_2PO_4, 10 mM HEPES, 5 mM Glucose at pH 7.3) (Pace *et al.*,

2014). Using a BioRad S3 Cell Sorter, parasites expressing both green and red fluorescence were sorted into a catch tube. Around 10-20,000 parasites were obtained during each sorting experiment. Parasites were sorted every time after egressing from the host cell monolayer until a population that was approximately 80% fluorescent was obtained. The mixed population was serially diluted into a 96-well plate to select for clonal populations.

For selection of host cells infected with GCaMP6f-mScarlet expressing parasites, host cells were treated with trypsin, centrifuged at 1700 rpm for 10 min and resuspended in 2 mL of Ringer's buffer. They were sorted with the same method as the parasites, except the settings in the flow cytometer were modified to select for host cells instead of parasites.

Plaque assay

hTERT host cells were grown in a 6 well plate for 7 days to ensure host cell confluence. Parasites were collected when 60-80% egressed from the host cell monolayer and passed through a 3 µm filter. 200 parasites were added to one well and allowed to grow for 7 days at 37°C. Host cell monolayer was then fixed with 70% ethanol and stained with crystal violet. Host cell monolayer was rinsed with 1x PBS.

Fura2-AM measurements

Parasites were incubated with Fura2-AM, the cell membrane permeable form of Fura2, a ratiometric Ca^{2+} indicator, as directed in Vella *et al (Vella et al., 2020)*. Briefly, confluent host cells were infected with 1 x 10^7 parasites in Dulbecco's Modified Eagle's Medium-high glucose (DMEM-HG) + 1% fetal bovine serum (FBS). After 24 hours the media was changed to fresh media, and the following day parasites were harvested once

70-80% lysed the host cell monolayer. Collected parasites were filtered through an 8 µm Nucleopore membrane to remove host cell debris and resuspended in Ringer's buffer with 5 µM Fura2-AM (AAT Bioquest) for 26 min at 26°C. Fura2-AM containing parasites were washed and resuspended in extracellular buffer to a final concentration of 1 x 10^9 parasites/mL and kept on ice. Fura2 has two excitation wavelengths, 340 nm when bound to Ca^{2+} and 380 nm when unbound to Ca^{2+}. The emission wavelength is 510 nm for both the bound and unbound state. The resulting ratiometric fluorescence values were used to calculate Ca^{2+} concentration (Grynkiewicz *et al.*, 1985). The Hitachi-7000 was used for detecting Fura2 fluorescence.

To validate zaprinast-resistant clones, the collection protocol is the same as above, however no chemical indicator was added to the parasites. Wavelengths used to detect GCaMP6 was an excitation of 485 nm and an emission of 510 nm and for mScarlet was an excitation of 569 nm and an emission of 594 nm. 50 µM and 100 µM zaprinast (Sigma-Aldrich) were used for analysis.

EMS treatment

RH-GCaMP6f-mScarlet-2 parasites were chemically mutagenized with the chemical mutagen ethyl methanesulfonate (EMS). One confluent T75 host cell flask was infected with 2 x 10^7 parasites. Twenty-four hours later, the infected host cell monolayer was washed, only leaving intracellular parasites. The parasites were left in DMEM-HG + 0.01% FBS for 10 min at 37°C. The media was then aspirated and replaced with DMEM-HG + 0.01% FBS + 10mM EMS for 4 hours at 37°C. After EMS exposure, extracellular parasites were washed away, and the intracellular parasites were collected by scraping and passing the infected host cell monolayer through a 25 1½ G needle. Host cell debris

was eliminated by passing the mixture through a 3 μM filter. Chemically mutagenized parasites were centrifuged at 1700 RPM for 10 min and washed with 1x PBS pH 7.4 to eliminate any remaining EMS. Parasites were resuspended in 1 mL of media and added to a new confluent T75 in DMEM-HG+10% FBS. Twenty-eight hours later, extracellular parasites were washed away, leaving only intracellular parasites.

Treatment for zaprinast-resistant mutants

100 μM of zaprinast was added to mutagenized parasites (in a T75) and left for 10 min at 37°C. After 10 min, the monolayer was washed until only intracellular parasites that were unable to egress in the presence of zaprinast remained. The intracellular parasites were collected via FACS sorting and then placed on a confluent host cell monolayer. This was repeated after each zaprinast treatment. The zaprinast treatment was repeated a total of 8 times in order to increase the probability of attaining a clone that is zaprinast resistant. The mixed population of zaprinast-induced egress mutants was serially diluted into a 96-well plate with confluent host cells where one parasite was seeded per well.

Plate reader and fluorometry analysis

For selection of RH-GCaMP6f-mScarlet, ten single clonal cell lines were obtained and tested in the plate reader for their response to extracellular Ca^{2+} and pharmacological drugs. Clonal cell lines were infected into a T75. After 24 hrs, the media was changed and 24 hrs later, the parasites were collected when they were 60-80% egressed from the host cell monolayer. The host cell monolayer was scraped and passed through an 8 μM filter, centrifuged at 1700 rpm for 10 min and resuspended in Ringer's buffer. 2 x 10^7 parasites were added into each well in a final volume of 100 μL. In the Synergy H1 hybrid

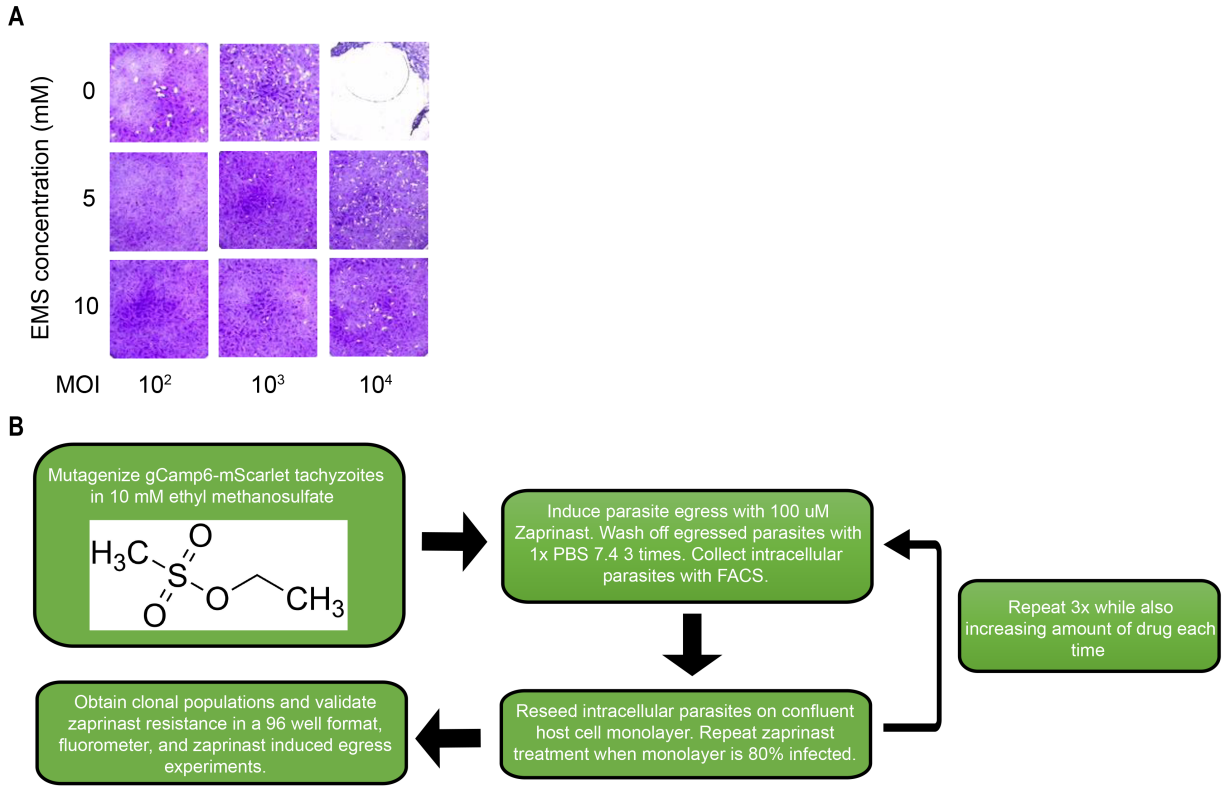

Figure 3.1 Forward genetic approach in *T. gondii*. A) Plaque assay of RH parasite exposed to different EMS concentrations at different MOI's (multiplicity of infection). B) Schematic describing method to obtain zaprinast resistant mutants. FACS= fluorescence-activated cell sorting.

reader, fluorescence intensity of GCaMP6f and mScarlet was measured using filter settings at 485 nm excitation/528 nm emission for GCaMP6f and 530 nm excitation/590 nm emission for mScarlet. The plate reader was set to 37 °C and the parasites were left to shake for 3 min prior to beginning fluorescence measurements. After shaking, basal fluorescence was measured for 3 min for a total of 6 reads. At 3 minutes, 20 µL of drug/stimulant or DMSO was injected into the wells, gently resuspended and then measured for an additional 4 min. Plate reader experiments were done in triplicate for each clone. 1 and 2 µM of thapsigargin and ionomycin, 100 µM zaprinast and 1.8 mM

Ca^{2+} was added. The two clones that (clones 2 and 5) produced the highest maximal green fluorescence in response to all stimulators were selected for further analysis.

For selection of zaprinast-resistant clones, the same plate reader settings as above were used. Once fully egressed out from a 96-well plate, each clonal population was transferred to a well in a 24 well plate with confluent host cells. Once mutants lysed the host cell, each mutant was collected, spun down for 10 min at 1700 RPM and resuspended in 250 µL of extracellular buffer. 100 µL of parasites were added into each well of 96-well plate and tested for its response to 100 µM zaprinast and DMSO. Additionally, the RH-GCaMP6f-mScarlet parent strain was tested as a control. The maximal green fluorescence in response to all stimulators was calculated for all clones as well as the average red fluorescence and were used to calculate ratiometric values.

Results

The chemical mutagen ethyl methanesulfonate (EMS), a commonly used mutagen when performing forward genetics in *T. gondii* was used to induce random mutations (Coleman & Gubbels, 2012). With this approach, a novel gene in *T. gondii* was identified containing a Ca^{2+}-dependent membrane binding domain (McCoy *et al.*, 2017). Parasite exposure to 10 mM of EMS is known to kill 70% of the population of parasites (Andrew Farrell, 2014). This dosage of EMS will induce about 100 single nucleotide variations in the surviving population (Andrew Farrell, 2014). Different EMS concentrations were tested with ranging concentrations of parasites to validate ideal conditions of EMS exposure. Through plaque assay analysis, we determined that 10 mM of EMS with 1 x 10^4 parasites was ideal (Fig.1A). The forward genetic approach to obtain zaprinast-resistant parasites is detailed in Fig. 1B.

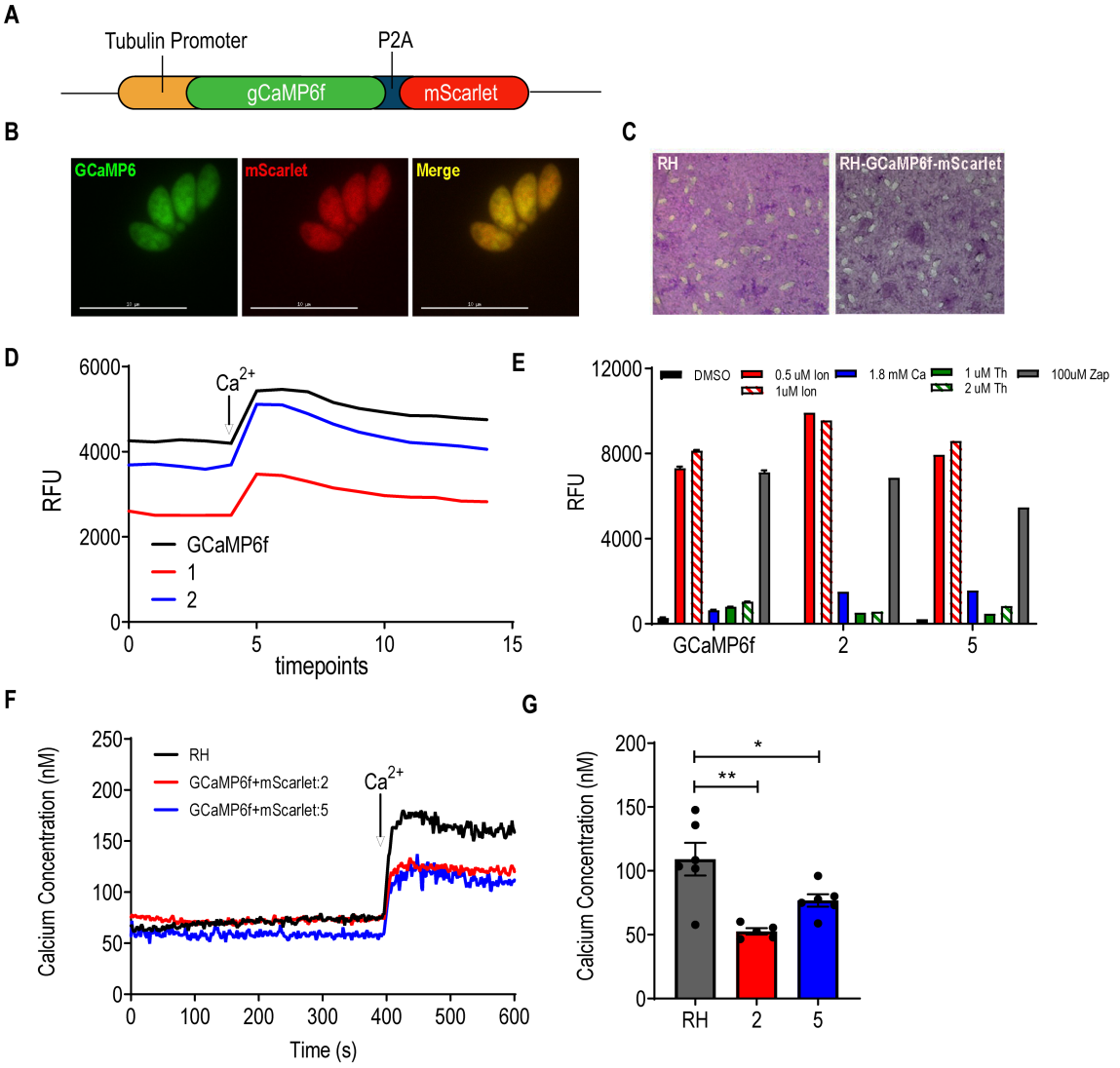

Figure 3.2 Characterization of GCaMP6f-mScarlet parasites. A) GCaMP6f-mScarlet plasmid used to transfect RH parasites. B) GCaMP6 and mScarlet fluorescent image. C) Plaque assay of GCaMP6f-mScarlet and RH parasites. D) GCaMP6 fluorescent measurement of parasite expressing GCaMP6 only (GCaMP6f) and GCaMP6f-mScarlet clones 1 and 2 after addition of 1.8 mM Ca^{2+}. E) Quantification of peak Ca^{2+} after addition of stimulants: 1.8 mM Ca^{2+}, 0.5 and 1 µM Thapsigargin (Th), 0.5 and 1 µM ionomycin (Io) and 100 µM Zaprinast (Zap). F) Representative image of Ca^{2+} measurements of GCaMP6f-mScarlet clone 2 loaded with FURA2-AM. 1.8 mM Ca^{2+} was added at 400 sec.G) Quantification of Ca^{2+} entry for RH, GCaMP6f-mScarlet Clone 2 and 5 from E. N=3. G indicates mean values of change in calcium from ± SEM and analyzed using t-test. *= p< 0.5, ** = p<0.01.

We engineered parasites expressing GCaMP6f, in combination with a red fluorescent protein (RFP), mScarlet (Bindels *et al.*, 2017), that is insensitive to Ca^{2+}, in a

type I strain of *T. gondii* (termed RH) (Fig. 2A). By measuring green and red fluorescence, we can estimate cytosolic Ca^{2+} concentration from the GFP:RFP ratio. GCaMP6f and mScarlet genes were cloned into a single expression vector and then transfected into RH parasites. GCaMP6f and mScarlet were cloned under the same promoter and linked by the 2A peptide in order to generate 1 to 1 ratio transcripts. Initially discovered in the foot and mouth disease virus, 2A is a 19 to 22 base pair oligopeptide (Martin D. Ryan, 1991). The 2A peptide contains a ribosome skipping site between the last glycine of the C-terminus and before the first proline specifically placed before the downstream gene, in this case mScarlet. The final product coordinates the simultaneous expression of GCaMP6f and mScarlet. Implementation of the 2A system will also prevents Forster resonance energy transfer from the green spectrum to the red spectrum, which can cause an undesired change in red fluorescence. Due to its high cleavage efficiency, the 2A peptide from porcine teschovirus-1 was used to ensure ratiometric expression of GCaMP6f and mScarlet (Kim *et al.*, 2011). After transfection into RH parasites, GCaMP6f and mScarlet expressing parasites were selected using fluorescence activating cell sorting (FACS) flow cytometry. Cells were selected based on simultaneous green and red fluorescence (Fig.2B). These parasites were sorted on 3 separate days to enrich for a GCaMP6f and mScarlet expressing population. RH-GCaMP6f-mScarlet (GCaMPf-mScarlet) parasites had a higher GFP:RFP ratio when exposed to pharmacological drugs known to increase intracellular levels of Ca^{2+} including thapsigargin, ionomycin, and zaprinast (Fig. 2C and D). Two clones that produced the highest maximal green fluorescence in response to all stimulators and had a low resting fluorescence (basal calcium level) were selected for further analysis.

GCaMP6f-mScarlet clone 2 Ca^{2+}-response phenotypes were compared to those of RH. To quantify intracellular concentrations of Ca^{2+} in these clones, parasites were incubated with Fura2-AM, the permeable form of Fura2, a ratiometric Ca^{2+} indicator that can be used to calculate intracellular Ca^{2+} concentration. Cytosolic Ca^{2+} concentrations were measured in response to increase in extracellular Ca^{2+}. We could detect Ca^{2+} influx in GCaMP6f-mScarlet clone 2, but Ca^{2+} influx was significantly lower than that of wildtype, after the addition of 1.8 mM of extracellular Ca^{2+}, suggesting that the GCaMP6f protein was sequestering Ca^{2+} and less intracellular Ca^{2+} was available for detection by FURA2 (Fig. 2F+G). We tested the ability of Fura2 loaded parasites to respond to other Ca^{2+} inhibitors and pharmacological agents and they responded similar to WT (data not shown). No difference in plaque size was observed between GCaMP6f-mScarlet clone 2 and WT infected cells, indicating that RH-GCaMP6f-mScarlet clone 2 parasites have a similar infection and lysis phenotype (Fig. 2C).

GCaMP6f-mScarlet clone 2 parasites were chemically mutagenized with EMS. Intracellular parasites were exposed to EMS for 4 hours at 37°C. Treated parasites were used to infect a confluent T75 and after 24 hrs, the culture was treated with 100 µM of zaprinast and left for 10 min at 37 °C. After 10 min, the monolayer was washed until only intracellular parasites that were unable to egress in the presence of zaprinast remained. Host cells containing intracellular parasites were isolated with FACS. FACS isolated host cells were seeded on a confluent host cell monolayer and the treatment was repeated 8 times to enrich for zaprinast-resistant clones. The mixed population of zaprinast-induced egress mutants were serially diluted into a 96-well plate where one parasite was seeded per well to obtain clonal cell lines. 63 zaprinast-induced egress mutants were analyzed

for their response to 50 and 100 μM zaprinast in the plate reader. Additionally, the RH-GCaMP6f-mScarlet parent was tested as a control (Fig. 3 C and D). Plate reader analysis demonstrated that the majority of clones exhibited either no, medium or high levels of zaprinast resistance. However, one parasite (clone 44), unexpectedly showed a 2-fold higher response to zaprinast.

12 zaprinast-resistant mutants were re-assayed to confirm resistance in the fluorescent spectrophotometer. The fluoromoter provides the advantage of analyzing a higher number of cells, therefore giving a more accurate response, and eliminating any false positives generated from the plate reader screen.

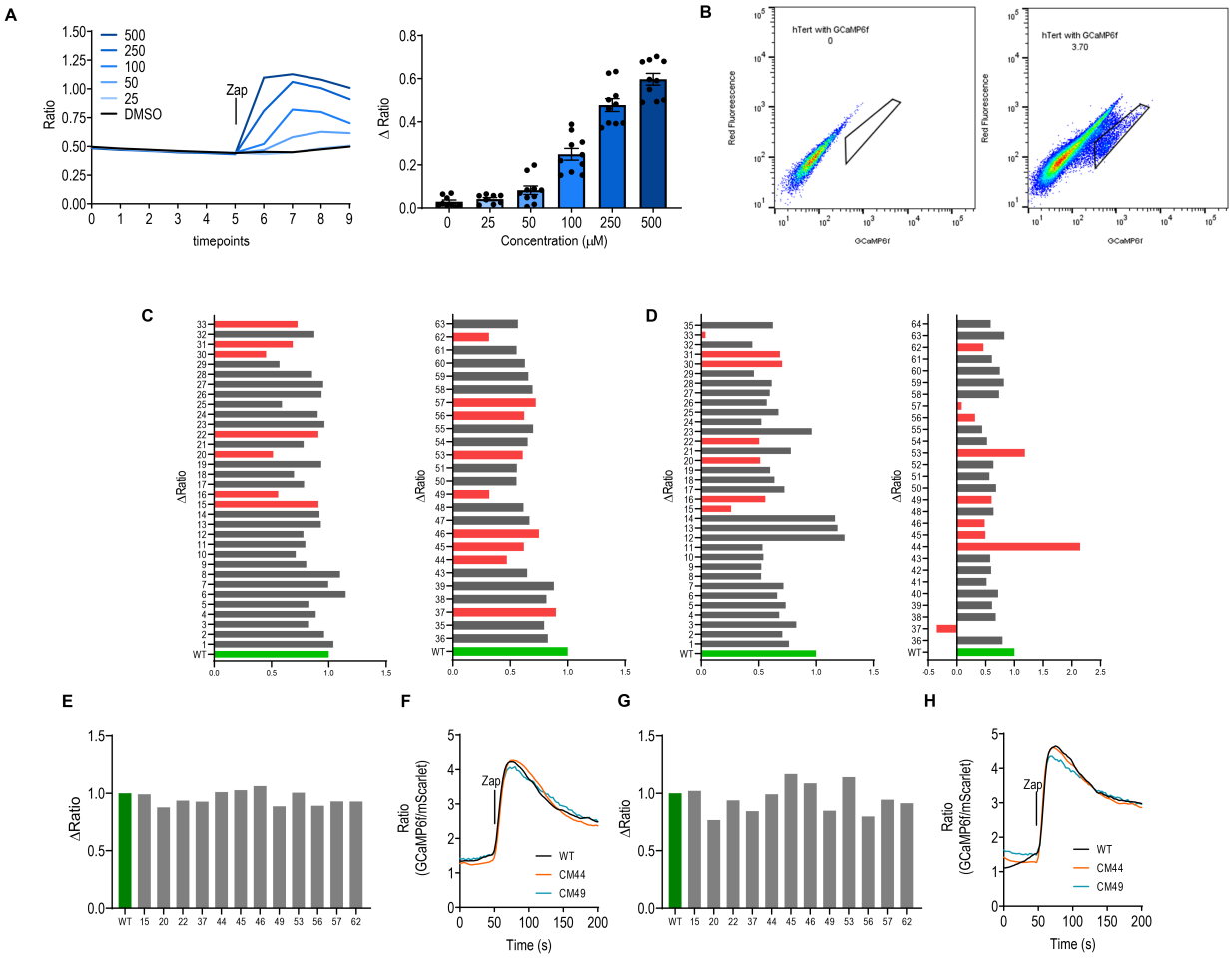

Figure 3.3 Validating zaprinast-resistant mutants. A) Dose dependent response of zaprinast using GCaMP6f-mScarlet clone. B) Histogram of host cells infected with and without GCaMP6f-mScarlet mutagenized parasites. C) Plate reader screen of potential mutants. Clones were collected from a 24 well plate, washed and resuspended in 100 µl of Ringer's buffer. 100 µM zaprinast was added to determine levels of resistance. Bar graphs quantify the ratiometric change in response to 100 µM zaprinast. Ratiometric change in mutants was normalized to GCaMP6f-mScarlet. 63 mutants were analyzed. Green indicates GCaMP6f-mScarlet and red indicates clones selected for further analysis. Ratio= GCaMP6f/mScarlet fluorescence change. D) Plate reader screen of potential mutants. Clones were collected from a 24 well plate, washed and resuspended in 100 µl of Ringer's buffer. 50 µM zaprinast was added to determine levels of resistance. Bar graphs quantify the ratiometric change in response to 50 µM zaprinast. Ratiometric change in mutants was normalized to GCaMP6f-mScarlet. 63 mutants were analyzed. Green indicates WT GCaMP6f-mScarlet and red indicates clones selected for further analysis. Ratio= GCaMP6f/mScarlet fluorescence change. N=2 for plate reader analysis. E) Bar graphs depict the quantification of fluorescence increase after addition of 50 µM of zaprinast in the fluorescence spectrophotometer. Ratio= GCaMP6f/mScarlet fluorescence change. F) Representative tracing of GCaMP6f-mScarlet and representative clones 44 and 49 in response to 50 µM zaprinast in the fluorescence spectrophotometer. G) Bar graphs depict the quantification of fluorescence increase after addition of 100 µM of zaprinast in the fluorescence spectrophotometer. Ratio= GCaMP6f/mScarlet fluorescence change. H) Representative tracing of GCaMP6f-mScarlet and representative clones 44 and 49 in response to 100 µM zaprinast in the fluorescent spectrophotometer.

Table 3.1 Fluorometric ratiometric increase of mutants in response to zaprinast.

Clone number	Ratio increase in response to 50 µM Zaprinast	Ratio increase in response to 100 µM Zaprinast
15	0.991434	1.021418
20	0.877634	0.767689
22	0.936575	0.938235
37	0.927476	0.844833
44	1.010719	0.991987
45	1.027832	1.168705
46	1.063519	1.087679
49	0.886921	0.848052
53	1.005364	1.141198
56	0.89134	0.79868
57	0.929048	0.944539
62	0.928224	0.913417

The zaprinast induced Ca^{2+} response of mutants is summarized in Table 1. Values are normalized to WT GCaMP6f-mScarlet (Fig. 3E and F). Clone 20's increase in Ca^{2+} after addition of 50 μM zaprinast was 12.3% smaller than that of wildtype. Clone 49 displayed an 11% difference and clone 52 a 10.9% difference. The percent fluorescence increase after 50 μM zaprinast was <8% than WT in Clones 15, 22, 37, 57 and 62. Clones 44, 45, 46, and 53 displayed a 0-6% increase in fluorescence. In response to 100 μM zaprinast, the increase in fluorescence for clone 20 was 23.2% smaller than WT and 20.3% for clone 56. Clone 37 displayed a 15.6% difference. Clones 22, 44, 57 and 62 displayed <9% difference in fluorescence than WT. Clone 15, 45, 46 and 53 all responded 2-14% higher than WT. Clone 20 seemed to have the most consistent response and would be the likeliest to show resistance to zaprinast in egress assays. However, the rest of the clones do not seem to exhibit any resistance and were likely false positives. As a whole, the mutants did not display levels of resistance that we had originally expected and did not appear to be resistant to zaprinast.

Discussion

In this work, we developed a ratiometric fluorescent cell line that can be used to measure *T. gondii* intracellular Ca^{2+} fluctuations in a high throughput manner. Using a forward genetic approach, we used EMS to mutagenize fluorescent parasites, selected for egress-deficient parasites and then attempted to isolate zaprinast-resistant mutants. We validated these mutants using the plate reader and the fluorometer and determined that ultimately, the enriched parasites were not resistant to zaprinast.

EMS was selected to induce random mutations in the *T. gondii* genome. Before the implementation of EMS, N-nitroso-N-ethylurea (ENU) was used in *T. gondii* to isolate

temperature-sensitive (Gubbels *et al.*, 2008) and Ca^{2+} ionophore-resistant mutants (Arrizabalaga *et al.*, 2004). EMS was the preferred mutagen because it targets G/C base pairs which are more frequently found in coding sequences (Coleman & Gubbels, 2012), as opposed to ENU which targets A/T base pairs and are likelier to be found in non-coding sequences. Canonically, a dosage of ENU had been used to induce 70% killing (Pfefferkorn, 1979). However, Farrell *et al* established that an EMS dose resulting in 90% killing induced around 100 SNVs in the entire genome, which is an average of one SNV per megabase (*T. gondii's* genome is comprised of 80 megabases) (Andrew Farrell, 2014). Optimization of the ideal dosage consisted of testing various doses of EMS, resulting in 70, 80 or 90% killing (3, 7.5, 10 mM EMS respectively), of the parasite population. The number of single nucleotide variants (SNVs) increased with increased killing percentage and the mutations generated were randomly distributed across the genome. Based on this study, we used 10 mM EMS to induce 90% killing in the RH-GCaMP6-mScarlet parasite population.

Developing a HTP method to measure intracellular Ca^{2+} in *T. gondii* is necessary to screen multiple clones for a phenotype of interest. In mammalian cells, both GECIs and fluorescent dyes have been implemented to study calcium in a HTP manner. A stable GCaMP6s fluorescent cell line in human embryonic kidney 293 (HEK-293) cell was generated and was successful in detecting Ca^{2+} entry and inhibition in response to Ca^{2+} influx agonists and antagonists in a 384 well plate format (Wu *et al.*, 2019). GCaMP6 was also expressed in the plasma membrane of Chinese hamster ovary cells. This system was effective in screening different voltage-gated channel inhibitors and thus found to be applicable for additional Ca^{2+} based HTP assays (Zhang *et al.*, 2022). Ca^{2+} assays have

also been commonly done using the fluorescent imaging plate reader (FLIPR) with specific Ca^{2+} assay kits to screen libraries in plates containing up to 1536 wells (Hodder *et al.*, 2004). The current drawback in *T. gondii* is the high amount of cells necessary to accurately and confidently measure intracellular Ca^{2+} levels. The FURA2 protocol requires at least 5 x 10^8 parasites to ensure proper saturation of the dye into the parasite cytosol, a quantity of cells that cannot be obtained from growing parasites in a 12 well plate or 24 well plate format. We were able to generate a cell line that stably expressed GCaMP6f and mScarlet to produce ratiometric values and in turn measure cytosolic Ca^{2+} levels.

Our goal was to isolate parasites that were deficient in zaprinast-induced egress, with the intention of discovering genes connected to the release of Ca^{2+} from the ER. In mammalian cells, the two main forms of Ca^{2+} release from the ER are through the ryanodine-receptor (Zalk *et al.*, 2007) and the inositol 1,4,5-triphosphate-receptor (Foskett *et al.*, 2007). These proteins oligomerize and form channels in the ER membrane, mediating Ca^{2+} release from the ER lumen. However, to date, orthologs of these proteins have not been identified in *T. gondii* and a mechanism of release from the ER has not been found. HTP approaches have led to the discovery of essential Ca^{2+} signaling molecules. An siRNA library targeting 2304 genes in HeLa cells lead to the discovery of Stromal interaction molecule 1 and 2 (STIM1+2) (Liou *et al.*, 2005). STIM proteins are Ca^{2+} sensing proteins that mediate store-operated calcium entry, a process that is activated after depletion of the ER and consists of replenishment of ER calcium by establishing junctions between the ER and plasma membrane. At the plasma membrane, STIM proteins interact with Ca^{2+} release-activated Ca^{2+} channels, ORAIs, and facilitate

Ca^{2+} influx and transport into the ER (Liou *et al.*, 2005; Zhang *et al.*, 2005). Up until the discovery of STIM proteins, store-operated Ca^{2+} entry was not fully understood. In *T. gondii*, a forward genetic approach resulted in the identification of the gene suppressor calcium-dependent egress 1 (SEC1) (McCoy *et al.*, 2017). CDPK3 knockout mutants were treated with EMS and intracellular parasites were exposed to the Ca^{2+} ionophore, A23187. CDPK3 mutants exhibited a delayed egress phenotype, and the authors were interested in obtaining parasites that were able to overcome this phenotype. Finally, those that egressed in the presence of A21387 were sent for whole genome sequencing and revealed a plasma membrane protein, conserved only in apicomplexans *Hammondia hammondi* and *Neospora caninum*, known as SEC1. The current model suggests that egress is dependent on SEC phosphorylation which can be mediated by CDPK3. Surprisingly SEC1 mutants did not impact Ca^{2+} oscillations and levels during egress. Using a HTP approach has proven to be successful in identification of novel genetic connections to intracellular Ca^{2+} signaling.

Several aspects of our approach could have impacted our results. Part of Tonkin *et al*'s approach was to treat 8 separate T75s culturing flasks, or 8 distinct populations. We only used 1 T75. Increasing the number of mixed populations might have increased our chances of obtaining a resistant population. Additionally, the parasites that have a reduced response to zaprinast in the plate reader could have been expanded and treated again to enhance the zaprinast resistant response. It is also possible that our screening method could not be improved. The mutants might have been egress deficient, but unaffected in their zaprinast stimulated Ca^{2+} response, something that would not have been detected by the plate reader or fluorometer. Lastly, it might be worth testing a higher

number of potential clones. In this screen, we tested 63 clones. Validating a higher number of clones might reveal a zaprinast-resistant mutant. It is important to continue investigating Ca^{2+} release mechanisms as release of Ca^{2+} from intracellular stores is necessary for major lytic cycle events and may lead to the identification of novel drug targets.

Chapter 4

A novel Clp protease system in the apicoplast of *Toxoplasma gondii*

Introduction

Calcium (Ca^{2+}) influx initiates different signaling cascades involved in cell proliferation, transcription, and communication (Clapham, 2007). In mammals, Ca^{2+} enters the cell via various channels such as voltage-gated Ca^{2+} channels (VGCC), ligand-gated or store-operated channels (CRAC or ORAI) and transient receptor channels (TRP) (Capiod, 2011). In *T. gondii*, the mechanisms of Ca^{2+} entry have not been entirely uncovered. Phylogenetic analyses of Ca^{2+} channels in protozoans by Prole and Taylor revealed that the *T. gondii* genome encodes two TRP channels (TRPPL-1 and TRPPL-2) and four L-type VGCCs (Prole & Taylor, 2011). Our lab characterized both TRP channels and found that TgTRPPL-1 localized to the endoplasmic reticulum (ER) (Hortua Triana, Marquez-Nogueras, Chang*, et al.*, 2018) and TgTRPPL-2 is a plasma and ER membrane channel involved in mediating Ca^{2+} influx (Marquez-Nogueras *et al.*, 2021). This study showed that TgTRPPL-2 conducts Ca^{2+}-dependent currents and is important for the parasite's pathogenic lytic cycle. In *T. gondii*, pharmacological evidence demonstrated that Ca^{2+} entry is inhibited by the dihydropyridine L-type VGCC inhibitor, nifedipine (Pace *et al.*, 2014). Dihydropyridines are a specific class of calcium channel blockers that can be further classified according to their specificity for targeting different types of VGCC (Takahara, 2009). These VGCCs are mainly expressed on cardiac tissue and vessels. Calcium channel blockers are commonly used for treating hypertension.

Blocking VGCC prevents Ca^{2+} entry that can stimulate contraction. Lessening the contraction of blood vessels, widens them and in turn lowers blood pressure. We found that Ca^{2+} entry can also be inhibited by exposing parasites to cilnidipine. Cilnidipine is specifically part of a fourth generation of calcium channel blockers and although initially designed to target L-type VGCC's, it can also target N-type VGCC (found on nerve cells) (Takahara, 2009), which haven't been identified in *T. gondii*. Unlike nifedipine, cilnidipine is not photosenstitive and more stable under long term conditions (Henk de Vries, 1998; Kulkarni *et al.*, 2020). Cilnidipine blocks about 40% of Ca^{2+} entry (data not published) and inhibits parasite growth (Marquez-Nogueras *et al.*, 2021). Identifying the targets of these inhibitors could lead to the discovery of novel *T. gondii* therapeutics.

An impactful *T. gondii* genome-wide CRISPR screen produced crucial information about the *T. gondii* genome, assembling data that predicts essentiality and dispensability of ~8000 genes (Sidik, Huet*, et al.*, 2016). This screen was also used as a tool to positively select for mutants sensitive to a particular drug. *T. gondii* nucleic acid formation depends on both a *de novo* and salvage pyrimidine pathway (Bzik, 2002). Uracil phosphoribosyltransferase (UPRT) is part of the salvage pathway and catalyzes the formation of uridine monophosphate (UMP), a precursor for cytosine and thymine nucleotides. The salvage pathway, and in turn UPRT, are not essential for the parasite due to the presence of the *de novo* pathway (Darrick Carter, 1997). 5-fluorodeoxyuridine (FUDR) is a nucleotide analog that inhibits DNA synthesis and is toxic to the parasite (Roos, 1995). UPRT catalyzes downstream products of FUDR that inhibit DNA synthesis. Deletion of UPRT allowed the parasite to survive in the presence of FUDR, establishing FUDR as a selection marker. Using this pathway as a proof of concept, the CRISPR

screen was performed in the presence of FUDR and results showed an increased abundance of sgRNAs against UPRT compared to the abundance of sgRNAs against all the others genes. These results suggest that the screen could be used as method to positively select mutants conferring resistance to a drug. We decided to use this approach to identify the potential target of cilnidipine. Collaborators at the Institute for Biomedical Research (Cambridge, MA) performed the CRISPR screen in the presence of cilnidipine. This screen produced a list of ~300 potential hits. We characterized the first hit on this list, a novel enzyme known as the caseinolytic protease ClpP, that localized to the apicoplast of *T. gondii*.

The apicoplast was formed during a secondary endosymbiotic event where a host cell engulfed a red algae cell containing a chloroplast (Striepen, 2011). Over time, in several apicomplexans such as *T. gondii*, the chloroplast lost photosynthetic activity, but retained its plastid structure. In *T. gondii*, the apicoplast is critical for fatty acid, isoprenoid and heme synthesis. The players and trajectory of these pathways vary from their human counterparts, highlighting them as potential drug targets (McFadden & Yeh, 2017; Striepen, 2011). For example, for fatty acid synthesis, humans use a fatty acid synthesis type I system which is comprised of a multimeric complex, whereas *T. gondii* uses a type II system consisting of sequential activity of several enzymes (Mazumdar *et al.*, 2006). ClpP is a highly conserved multimeric enzyme found in bacteria, the mitochondria of humans and plastids of lower eukaryotes (Yu & Houry, 2007). ClpP degrades misfolded or damaged proteins, functioning as a critical regulator of protein homeostasis. It's substrates include enzymes involved in cellular stress responses, transcription, and metabolism (Feng *et al.*, 2013; Flynn *et al.*, 2003; Gispert *et al.*, 2013; Olinares *et al.*,

2011). ClpP forms an ATP-dependent proteolytic core, comprised of two stacked heptameric ClpP rings. ClpP is a serine protease and alone degrades peptides (7-15 amino acids), however when combined with a hexameric chaperone, it can degrade larger substrates. The Clp chaperone belongs to a family of AAA+ ATPases and aids in the unfolding and translocation of target substrates. Assembly of the protease and chaperone leads to the formation of the Clp protease machinery. This complex is a novel proteolytic system in the apicoplast of *T. gondii* and could serve as a potential drug target in apicomplexans. In this work we characterize TgClpP as a potential target of cilnidipine.

Materials and Methods

Cell Culturing

All *T. gondii* parasites were grown in immortalized human foreskin fibroblasts (hTERT) host cells at 37º C at a 5% CO_2 level. Parasites were cultured in Dulbecco's modified minimal essential media with high glucose (DMEM-HG) media supplemented with 1% fetal bovine serum (FBS) and host cells were grown in DMEM-HG supplemented with 10% FBS.

CRISPR screen

The screen was done using the recently published genome-wide CRISPR protocol for *T. gondii* (Sidik, Huet*, et al.*, 2016) by our collaborators at Institute for Biomedical Research (Cambridge, MA). In summary, a sgRNA library was constructed, consisting of 10 sgRNAs for each coding protein-coding gene in the *T. gondii* genome. The library was transfected into the type I RH cell line grown in several different host cell confluent T-175s. Parasites underwent three rounds of passage (each time parasites lysed, they were passaged to new confluent T175s) before dividing the parasites into two populations. A

portion of the parasites was also collected at each passage for analysis. These populations were cultured for one week in the absence or presence of 5 μM cilnidipine. Parasites in the presence of cilnidipine were collected for analysis after the first lysis. After extraction of genomic DNA from these populations, the sgRNAs were amplified and sequenced using the Illumina HiSeq 2500. The relative abundance of sgRNA for all of the genes in the library (in the vehicle and cilnidipine treated population) was measured and quantified. These values were used to calculate the $\log_2$ fold change in relative abundance of the sgRNAs.

Generating tagged and conditional knockdown cell line

To generate mutants, a CRISPR-Cas9 mediated genome editing approach was taken. The TATiΔku80 cell line was used to generate TgClpP1-3xHA. The pLIC-3xHA plasmid containing a chloramphenicol resistant cassette was amplified with primers containing 35 bp of homology to the 3' end of TgClpP1. The pSAG:CAS9-U6:sgUPRT plasmid was modified to encode for an sgRNA sequence homologous to the 3' end of TgClpP1. 4 μg of the plasmid and 500 ng of the repair template was transfected into TATiΔku80 and positive mutants were selected with 20 μM chloramphenicol. After 4 passages a stable population was obtained, and the mixed population was subcloned to isolate for a clonal cell line. The clonal cell line, TgClpP1-3xHA, was validated with PCR (data not shown), western blot analysis and IFA. In the TgClpP1-3xHA background, a tetracycline inducible knockdown mutant of TgClpP1 was generated. The pSAG:CAS9-U6:sgUPRT plasmid was modified to encode for an sgRNA homologous to the 5' region of the UTR of TgClpP1. A repair template consisting of the TetO response element and a DHFR resistance cassette (Sheiner *et al.*, 2011) was amplified using primers

possessing 35 bp of homology to the 5' UTR of TgClpP1. Parasites were selected using the same method as TgClpP1-3xHA, except positive clones were selected using 1 μM pyrimethamine. Ultimately, a clonal cell line was obtained (iΔTgClpP1-3xHA) and was validated by observing downregulation of iΔTgClpP1-3xHA in the presence of 0.5 mg/ml anhydrotetracycline (ATc) through IFA and western blot analysis.

Antibodies

To probe for TgClpP1-3xHA lysate in a western blot, mouse αHA (1:1000) was used and mouse αtubulin (1:10,000) was used as a control. The secondary antibody was Goat αHA Alexa Fluor IRDye 800CW (1:10,000). For immunofluorescence assays, the protocol was performed as previously described in Marquez-Nogueras *et al* (Marquez-Nogueras *et al.*, 2021). Mouse αHA (1:100) and rabbit αHSP60 (1:500) were used. Secondary antibodies used were goat αmouse Alexa Fluor 488 dye and goat αrabbit 546 dye (Thermo-Fischer).

Growth assay and plaque assay

For experiments that required parasites preincubated in ATc, one drop of the completely lysed parasites was passed to a T25 and allowed to grow for 3 days in the presence of 0.5 mg/ml ATc. These parasites were then used for either the growth or plaque assays and exposed to ATc for an additional 6-7 days.

Growth assays were carried out with iΔTgClpP11-3xHA parasites expressing RFP protein, TdTomato. Parasites were transfected with 20 μg of RFP containing plasmid and selected through FACS using the S3 Cell Sorter (BioRad). A clonal cell line was selected after serial limited dilution (iΔTgClpP1-RFP). For all growth assays, 4000 RFP expressing parasites were seeded in a 96 well plate containing a monolayer of hTERT cells seeded

one to two days before. Growth assays were carried out in DMEM-HG media without phenol red (Thermo-Fischer) to prevent interference with the red channel. The fluorescence of the parasites was measured every day at a 544 nm excitation and 590 nm emission wavelength around the same time for 6 days. 0.5 mg/ml of ATc was added to induce downregulation and 1, 2, 4, 5, 8, 10 and 12 μM cilndipine was added as indicated.

For plaque assays, 200 iΔTgClpP1-3xHA or TATiΔku80 parasites were seeded on a confluent host cell monolayer and allowed to growth for 7 days. The monolayer was then fixed with 70% ethanol and stained with crystal violet. The size of the plaque areas were quantified for each condition using ImageJ.

Results

To determine the potential targets of cilnidipine, the previously established CRISPR screen (Sidik, Huet*, et al.*, 2016) was done in the presence and absence of 5 μM cilnidipine. Parasites were transfected with the genome-wide sgRNA library and after 3 passages, the relative sgRNA abundance was quantified. The top ten hits consisted of sgRNAs with the highest change in relative abundance after exposure to cilndipine, suggesting the absence of these genes confers potential resistance to cilnidipine. The list and annotation of the hits is summarized in Table 1. The top ten hits consisted of 4 hypothetical proteins (TGGT1_274150, 265510, 243200 and 281440), 3 nucleic acid metabolism proteins (TGGT1_310380, 271625B, and 239480), a putative GTPase (TGGT1_312050) and thioredoxin protein Atrx1 (TGGT1_312110) (Biddau *et al.*, 2018). For this study, we characterized the gene with the highest relative change in sgRNA abundance, TGGT1_318320, a ClpP domain-containing protein. All of the genes in this

list also possess a negative CRISPR phenotype score, suggesting they are indispensable for *T. gondii*.

Table 4.1. Results of top 10 hits from Cilnidipine CRISPR screen.

Gene ID	Change in sgRNA relative abundance	Fitness score	Annotation
TGGT1_318320	6.8	-2.7	ATP-dependent Clp endopeptidase, proteolytic subunit ClpP domain-containing protein
TGGT1_274150	4.6	-3.6	hypothetical protein
TGGT1_301380	4.4	-4.8	elongation factor Tu GTP binding domain-containing protein
TGGT1_265510	3.9	-2.2	hypothetical protein
TGGT1_271625B	3.8	-4.8	serine-tRNA ligase
TGGT1_243200	3.7	-3.95	hypothetical protein
TGGT1_239480	3.5	-1.7	RNB family domain-containing protein
TGGT1_281440	3.3	-4.8	hypothetical protein
TGGT1_312110	3.3	-4.2	apicoplast-associated thioredoxin family protein Atrx1
TGGT1_312050	3.3	-2.8	putative small GTPase Rab2

The ClpP protease contains a conserved proteolytic active site comprised of three amino acidic residues, Ser-His-Asp (Fig. 1B). However, in addition to ClpP, organisms like, *Arabidopsis thaliana (A. thaliana)* and *Plasmodium falciparum (P. falciparum)*, contain a ClpP-like protein that does not contain the catalytic triad, known as a ClpR(El Bakkouri *et al.*, 2010; Zheng *et al.*, 2002) (Fig. 1A+B). A BLAST search of the *T. gondii* genome using PfClpP revealed that *T. gondii* encodes for another ClpP protein, TGGT1_203270, (TgClpP2) and a ClpR, TGGT1_213115 (TgClpR) (Florentin *et al.*, 2017; Florentin *et al.*, 2020). Further investigation of the sequence showed that TgClpP1 lacks an active site and might function as a ClpR. Protein sequences of the active site showed that the predicted TgClpP1 does not contain the canonical ClpP catalytic triad, much like TgClpR. On the other hand, TgClpP2 does contain the catalytic triad,

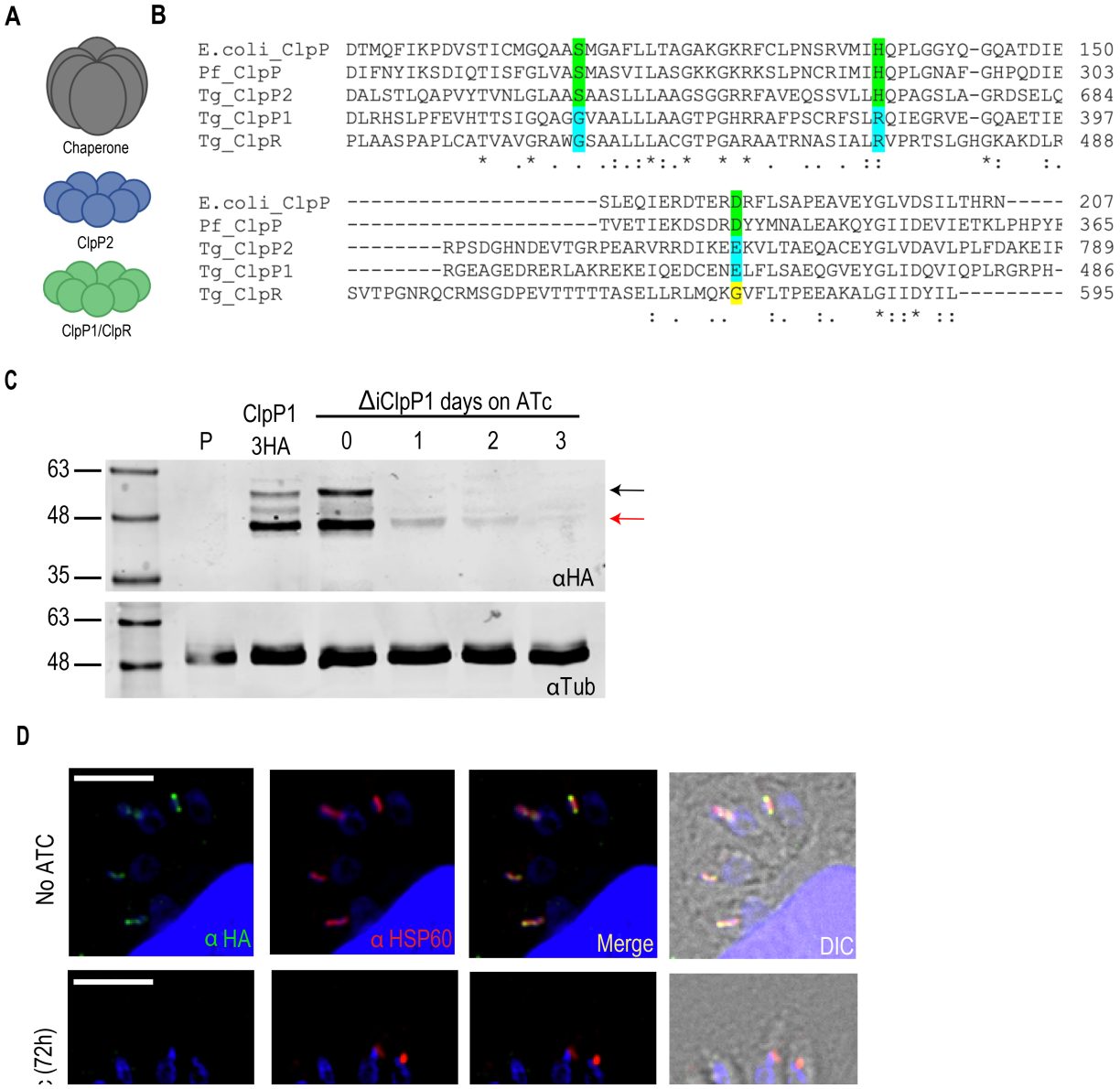

Figure 4.1 TgClpP1 is processed before transport to the apicoplast. A) Predicted Clp machinery in *T. gondii*. The chaperone remains unidentified. TgClpP2 subunits form the catalytically active ring. TgClpP1 and TgClpR assemble into a dimeric catalytically inactive ring. B) Multiple sequence alignment of active site of *E. coli* ClpP (WP 106489817.1), *P. falciparum* ClpP (PF3D7_0307400), *T. gondii* ClpP2 (TGGT1_203270), ClpP1 (TGGT1_318320), and ClpR (TGGT1_213115). Green indicates active site. Accession or gene ID numbers are in parentheses. C) Western blot analysis of TATiΔku80 parental (P), TgClpP1-3xHA, and iΔTgClpP1-3xHA lysates. iΔTgClpP1-3xHA was exposed to 0, 1, 2, and 3 days of ATc. The black arrow indicates mature TgClpP1 (56 kDa) and the red arrow indicates mature TgClpP1 (48 kDa). Tubulin was used as a loading control. D) Intracellular IFA of iΔTgClpP1-3xHA cells exposed to 0 or 3 days of ATc with αHA and colocalization with apicoplast marker, αHSP60.

suggesting it could be the true TgClpP. This also suggests that the *T. gondii* Clp protease core is comprised of a ClpP ring and ClpR ring, much like *A. thaliana* (Peltier *et al.*, 2004; Rudella *et al.*, 2006; Zheng *et al.*, 2002) and *P. falciparum* (Fig. 1A) (Florentin *et al.*, 2017; Florentin *et al.*, 2020). All of the Clp proteins described in this study have predicted essential phenotypic scores implying that the Clp machinery is essential for the parasite (ToxoDB) (Sidik, Huet*, et al.*, 2016).

To investigate the function of the Clp complex in *T. gondii*, we first endogenously tagged the C-terminal end of TgClpP1 with a 3x-hemagglutinin (3xHA) tag in the TATiΔku80 cell line using a CRISPR/Cas9 approach (TgClpP1-3xHA) (Fig. 1C). The TATiΔku80 cell line is characterized by two important components. The first being the absence of the Ku80 gene, a protein that can mediate non-homologous end-joining (Huynh & Carruthers, 2009). In the ΔKu80 cell line, the parasites will only be able to repair DNA double stranded breaks using homologous recombination, and proper repair can occur with homology arms consisting of as little as 30-40 bp with the implementation of CRISPR/Cas9 machinery. Secondly, this cell line constitutively expresses a tetracycline-regulated transactivator (TATi) (Sheiner *et al.*, 2011). In the presence of tetracycline (ATc), TATi will unbind from a tetracycline response element (located upstream of the regulated gene), leading to downregulation of the gene of interest. Insertion of a tetracycline-regulated promoter at the N-terminus of TgClpP1, in the TgClpP1-3xHA background, produced a conditional knockdown mutant (iΔTgClpP1-3xHA) (Fig. 1C). Downregulation of iΔTgClpP1-3xHA in the presence of ATc was validated through western blot analysis. TgClpP1 expression was significantly reduced after 1 day of exposure to ATc and became undetectable by 3 days. TgClpP1

downregulation was specific because the expression of tubulin remained unaffected. The expected size of TgClpP1-3xHA is 57 kDa and the band size from the western blot appears right under 63 kDa. However, another band with a lower molecular mass appeared under the 57 kDa band. PfClpP and ClpR proteins are processed into a mature zymogen before translocation to the apicoplast (El Bakkouri *et al.*, 2010; Florentin *et al.*, 2017; Florentin *et al.*, 2020). ClpP1 contains a transmembrane domain at the N-terminus end, which is most likely cleaved before becoming fully processed and transported to its final destination. A faint band is observed between these two bands indicating a version of TgClpP1 where the signal peptide is removed, but not the apicoplast signaling peptide. Removing the sequence before the transmembrane domain corresponds to a protein size of 46 kDa, similar to the migration of the two bands observed in the western blot analysis is indicative of immature and mature TgClpP1. Downregulation of TgClpP1-3xHA was further confirmed with immunofluorescence staining. In the absence of ATc, iΔTgClpP1-3xHA co-localized with the apicoplast marker heat shock protein 60 (HSP60). After 3 days of ATc exposure, iΔTgClpP1-3xHA localization was no longer detected, and apicoplast integrity was compromised and displayed a punctate localization. These data suggest that TgClpP1 localizes to the apicoplast and is important for apicoplast biogenesis and segregation.

The viability of iΔTgClpP1-3xHA was first tested with plaque assays. Plaque assays were done over the course of 7 days. The size of plaques formed by iΔTgClpP1-3xHA exposed to ATc was significantly smaller than iΔTgClpP1-3xHA cells not exposed to ATc. As a control, the TATiΔku80 strain was also analyzed by plaque assay in the presence and absence of ATc, and no difference in plaque size was observed, as

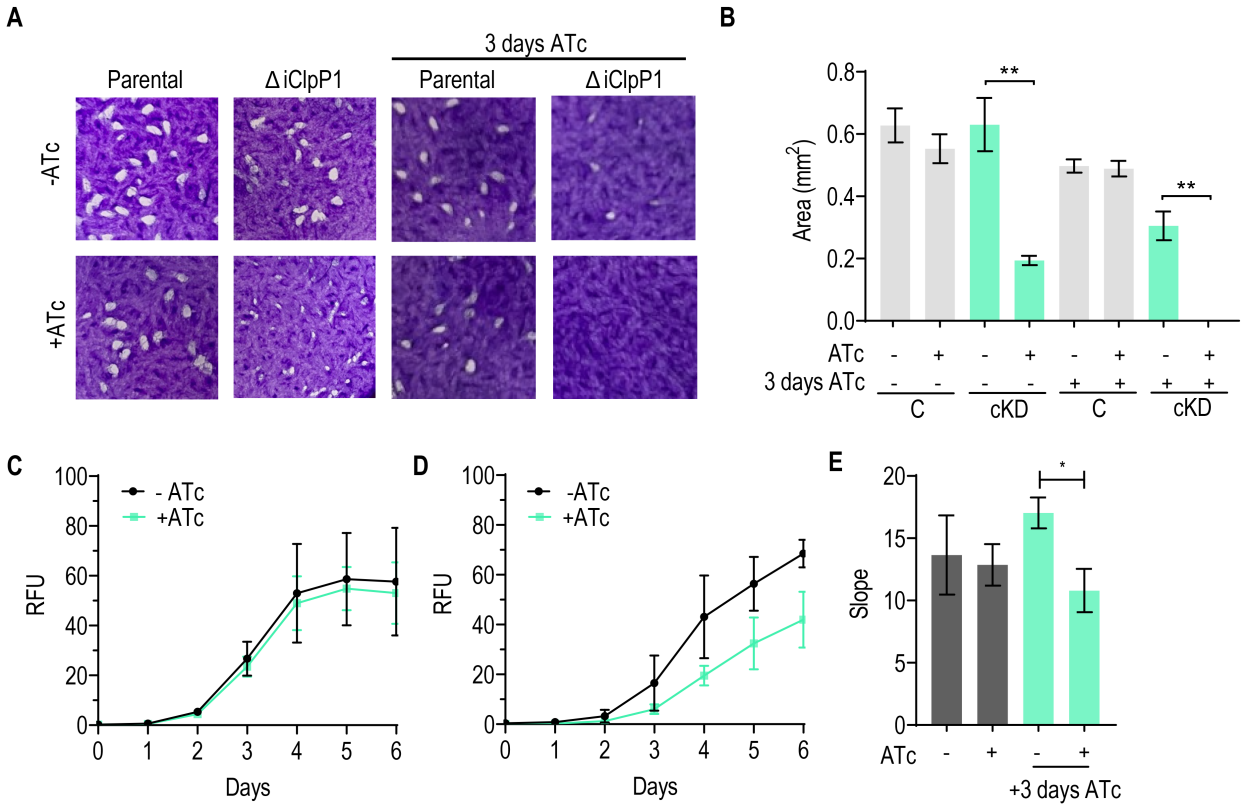

Figure 4.2 TgClpP1 is essential for the *T. gondii* lytic cycle. A) Plaque assays of TATiΔku80 (parental) and iΔTgClpP1-3xHA grown in + or – ATc for 7 days. 3 days ATc indicates parasites incubated in ATc for 3 additional days immediately prior to being seeded for the plaque assay experiment. B) Quantification of plaque area from A. Data is from 3 independent trials. 15 plaques were analyzed for each condition. C) Growth assay of iΔTgClpP1-3xHA-RFP in + or – ATc for 6 days. D) Growth assay of iΔTgClpP1-3xHA-RFP, preincubated in ATc for 3 days prior, in + or – ATc for 6 days. E) Slope of C) and D) from 2-5 days. Data is from 3 independent trials done in triplicate. B) and E), data indicates the mean ± SEM from 3 independent experiments. Data was analyzed with Student's t-test and *p<0.05 and **p<0.01.

expected. Drugs targeting the apicoplast function at a slower rate due to a phenomenon known as the delayed death phenotype (Kennedy *et al.*, 2019). This phenomenon has also been observed in the characterization of several apicoplast proteins such as, acyl carrier protein (ACP) (Mazumdar *et al.*, 2006) and integral membrane protein TgTic20 (van Dooren *et al.*, 2008). To address the potential delayed death phenotype, iΔTgClpP1-3xHA was preincubated in 3 days of ATc prior to seeding the plaque assay, and after 7 days the plaque sizes of iΔTgClpP1-3xHA were undetectable. Plate reader growth assays

using mutant parasites expressing RFP resulted in no difference in the growth kinetics between iΔTgClpP1-3xHA +/- ATc (Fig. 2C+E). However, after incubating the parasites in ATc for 3 days prior to the growth assay, a difference in the growth rate was detected Fig. 2D+E). The physiological role and mechanisms of action of the *T. gondii* Clp proteins are unknown. Here we showed that iΔTgClpP1-3xHA is important for the parasite's lytic cycle. Our results suggest that they might play an important role in apicoplast biogenesis and homeostasis.

To determine whether TgClpP1 was a target of cilnidipine, growth assays with RFP parasites were done in the presence of varying concentrations of cilnidipine. Cilnidipine inhibits growth of iΔTgClpP1-3xHA parasites in a dose dependent manner and the IC_{50} is around 2 μM (Fig. 3 A+B). In the knockdown mutants, there was no difference in percentage of parasites surviving in response to various cilnidipine concentrations (Fig. 3C+D). To ensure that this wasn't due to the delayed death phenotype induced by the absence of apicoplast specific proteins, we preincubated the parasites for 3 days in ATc. However, the results did not demonstrate any difference in the growth rate between the knockdown and cells consisting of wildtype expression levels of TgClpP1 (Fig. 3E-H). This indicates that the absence of ClpP1 does not confer resistance to cilnidipine, and ultimately suggests that TgClpP1 is not a target of cilnidipine.

Discussion

In this work, we implemented a CRISPR genome-wide screen in *T. gondii* in the presence of the VGCC inhibitor, cilnidipine. We were interested in determining the molecular target of cilnidipine and investigated the top hit from this screen, TgClpP1, to

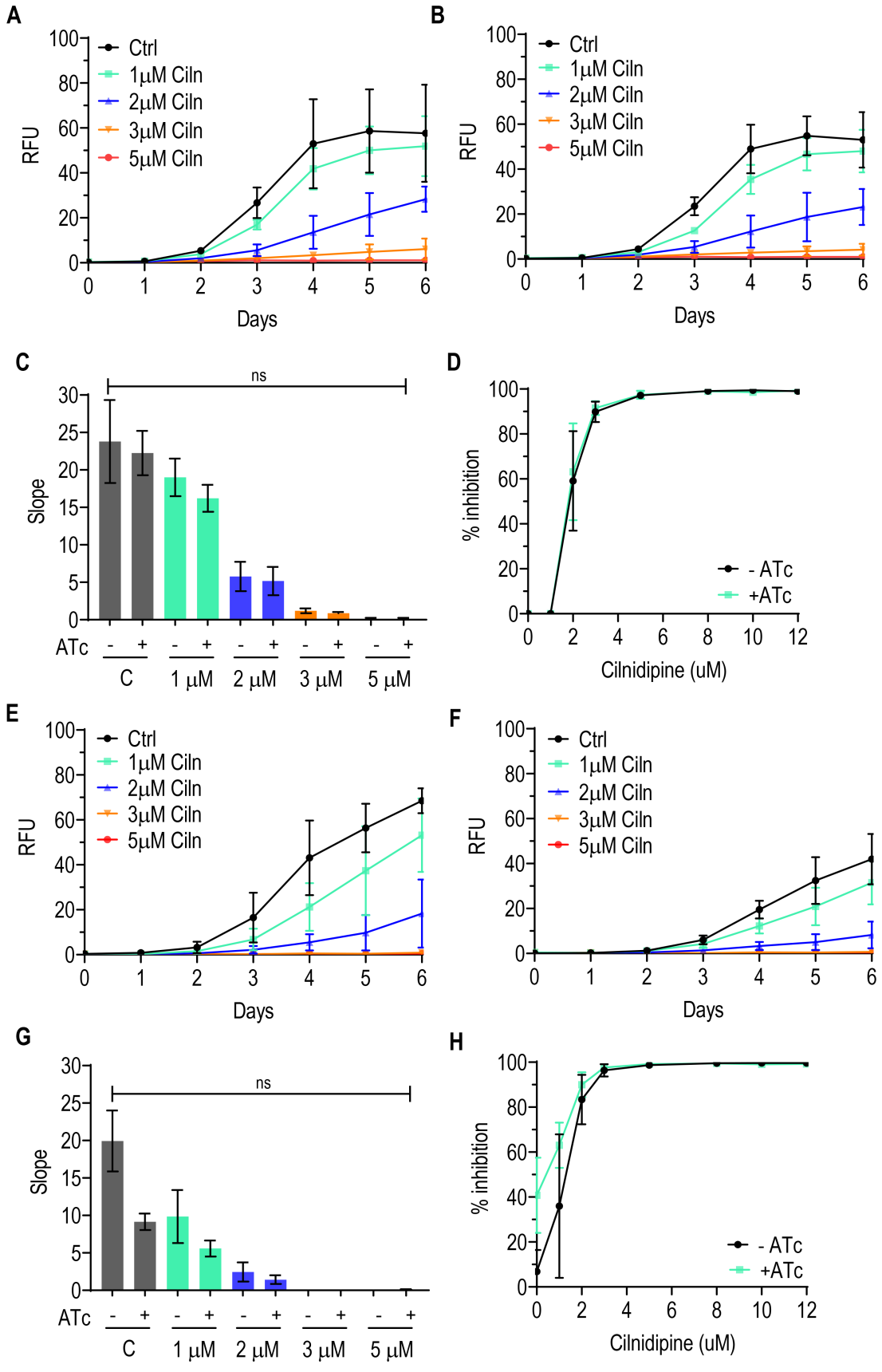
A
RFU
Days
Ctrl
1μM Ciln
2μM Ciln
3μM Ciln
5μM Ciln
B
RFU
Days
Ctrl
1μM Ciln
2μM Ciln
3μM Ciln
5μM Ciln
C
Slope
ns
ATc
C
1 μM
2 μM
3 μM
5 μM
D
% inhibition
- ATc
+ATc
Cilnidipine (uM)
E
RFU
Days
Ctrl
1μM Ciln
2μM Ciln
3μM Ciln
5μM Ciln
F
RFU
Days
Ctrl
1μM Ciln
2μM Ciln
3μM Ciln
5μM Ciln
G
Slope
ns
ATc
C
1 μM
2 μM
3 μM
5 μM
H
% inhibition
- ATc
+ATc
Cilnidipine (uM)

Fig. 4.3 iΔTgClpP1-3xHA is not resistant to cilnidipine. Growth assay of iΔTgClpP1-3xHA-RFP – ATc for 6 days in the presence of 0, 1, 2, 3 and 5 μM of cilndipine. B) Growth assay of iΔTgClpP1-3xHA-RFP + ATc for 6 days in the presence of 0, 1, 2, 3 and 5 μM of cilndipine. C) Slope of A) and B) from 2-4 days. Data is from 3 independent trials done in triplicate. D) % Inhibition dose response curve of iΔTgClpP1-3xHA-RFP + and – ATc in the presence of various cilnidipine concentrations on day 3 of growth. E) Growth assay of iΔTgClpP1-3xHA-RFP – ATc for 6 days in the presence of 0, 1, 2, 3 and 5 μM of cilnidipine, exposed to ATc 3 days prior to experiment. F) Growth assay of iΔTgClpP1-3xHA-RFP + ATc for 6 days in the presence of 0, 1, 2, 3 and 5 μM of cilnidipine, exposed to ATc 3 days prior to experiment. G) Slope of E) and F) from 2-4 days. Data is from 2 independent trials done in triplicate. H) % Inhibition dose response curve of iΔTgClpP1-3xHA-RFP + and – Atc (and grown in ATc 3 days prior) in the presence of various cilnidipine concentrations.

determine its specificity for cilnidipine. Our results showed that TgClpP1 does not appear to be a direct target of cilnidipine.

To obtain a possible hit list of cilnidipine, a CRISPR screen was performed in the presence of 5 μM cilnidipine. The genes demonstrating an increase in relative abundance of sgRNA did not appear to be related to Ca^{2+} signaling or regulation. Two of the genes from the screen, TgAtrx1 and TgClpP1 are both apicoplast specific proteins. Genes involved in tRNA biology and DNA replication also appeared. The remaining genes are hypothetical proteins that require further investigation. One unifying factor of this list is that they are all predicted as essential. The absence of these genes allowed the parasite to adapt to 5 μM of cilnidipine. It is difficult to understand why the absence of essential genes would benefit the parasite to survive in a toxic environment.

In addition to the top ten genes from the list, a large number of proteins from the list contained a 2-fold change in sgRNA relative abundance (data not shown), as opposed to the 6-fold change observed with TgClpP1 (Table 1). Several of these proteins did not contain an essential phenotype score. It is possible that targeting these proteins might reveal cilnidipine targets. Screening multiple proteins of interest from the list to increase

the possibility of finding a cilnidipine target could also reveal potential candidates. It is also possible that cilnidipine has off target effects. Our group established that 40 μM of cilnidpine is required to observe inhibition of Ca^{2+} entry (data not published), however the screen was performed in 5 μM cilnidipine, which is still an extremely potent amount of cilnidipine (Marquez-Nogueras *et al.*, 2021), but does not appear to have immediate Ca^{2+} inhibitory effects (Fig. 3A).

TgClpP1 was the primary candidate produced in the cilnidipine CRISPR screen. Since Atrx1 also appeared in the hit list, it raises the question whether the apicoplast plays a role in modulating Ca^{2+} influx. The apicoplast has been shown to contain Ca^{2+} and can sequester Ca^{2+} specifically from the ER, potentially through modulation of an apicoplast *T. gondii* Two-Pore Channel (TgTPC) (Li *et al.*, 2021). Is it possible that the apicoplast expresses an unidentified channel on its membrane that is a target of cilndipine? The investigation of TgClpP1 suggests that the apicoplast could serve as an important mechanism to handle stressful Ca^{2+} conditions in *T. gondii*. Additional studies need to be done to test this hypothesis.

Although TgClpP1 was not the apparent target of cilnidipine, the Clp machinery is a novel proteolytic system in *T. gondii* and this is the first time the apicoplast has been shown to have a role in protein degradation regulation. The Clp machinery is comprised of the chaperone and the proteolytic rings. In *P. falciparum*, Clp complex members have been identified and consist of the PfClpC chaperone, PfClpP and PfClpR (Florentin *et al.*, 2020). The complex localizes to the apicoplast, and processes proteins involved in translation, chaperone activity, redox biology, and lipid metabolism. Additionally, *P. falciparum* expresses ClpS, an adaptor protein hypothesized to be important for recruiting

Clp protein targets (AhYoung *et al.*, 2016; Florentin *et al.*, 2020; Peltier *et al.*, 2004). A ClpS homolog is also found in *T. gondii* (TGGT1_295910). It is also possible that TgClpP1 is responsible for processing the true target of cilnidipine or modulates another protein that interacts with the target of cilnidipine.

Although cilnidipine did not function as a ClpP inhibitor, ClpP protease activity has been tested and several inhibitors and stimulators have been identified. β-lactones are known inhibitors of ClpP that bind to the active site and block proteolytic activity (Gersch *et al.*, 2013). These compounds were first identified in *Staphylococcus aureus* (Bottcher & Sieber, 2008; Böttcher & Sieber, 2008) and are efficient in inhibiting PfClpP activity as well (El Bakkouri *et al.*, 2010; Rathore *et al.*, 2010). Acyldepeptidases (ADEPs) are a group of antibacterial drugs that also target ClpP in an unprecedented fashion. Normally ClpP binds to the Clp chaperone to process proteins, as opposed to just small peptides. ADEPs bind to the N-terminal region of ClpP and enlarge the pore of the ClpP heptameric ring causing proteolysis of larger products and unregulated levels of protease activity (Janine Kirstein, 2008). It is possible to test the catalytic activity of recombinant TgClpP1, 2 and ClpR in response to these various compounds to determine their specificity. Additionally, these compounds could be tested to determine their effect on the viability of *T. gondii*. These findings will show the importance of studying the mechanism of protease activity in plastids and simultaneously pave the path for protease targeted therapy in *T. gondii.*

CHAPTER 5

CONCLUSIONS AND FUTURE DIRECTIONS

In this work, we attempted several different strategies to uncover the mechanisms of Ca^{2+} signaling in *T. gondii*. Until now, only one calcium entry channel on the plasma membrane of the parasite has been identified and no release mechanisms from the ER have been identified. These are crucial and essential signaling molecules for parasite pathogenesis, and yet we know very little if anything about these proteins. Our lab and others in the *T. gondii* community have made significant progress on assembling the *T. gondii* Ca^{2+} signaling toolkit, but there is much yet left to uncover and understand.

In the literature review in this thesis (chapter 1), we explain the relationship between the ions, Ca^{2+} and protons, a topic that isn't often discussed and the literature available on this interaction is far and few between. To date, the relationship between protons and Ca^{2+}, two ions that need to be highly regulated and can impact function of a wide range of proteins through binding and release mechanisms, is not entirely understood. In vitro, Ca^{2+} and protons interact in a significantly different manner than in vivo, and they can compete with one another. It isn't often that genes encoding for Ca^{2+} related proteins are investigated for their role in pH regulation and vice versa. However, learning about this dynamic could allow us to learn more about the overall pathogenesis of the parasites, as these two ions can stimulate different parts of the lytic cycle.

In the second chapter, we investigate the relationship between protons and Ca^{2+} by determining the role of calcium/proton exchanger, TgCAXL1, in the lytic cycle of *T. gondii.* We find that TgCAXL1 affects Ca^{2+} signaling and homeostasis as well as pH regulation. Calcium/proton exchangers are generally expressed on highly acidic organelles or on the mitochondria. Discovery of a calcium/proton exchanger that displays dual localization on the ER and Golgi apparatus is novel. It brings into question the role of the endoplasmic reticulum in pH regulation. Although the ER is a bona fide

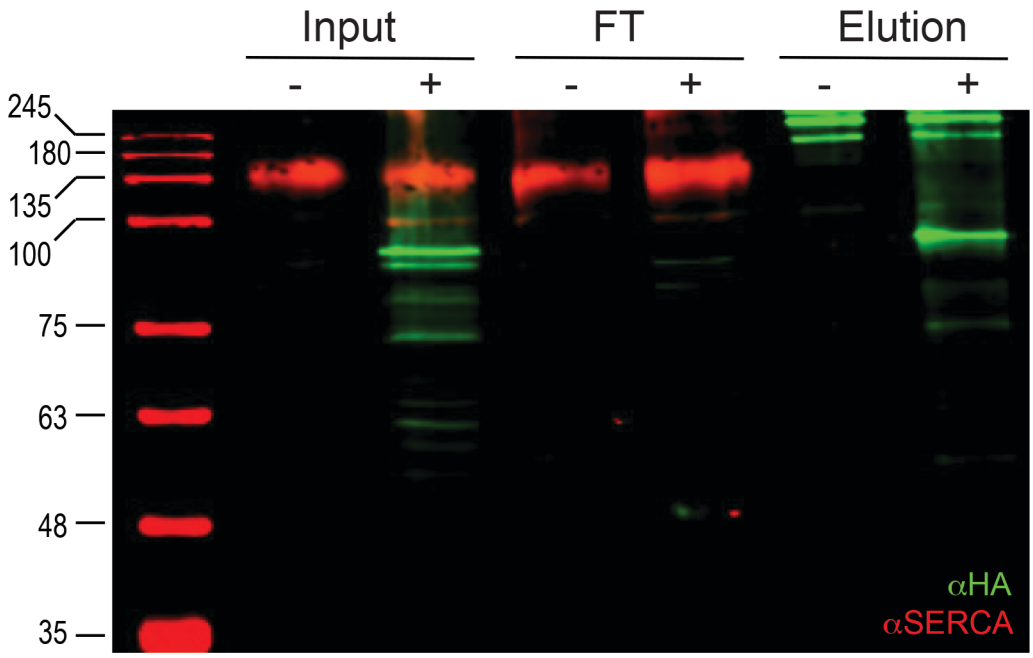

Figure 5.1 Co-immunoprecipation of TgCAXL1smHA. Western blot analysis of pull down of TgCAXL1smHA parasites and TATiΔKu80 negative control cell line. 2 x 10^8 were collected and incubated with HA conjugated beads. Input, flow through (FT) and immunoprecipitated (elution) samples were probed with rat-αHA and guinea pig-αSERCA. TgCAXL1smHA expected band size is 76 kDa and SERCA is 119 kDa. – indicates lysate from TATiΔKu80 lysate and + indicates TgCAXL1-SM lysate. FT= flow through. Protocol for this experiment is in Chapter 2 Materials and Methods.

Ca^{2+} store, it further supports that pH regulation and Ca^{2+} signaling cannot be separated. Future experiments consist of identifying interacting partners of TgCAXL1. We showed that TgCAXL1 affects TgSERCA activity, however under our co-immunoprecipitation conditions, we were not able to detect interaction (Fig. 5.1). It is

possible that the interaction between the two proteins is brief, and proximity labeling with TurboID might produce more representative results. It is also possible that TgCAXL1 and TgSERCA interact in an indirect manner, or there is another protein involved that mediates this interaction.

As previously mentioned, our lab is very interested in identifying novel Ca^{2+} signaling molecules. Reverse genetic approaches have allowed the community to advance a great deal in our knowledge about Ca^{2+} regulation, but we hypothesized that taking a forward genetic approach might reveal a novel gene. While our approaches by randomly mutagenizing the genome and subjecting the parasite to drug stress (chapter 3) and performing a positive selection drug strategy with a CRISPR genome-wide screen (chapter 4) were unsuccessful, we learned that we need to employ a different strategy. One potential strategy to identify ER calcium release proteins is to perform subcellular fractionation to enrich and isolate proteins only found at the ER membrane. Using this method in *T. gondii*, Ca^{2+} uptake mechanisms was discovered in acidocalcisomes (Rohloff *et al.*, 2011), the mitochondria complexome profile was determined (Maclean *et al.*, 2021), and the localization of over ~2,500 proteins within the parasite was predicted and shared on ToxoDB (Barylyuk *et al.*, 2020).

To conclude, the work in this dissertation has been novel and unique. We have tested several forward genetic methods and canonical reverse genetic techniques to characterize different proteins in the protozoan *T. gondii*. In doing so, we learned that TgCAXL1 is a novel calcium/proton exchanger and that pH is highly essential for Ca^{2+} signaling molecules. Ultimately, this work will broaden our understanding of the role of ions in *T. gondii* pathogenesis.

Bibliography

AhYoung, A. P., Koehl, A., Vizcarra, C. L., Cascio, D., & Egea, P. F. (2016). Structure of a putative ClpS N-end rule adaptor protein from the malaria pathogen Plasmodium falciparum. *Protein Sci, 25*(3), 689-701. doi:10.1002/pro.2868

Alday, P. H., & Doggett, J. S. (2017). Drugs in development for toxoplasmosis: advances, challenges, and current status. *Drug Des Devel Ther, 11*, 273-293. doi:10.2147/DDDT.S60973

Andrew Farrell, B. I. C., Brian Benenati1, Kevin M Brown, Ira J Blader, Gabor T Marth and Marc-Jan Gubbels. (2014). Whole genome profiling of spontaneous and chemically induced mutations in Toxoplasma gondii. *BMC Genomics, 15*, 534.

Angelika Herm-Gotz, S. W., Rolf Stratmann, S. F.-B., Christine Ruff, Edgar Meyhofer, Thierry Soldati, Dietmar J.Manstein, Michael A.Geeves and, & Soldati, D. (2002). Toxoplasma gondii myosin A and its light chain a fast single-headed. *The EMBO Jounrnal, 21*, 2149-2158.

Ann-Marie Gunteski-Hamblin, D. M. C., and Gary E. Shull. (1992). Molecular Cloning and Tissue Distribution of Alternatively Spliced mRNAs

Encoding Possible Mammalian Homologues of the Yeast Secretory Pathway Calcium Pump. *Biochemistry, 31*, 7600-7608. doi:10.1021/bi00148a023,

Arrizabalaga, G., Ruiz, F., Moreno, S., & Boothroyd, J. C. (2004). Ionophore-resistant mutant of Toxoplasma gondii reveals involvement of a sodium/hydrogen exchanger in calcium regulation. *J Cell Biol, 165*(5), 653-662. doi:10.1083/jcb.200309097

Atakpa, P., van Marrewijk, L. M., Apta-Smith, M., Chakraborty, S., & Taylor, C. W. (2019). GPN does not release lysosomal Ca(2+) but evokes Ca(2+) release from the ER by increasing the cytosolic pH independently of cathepsin C. *J Cell Sci, 132*(3). doi:10.1242/jcs.223883

Bammens, R., Mehta, N., Race, V., Foulquier, F., Jaeken, J., Tiemeyer, M., . . . Flanagan-Steet, H. (2015). Abnormal cartilage development and altered N-glycosylation in Tmem165-deficient zebrafish mirrors the phenotypes associated with TMEM165-CDG. *Glycobiology, 25*(6), 669-682. doi:10.1093/glycob/cwv009

Barylyuk, K., Koreny, L., Ke, H., Butterworth, S., Crook, O. M., Lassadi, I., . . . Waller, R. F. (2020). A Comprehensive Subcellular Atlas of the Toxoplasma Proteome via hyperLOPIT Provides Spatial Context for Protein Functions. *Cell Host Microbe, 28*(5), 752-766 e759. doi:10.1016/j.chom.2020.09.011

Biddau, M., Bouchut, A., Major, J., Saveria, T., Tottey, J., Oka, O., . . . Sheiner, L. (2018). Two essential Thioredoxins mediate apicoplast biogenesis, protein import, and gene expression in Toxoplasma gondii. *PLoS Pathog, 14*(2), e1006836. doi:10.1371/journal.ppat.1006836

Bindels, D. S., Haarbosch, L., van Weeren, L., Postma, M., Wiese, K. E., Mastop, M., . . . Gadella, T. W., Jr. (2017). mScarlet: a bright monomeric red fluorescent protein for cellular imaging. *Nat Methods, 14*(1), 53-56. doi:10.1038/nmeth.4074

Birgisdottir, A., Asbjornsdottir, H., Cook, E., Gislason, D., Jansson, C., Olafsson, I., . . . Thjodleifsson, B. (2006). Seroprevalence of Toxoplasma gondii in Sweden, Estonia and Iceland. *Scand J Infect Dis, 38*(8), 625-631. doi:10.1080/00365540600606556

Björn F. C. Kafsack, J. D. O. P., Isabelle Coppens, Sandeep Ravindran, John C. Boothroyd, Vern B. Carruthers. (2009). Rapid Membrane Disruption by a Perforin-Like Protein Facilitates Parasite Exit from Host Cells. *Science 323*.

Blader, I. J., Coleman, B. I., Chen, C. T., & Gubbels, M. J. (2015). Lytic Cycle of Toxoplasma gondii: 15 Years Later. *Annu Rev Microbiol, 69*, 463-485. doi:10.1146/annurev-micro-091014-104100

Boczek, T., Lisek, M., Ferenc, B., Kowalski, A., Stepinski, D., Wiktorska, M., & Zylinska, L. (2014). Plasma membrane Ca2+-ATPase isoforms composition regulates cellular pH homeostasis in differentiating PC12 cells in a manner dependent on cytosolic Ca2+ elevations. *PLoS One, 9*(7), e102352. doi:10.1371/journal.pone.0102352

Borges-Pereira, L., Budu, A., McKnight, C. A., Moore, C. A., Vella, S. A., Hortua Triana, M. A., . . . Moreno, S. N. J. (2015). Calcium Signaling throughout the Toxoplasma gondii Lytic Cycle: A STUDY USING GENETICALLY ENCODED CALCIUM INDICATORS. *J Biol Chem, 290*(45), 26914-26926. doi:10.1074/jbc.M115.652511

Bottcher, T., & Sieber, S. A. (2008). Beta-lactones as privileged structures for the active-site labeling of versatile bacterial enzyme classes. *Angew Chem Int Ed Engl, 47*(24), 4600-4603. doi:10.1002/anie.200705768

Böttcher, T., & Sieber, S. A. (2008). β-lactones as specific inhibitors of ClpP attenuate the production of extracellular virulence factors of Staphylococcus aureus. *Journal of the American Chemical Society, 130*(44), 14400-14401.

Brydges, S. D., Harper, J. M., Parussini, F., Coppens, I., & Carruthers, V. B. (2008). A transient forward-targeting element for microneme-regulated secretion in Toxoplasma gondii. *Biol Cell, 100*(4), 253-264. doi:10.1042/BC20070076

Bzik, B. A. F. D. J. (2002). De novo pyrimidine biosynthesis is required for virulence of Toxoplasma gondii. *Nature, 415*.

Cai, X., & Lytton, J. (2004). The cation/Ca(2+) exchanger superfamily: phylogenetic analysis and structural implications. *Mol Biol Evol, 21*(9), 1692-1703. doi:10.1093/molbev/msh177

Capiod, T. (2011). Cell proliferation, calcium influx and calcium channels. *Biochimie, 93*(12), 2075-2079. doi:10.1016/j.biochi.2011.07.015

Chikashi Toyoshima, M. N., Hiromi Nomura & Haruo Ogawa. (2000). Crystal structure of the calcium pump of sarcoplasmic reticulum at 2.6 A resolution. *Nature, 405*.

Clapham, D. E. (2007). Calcium signaling. *Cell, 131*(6), 1047-1058. doi:10.1016/j.cell.2007.11.028

Coleman, B. I., & Gubbels, M. J. (2012). A genetic screen to isolate Toxoplasma gondii host-cell egress mutants. *J Vis Exp*(60). doi:10.3791/3807

Colinet, A. S., Sengottaiyan, P., Deschamps, A., Colsoul, M. L., Thines, L., Demaegd, D., . . . Morsomme, P. (2016). Yeast Gdt1 is a Golgi-localized calcium transporter required for stress-induced calcium signaling and protein glycosylation. *Sci Rep, 6*, 24282. doi:10.1038/srep24282

Courret, N., Darche, S., Sonigo, P., Milon, G., Buzoni-Gatel, D., & Tardieux, I. (2006). CD11c- and CD11b-expressing mouse leukocytes transport single Toxoplasma gondii tachyzoites to the brain. *Blood, 107*(1), 309-316. doi:10.1182/blood-2005-02-0666

Cunningham, K. W. (2011). Acidic calcium stores of Saccharomyces cerevisiae. *Cell Calcium, 50*(2), 129-138. doi:10.1016/j.ceca.2011.01.010

Da Gama, L. M., Ribeiro-Gomes, F. L., Guimaraes, U., Jr., & Arnholdt, A. C. (2004). Reduction in adhesiveness to extracellular matrix components, modulation of adhesion molecules and in vivo migration of murine macrophages infected with Toxoplasma gondii. *Microbes Infect, 6*(14), 1287-1296. doi:10.1016/j.micinf.2004.07.008

Darrick Carter, R. G. K. D., David Roos, Buddy Ullman (1997). Expression, purification, and characterization of uracil phosphoribosyltransferase from Toxoplasma gondii. *Molecular and Biochemical Parasitology, 87*, 137-144.

Demaegd, D., Colinet, A. S., Deschamps, A., & Morsomme, P. (2014). Molecular evolution of a novel family of putative calcium transporters. *PLoS One, 9*(6), e100851. doi:10.1371/journal.pone.0100851

Demaegd, D., Foulquier, F., Colinet, A. S., Gremillon, L., Legrand, D., Mariot, P., . . . Morsomme, P. (2013). Newly characterized Golgi-localized family of proteins is involved in calcium and pH homeostasis in yeast and human cells. *Proc Natl Acad Sci U S A, 110*(17), 6859-6864. doi:10.1073/pnas.1219871110

DeMarco, S. J., & Strehler, E. E. (2001). Plasma membrane Ca2+-atpase isoforms 2b and 4b interact promiscuously and selectively with members of the membrane-associated guanylate kinase family of PDZ (PSD95/Dlg/ZO-1) domain-containing proteins. *J Biol Chem, 276*(24), 21594-21600. doi:10.1074/jbc.M101448200

Dereeper, A., Guignon, V., Blanc, G., Audic, S., Buffet, S., Chevenet, F., . . . Gascuel, O. (2008). Phylogeny.fr: robust phylogenetic analysis for the non-specialist. *Nucleic Acids Res, 36*(Web Server issue), W465-469. doi:10.1093/nar/gkn180

Ding, J., Luo, A. F., Hu, L., Wang, D., & Shao, F. (2014). Structural basis of the ultrasensitive calcium indicator GCaMP6. *Sci China Life Sci, 57*(3), 269-274. doi:10.1007/s11427-013-4599-5

Dolman, N. J., & Tepikin, A. V. (2006). Calcium gradients and the Golgi. *Cell Calcium, 40*(5-6), 505-512. doi:10.1016/j.ceca.2006.08.012

Dubey, J. P. (2004). Toxoplasmosis - a waterborne zoonosis. *Vet Parasitol, 126*(1-2), 57-72. doi:10.1016/j.vetpar.2004.09.005

Dubey, J. P., & Jones, J. L. (2008). Toxoplasma gondii infection in humans and animals in the United States. *Int J Parasitol, 38*(11), 1257-1278. doi:10.1016/j.ijpara.2008.03.007

Dubey, J. P., Lago, E. G., Gennari, S. M., Su, C., & Jones, J. L. (2012). Toxoplasmosis in humans and animals in Brazil: high prevalence, high burden of disease, and epidemiology. *Parasitology, 139*(11), 1375-1424. doi:10.1017/S0031182012000765

Dubey, J. P., Murata, F. H. A., Cerqueira-Cezar, C. K., Kwok, O. C. H., & Grigg, M. E. (2020). Recent epidemiologic and clinical importance of Toxoplasma gondii infections in marine mammals: 2009-2020. *Vet Parasitol, 288*, 109296. doi:10.1016/j.vetpar.2020.109296

Dulary, E., Yu, S. Y., Houdou, M., de Bettignies, G., Decool, V., Potelle, S., . . . Foulquier, F. (2018). Investigating the function of Gdt1p in yeast Golgi glycosylation. *Biochim Biophys Acta Gen Subj, 1862*(3), 394-402. doi:10.1016/j.bbagen.2017.11.006

El Bakkouri, M., Pow, A., Mulichak, A., Cheung, K. L., Artz, J. D., Amani, M., . . . Houry, W. A. (2010). The Clp chaperones and proteases of the human malaria parasite Plasmodium falciparum. *J Mol Biol, 404*(3), 456-477. doi:10.1016/j.jmb.2010.09.051

Elijah W. Stommel, K. H. E., Joseph D. Schwartzman, and Lloyd H. Kasper. (1997). Toxoplasma gondii: Dithiol-Induced Ca2+ Flux Causes Egress of Parasites from the Parasitophorous Vacuole. *Experimental Parasitology, 87*, 88-97.

Elmore, S. A., Jones, J. L., Conrad, P. A., Patton, S., Lindsay, D. S., & Dubey, J. P. (2010). Toxoplasma gondii: epidemiology, feline clinical aspects, and prevention. *Trends Parasitol, 26*(4), 190-196. doi:10.1016/j.pt.2010.01.009

Espinoza-Fonseca, L. M. (2017). The Ca(2+)-ATPase pump facilitates bidirectional proton transport across the sarco/endoplasmic reticulum. *Mol Biosyst, 13*(4), 633-637. doi:10.1039/c7mb00065k

F. Wuytack, L. R., L. Missiaen. (2002). Molecular physiology of the SERCA and SPCA pumps. *Cell Calcium 35*(5-6), 279-305

. doi:10.1016/S0143-4160(02)00184-7

Fasolato, C., Zottini, M., Clementi, E., Zacchetti, D., Meldolesi, J., & Pozzan, T. (1991). Intracellular Ca2+ pools in PC12 cells. Three intracellular pools are distinguished by their turnover and mechanisms of Ca2+ accumulation, storage, and release. *Journal of Biological Chemistry, 266*(30), 20159-20167. doi:10.1016/s0021-9258(18)54904-8

Feng, J., Michalik, S., Varming, A. N., Andersen, J. H., Albrecht, D., Jelsbak, L., . . . Frees, D. (2013). Trapping and proteomic identification of cellular substrates of the ClpP protease in Staphylococcus aureus. *J Proteome Res, 12*(2), 547-558. doi:10.1021/pr300394r

Fink, K. W. C. a. G. R. (1996). Calcineurin Inhibits VCX1-Dependent H?/Ca2? Exchange and Induces Ca2? ATPases in Saccharomyces cerevisiae. *Molecular and cellulary biology, 16*, 2226-2237.

Florentin, A., Cobb, D. W., Fishburn, J. D., Cipriano, M. J., Kim, P. S., Fierro, M. A., . . . Muralidharan, V. (2017). PfClpC Is an Essential Clp Chaperone Required for Plastid Integrity and Clp Protease Stability in Plasmodium falciparum. *Cell Rep, 21*(7), 1746-1756. doi:10.1016/j.celrep.2017.10.081

Florentin, A., Stephens, D. R., Brooks, C. F., Baptista, R. P., & Muralidharan, V. (2020). Plastid biogenesis in malaria parasites requires the interactions and catalytic activity of the Clp proteolytic system. *Proc Natl Acad Sci U S A, 117*(24), 13719-13729. doi:10.1073/pnas.1919501117

Flynn, J. M., Neher, S. B., Kim, Y.-I., Sauer, R. T., & Baker, T. A. (2003). Proteomic Discovery of Cellular Substrates of the ClpXP Protease Reveals Five Classes of ClpX-Recognition Signals. *Molecular Cell, 11*(3), 671-683. doi:10.1016/s1097-2765(03)00060-1

Foskett, J. K., White, C., Cheung, K. H., & Mak, D. O. (2007). Inositol trisphosphate receptor Ca2+ release channels. *Physiol Rev, 87*(2), 593-658. doi:10.1152/physrev.00035.2006

Foulquier, F., Amyere, M., Jaeken, J., Zeevaert, R., Schollen, E., Race, V., . . . Matthijs, G. (2012). TMEM165 deficiency causes a congenital disorder of glycosylation. *Am J Hum Genet, 91*(1), 15-26. doi:10.1016/j.ajhg.2012.05.002

Francia, M. E., & Striepen, B. (2014). Cell division in apicomplexan parasites. *Nat Rev Microbiol, 12*(2), 125-136. doi:10.1038/nrmicro3184

Fredy Cifuentesa, C. E. G., Tatiana Fiordelisioa, Georgina Guerreroa, F. Anthony Laib, Arturo Hernandez-Cruza. (2001). A ryanodine fluorescent derivative reveals the presence of high-affinity ryanodine binding sites in the Golgi complex of rat sympathetic neurons, with possible functional roles in intracellular Ca2+ signaling

. *Cellular Signaling, 13*, 353-362.

Frenal, K., Polonais, V., Marq, J. B., Stratmann, R., Limenitakis, J., & Soldati-Favre, D. (2010). Functional dissection of the apicomplexan glideosome molecular architecture. *Cell Host Microbe, 8*(4), 343-357. doi:10.1016/j.chom.2010.09.002

Gadsby, D. C. (2009). Ion channels versus ion pumps: the principal difference, in principle. *Nat Rev Mol Cell Biol, 10*(5), 344-352. doi:10.1038/nrm2668

Gaskins, E., Gilk, S., DeVore, N., Mann, T., Ward, G., & Beckers, C. (2004). Identification of the membrane receptor of a class XIV myosin in Toxoplasma gondii. *J Cell Biol, 165*(3), 383-393. doi:10.1083/jcb.200311137

Gersch, M., Gut, F., Korotkov, V. S., Lehmann, J., Bottcher, T., Rusch, M., . . . Sieber, S. A. (2013). The mechanism of caseinolytic protease (ClpP) inhibition. *Angew Chem Int Ed Engl, 52*(10), 3009-3014. doi:10.1002/anie.201204690

Gispert, S., Parganlija, D., Klinkenberg, M., Drose, S., Wittig, I., Mittelbronn, M., . . . Auburger, G. (2013). Loss of mitochondrial peptidase Clpp leads to infertility, hearing loss plus growth retardation via accumulation of CLPX, mtDNA and inflammatory factors. *Hum Mol Genet, 22*(24), 4871-4887. doi:10.1093/hmg/ddt338

Goujon, M., McWilliam, H., Li, W., Valentin, F., Squizzato, S., Paern, J., & Lopez, R. (2010). A new bioinformatics analysis tools framework at EMBL-EBI. *Nucleic Acids Res, 38*(Web Server issue), W695-699. doi:10.1093/nar/gkq313

Grynkiewicz, G., Poenie, M., & Tsien, R. Y. (1985). A new generation of Ca2+ indicators with greatly improved fluorescence properties. *Journal of Biological Chemistry, 260*(6), 3440-3450. doi:10.1016/s0021-9258(19)83641-4

Gubbels, M. J., Lehmann, M., Muthalagi, M., Jerome, M. E., Brooks, C. F., Szatanek, T., . . . White, M. W. (2008). Forward genetic analysis of the apicomplexan cell division cycle in Toxoplasma gondii. *PLoS Pathog, 4*(2), e36. doi:10.1371/journal.ppat.0040036

Guttery, D. S., Pittman, J. K., Frenal, K., Poulin, B., McFarlane, L. R., Slavic, K., . . . Staines, H. M. (2013). The Plasmodium berghei Ca(2+)/H(+) exchanger, PbCAX, is essential for tolerance to environmental Ca(2+) during sexual development. *PLoS Pathog, 9*(2), e1003191. doi:10.1371/journal.ppat.1003191

Hammoudi, P. M., Jacot, D., Mueller, C., Di Cristina, M., Dogga, S. K., Marq, J. B., . . . Soldati-Favre, D. (2015). Fundamental Roles of the Golgi-Associated

Toxoplasma Aspartyl Protease, ASP5, at the Host-Parasite Interface. *PLoS Pathog, 11*(10), e1005211. doi:10.1371/journal.ppat.1005211
Harker, K. S., Ueno, N., & Lodoen, M. B. (2015). Toxoplasma gondii dissemination: a parasite's journey through the infected host. *Parasite Immunol, 37*(3), 141-149. doi:10.1111/pim.12163
Henk de Vries, G. M. J. B. v. H. (1998). Photoreactivity of nifedipine in vitro and in vivo. *Journal of Photochemistryand Photobiology*(43), 217-221.
Hodder, P., Mull, R., Cassaday, J., Berry, K., & Strulovici, B. (2004). Miniaturization of intracellular calcium functional assays to 1536-well plate format using a fluorometric imaging plate reader. *J Biomol Screen, 9*(5), 417-426. doi:10.1177/1087057104264038
Hortua Triana, M. A., Marquez-Nogueras, K. M., Chang, L., Stasic, A. J., Li, C., Spiegel, K. A., . . . Moreno, S. N. J. (2018). Tagging of Weakly Expressed Toxoplasma gondii Calcium-Related Genes with High-Affinity Tags. *J Eukaryot Microbiol, 65*(5), 709-721. doi:10.1111/jeu.12626
Hortua Triana, M. A., Marquez-Nogueras, K. M., Vella, S. A., & Moreno, S. N. J. (2018). Calcium signaling and the lytic cycle of the Apicomplexan parasite Toxoplasma gondii *Biochim Biophys Acta Mol Cell Res, 1865*(11 Pt B), 1846-1856. doi:10.1016/j.bbamcr.2018.08.004
Howard, B. L., Harvey, K. L., Stewart, R. J., Azevedo, M. F., Crabb, B. S., Jennings, I. G., . . . Gilson, P. R. (2015). Identification of potent phosphodiesterase inhibitors that demonstrate cyclic nucleotide-dependent functions in apicomplexan parasites. *ACS Chem Biol, 10*(4), 1145-1154. doi:10.1021/cb501004q
Huynh, M.-H., & Carruthers, V. B. (2021). Toxoplasma gondii excretion of glycolytic products is associated with acidification of the parasitophorous vacuole during parasite egress. *BioRxiv*. doi:10.1101/2021.11.25.469974
Huynh, M. H., & Carruthers, V. B. (2009). Tagging of endogenous genes in a Toxoplasma gondii strain lacking Ku80. *Eukaryot Cell, 8*(4), 530-539. doi:10.1128/EC.00358-08
Huynh, M. H., & Carruthers, V. B. (2022). Toxoplasma gondii excretion of glycolytic products is associated with acidification of the parasitophorous vacuole during parasite egress. *PLoS Pathog, 18*(5), e1010139. doi:10.1371/journal.ppat.1010139
Inesi, G., & Tadini-Buoninsegni, F. (2014). Ca(2+)/H (+) exchange, lumenal Ca(2+) release and Ca (2+)/ATP coupling ratios in the sarcoplasmic reticulum ATPase. *J Cell Commun Signal, 8*(1), 5-11. doi:10.1007/s12079-013-0213-7
Innes, E. A. (2010). A brief history and overview of Toxoplasma gondii. *Zoonoses Public Health, 57*(1), 1-7. doi:10.1111/j.1863-2378.2009.01276.x
J. P. DUBEY, D. S. L., AND C. A. SPEER. (1998). Structures of Toxoplasma gondii Tachyzoites, Bradyzoites, and Sporozoites and Biology and Development of Tissue Cysts. *CLINICAL MICROBIOLOGY REVIEWS, 11*, 267-299.
Jackson, A. J., Clucas, C., Mamczur, N. J., Ferguson, D. J., & Meissner, M. (2013). Toxoplasma gondii Syntaxin 6 is required for vesicular transport between endosomal-like compartments and the Golgi complex. *Traffic, 14*(11), 1166-1181. doi:10.1111/tra.12102

James, P., Maeda, M., Fischer, R., Verma, A. K., Krebs, J., Penniston, J. T., & Carafoli, E. (1988). Identification and primary structure of a calmodulin binding domain of the Ca2+ pump of human erythrocytes. *Journal of Biological Chemistry, 263*(6), 2905-2910. doi:10.1016/s0021-9258(18)69154-9

Janine Kirstein, A. H., Hauke Lilie, Ronny Schmidt, Helga Rubsamen-Waigmann, Heike Brotz-Oesterhelt, Axel Mogk, Kursad Turgay. (2008). The antibiotic ADEP reprogrammes ClpP switching it from a regulated to an uncontrolled. *EMBO Molecular Medicine, 1*, 37-49.

Jesper V. Moller, B. J., Marc le Maire (1996). Structural organization, ion transport, and energy transduction of P-type ATPases. *Biochimica et Biophysica Acta, 1286*.

Junichi Nakai, M. O., and Keiji Imoto. (2001). A high signal-to-noise Ca2+ probe composed of a single green fluorescent protein. *Nature Biotechnology, 19*.

Kafsack, B. F., Beckers, C., & Carruthers, V. B. (2004). Synchronous invasion of host cells by Toxoplasma gondii. *Mol Biochem Parasitol, 136*(2), 309-311. doi:10.1016/j.molbiopara.2004.04.004

Ke Hu, T. M., Boris Striepen, Con J. M. Beckers, David S. Roos, and John M. Murray. (2002). Daughter Cell Assembly in the Protozoan Parasite Toxoplasma gondii *Molecular Biology of the Cell, 13*, 503-606. doi:10.1091/mbc.01-

Kennedy, K., Crisafulli, E. M., & Ralph, S. A. (2019). Delayed Death by Plastid Inhibition in Apicomplexan Parasites. *Trends in Parasitology, 35*(10), 747-759. doi:10.1016/j.pt.2019.07.010

Kim, J. H., Lee, S. R., Li, L. H., Park, H. J., Park, J. H., Lee, K. Y., . . . Choi, S. Y. (2011). High cleavage efficiency of a 2A peptide derived from porcine teschovirus-1 in human cell lines, zebrafish and mice. *PLoS One, 6*(4), e18556. doi:10.1371/journal.pone.0018556

Krishna, S., Woodrow, C., Webb, R., Penny, J., Takeyasu, K., Kimura, M., & East, J. M. (2001). Expression and functional characterization of a Plasmodium falciparum Ca2+-ATPase (PfATP4) belonging to a subclass unique to apicomplexan organisms. *J Biol Chem, 276*(14), 10782-10787. doi:10.1074/jbc.M010554200

Kulkarni, A., Shirsat, M. K., & Tiwari, B. (2020). Development and Validation of Stability Indicating RP-HPLC Method for Estimation of Cilnidipine. *Journal of Drug Delivery and Therapeutics, 10*(1), 97-100. doi:10.22270/jddt.v10i1.3846

Laurence Pelletier, C. A. S., Marc Pypaert, David Sheff, Huan M. Ngo, Nitin Roper, Cynthia Y. He, Ke Hu, Derek Toomre, Isabelle Coppens, David S. Roos, Keith A. Joiner & Graham Warren. (2002). Golgi biogenesis in Toxoplasma gondii. *Nature, 418*(548-552). doi:10.1038/nature00864

Lehane, A. M., Dennis, A. S. M., Bray, K. O., Li, D., Rajendran, E., McCoy, J. M., . . . van Dooren, G. G. (2019). Characterization of the ATP4 ion pump in Toxoplasma gondii. *J Biol Chem, 294*(14), 5720-5734. doi:10.1074/jbc.RA118.006706

Li, S., Hao, B., Lu, Y., Yu, P., Lee, H. C., & Yue, J. (2012). Intracellular alkalinization induces cytosolic Ca2+ increases by inhibiting sarco/endoplasmic reticulum Ca2+-ATPase (SERCA). *PLoS One, 7*(2), e31905. doi:10.1371/journal.pone.0031905

Li, Z. H., King, T. P., Ayong, L., Asady, B., Cai, X., Rahman, T., . . . Moreno, S. N. J. (2021). A plastid two-pore channel essential for inter-organelle communication

and growth of Toxoplasma gondii. *Nat Commun, 12*(1), 5802. doi:10.1038/s41467-021-25987-5
Liou, J., Kim, M. L., Heo, W. D., Jones, J. T., Myers, J. W., Ferrell, J. E., Jr., & Meyer, T. (2005). STIM is a Ca2+ sensor essential for Ca2+-store-depletion-triggered Ca2+ influx. *Curr Biol, 15*(13), 1235-1241. doi:10.1016/j.cub.2005.05.055
Lipmann, S. E. a. F. (1962). Adenosine triphosphate-linked concentration of calcium ions in a particulate fraction of rabbit muscle. *The Journal of Cell Biology*.
Lourido, S., Tang, K., & Sibley, L. D. (2012). Distinct signalling pathways control Toxoplasma egress and host-cell invasion. *EMBO J, 31*(24), 4524-4534. doi:10.1038/emboj.2012.299
Luo, G. Z., Wang, H. W., Huang, J., Tian, A. G., Wang, Y. J., Zhang, J. S., & Chen, S. Y. (2005). A putative plasma membrane cation/proton antiporter from soybean confers salt tolerance in Arabidopsis. *Plant Mol Biol, 59*(5), 809-820. doi:10.1007/s11103-005-1386-0
Luo, S., Ruiz, F. A., & Moreno, S. N. (2005). The acidocalcisome Ca2+-ATPase (TgA1) of Toxoplasma gondii is required for polyphosphate storage, intracellular calcium homeostasis and virulence. *Mol Microbiol, 55*(4), 1034-1045. doi:10.1111/j.1365-2958.2004.04464.x
Maclean, A. E., Bridges, H. R., Silva, M. F., Ding, S., Ovciarikova, J., Hirst, J., & Sheiner, L. (2021). Complexome profile of Toxoplasma gondii mitochondria identifies divergent subunits of respiratory chain complexes including new subunits of cytochrome bc1 complex. *PLoS Pathog, 17*(3), e1009301. doi:10.1371/journal.ppat.1009301
Makani, S., & Chesler, M. (2010). Rapid rise of extracellular pH evoked by neural activity is generated by the plasma membrane calcium ATPase. *J Neurophysiol, 103*(2), 667-676. doi:10.1152/jn.00948.2009
Marquez-Nogueras, K. M., Hortua Triana, M. A., Chasen, N. M., Kuo, I. Y., & Moreno, S. N. (2021). Calcium signaling through a transient receptor channel is important for Toxoplasma gondii growth. *Elife, 10*. doi:10.7554/eLife.63417
Martin D. Ryan, A. M. Q. K. a. G. P. T. (1991). Cleavage of foot-and-mouth disease virus polyprotein is mediated by residues located within a 19 amino acid sequence. *Journal of General Virology, 72*, 2727-2732.
Martorelli Di Genova, B., & Knoll, L. J. (2020). Comparisons of the Sexual Cycles for the Coccidian Parasites Eimeria and Toxoplasma. *Front Cell Infect Microbiol, 10*, 604897. doi:10.3389/fcimb.2020.604897
Mazumdar, J., E, H. W., Masek, K., C, A. H., & Striepen, B. (2006). Apicoplast fatty acid synthesis is essential for organelle biogenesis and parasite survival in Toxoplasma gondii. *Proc Natl Acad Sci U S A, 103*(35), 13192-13197. doi:10.1073/pnas.0603391103
McCoy, J. M., Stewart, R. J., Uboldi, A. D., Li, D., Schroder, J., Scott, N. E., . . . Tonkin, C. J. (2017). A forward genetic screen identifies a negative regulator of rapid Ca(2+)-dependent cell egress (MS1) in the intracellular parasite Toxoplasma gondii. *J Biol Chem, 292*(18), 7662-7674. doi:10.1074/jbc.M117.775114
McFadden, G. I., & Yeh, E. (2017). The apicoplast: now you see it, now you don't. *Int J Parasitol, 47*(2-3), 137-144. doi:10.1016/j.ijpara.2016.08.005

Melchionda, M., Pittman, J. K., Mayor, R., & Patel, S. (2016). Ca2+/H+ exchange by acidic organelles regulates cell migration in vivo. *J Cell Biol, 212*(7), 803-813. doi:10.1083/jcb.201510019

Miranda, K., Pace, D. A., Cintron, R., Rodrigues, J. C., Fang, J., Smith, A., . . . Moreno, S. N. (2010). Characterization of a novel organelle in Toxoplasma gondii with similar composition and function to the plant vacuole. *Mol Microbiol, 76*(6), 1358-1375. doi:10.1111/j.1365-2958.2010.07165.x

Mizutani, C. T. T. (2004). Crystal structure of the calcium pump with a bound ATP analogue. *Nature, 430*.

Molinari, G., & Nervo, E. (2021). Role of protons in calcium signaling. *Biochem J, 478*(4), 895-910. doi:10.1042/BCJ20200971

Montoya, J. G., & Remington, J. S. (2008). Management of Toxoplasma gondii infection during pregnancy. *Clin Infect Dis, 47*(4), 554-566. doi:10.1086/590149

Morlon-Guyot, J., Berry, L., Chen, C. T., Gubbels, M. J., Lebrun, M., & Daher, W. (2014). The Toxoplasma gondii calcium-dependent protein kinase 7 is involved in early steps of parasite division and is crucial for parasite survival. *Cell Microbiol, 16*(1), 95-114. doi:10.1111/cmi.12186

N. D. Levine, J. O. C., F. E. G. Cox, G. Deroux, J. Grain, B. M. Honiberg G. F. Leedale, A. R. Loeblich, J. Lom, D. Lynn, E. G. Merinfeld, F. C. Page,, & G. Poljansky, V. S., J. Vavra, and F. G. Wallace. (1980). Newly Revised Classification of the Protozoa. *The Journal of Protozoology 27*.

Nagamune, K., Beatty, W. L., & Sibley, L. D. (2007). Artemisinin induces calcium-dependent protein secretion in the protozoan parasite Toxoplasma gondii. *Eukaryot Cell, 6*(11), 2147-2156. doi:10.1128/EC.00262-07

Nagamune, K., Hicks, L. M., Fux, B., Brossier, F., Chini, E. N., & Sibley, L. D. (2008). Abscisic acid controls calcium-dependent egress and development in Toxoplasma gondii. *Nature, 451*(7175), 207-210. doi:10.1038/nature06478

Nagamune, K., & Sibley, L. D. (2006). Comparative genomic and phylogenetic analyses of calcium ATPases and calcium-regulated proteins in the apicomplexa. *Mol Biol Evol, 23*(8), 1613-1627. doi:10.1093/molbev/msl026

Olinares, P. D., Kim, J., Davis, J. I., & van Wijk, K. J. (2011). Subunit stoichiometry, evolution, and functional implications of an asymmetric plant plastid ClpP/R protease complex in Arabidopsis. *Plant Cell, 23*(6), 2348-2361. doi:10.1105/tpc.111.086454

Omasits, U., Ahrens, C. H., Muller, S., & Wollscheid, B. (2014). Protter: interactive protein feature visualization and integration with experimental proteomic data. *Bioinformatics, 30*(6), 884-886. doi:10.1093/bioinformatics/btt607

Pace, D. A., McKnight, C. A., Liu, J., Jimenez , V., & Moreno, S. N. J. (2014). Calcium Entry in Toxoplasma gondii and its Enhancing Effect of Invasion-linked Traits. *Journal of Biological Chemistry, 289*(49), viii-ix. doi:10.1016/s0021-9258(20)47385-5

Palmgren, K. B. A. a. M. G. (1998). Evolution of Substrate Specificities in the P-Type ATPase Superfamily. *Journal of Molecular Evolution, 46*, 86-101.

Paolo Pinton, T. P. a. R. R. (1998). The Golgi apparatus is an inositol 1,4,5-trisphosphate-sensitive Ca2+? store, with functional properties distinct from those of the endoplasmic reticulum. *The EMBO Jounrnal, 17*, 5298-5308.

Patel, S., & Docampo, R. (2010). Acidic calcium stores open for business: expanding the potential for intracellular Ca2+ signaling. *Trends Cell Biol, 20*(5), 277-286. doi:10.1016/j.tcb.2010.02.003

Peltier, J. B., Ripoll, D. R., Friso, G., Rudella, A., Cai, Y., Ytterberg, J., . . . van Wijk, K. J. (2004). Clp protease complexes from photosynthetic and non-photosynthetic plastids and mitochondria of plants, their predicted three-dimensional structures, and functional implications. *J Biol Chem, 279*(6), 4768-4781. doi:10.1074/jbc.M309212200

Persson, E. K., Agnarson, A. M., Lambert, H., Hitziger, N., Yagita, H., Chambers, B. J., . . . Grandien, A. (2007). Death receptor ligation or exposure to perforin trigger rapid egress of the intracellular parasite Toxoplasma gondii. *J Immunol, 179*(12), 8357-8365. doi:10.4049/jimmunol.179.12.8357

Peter Brodin, R. F., Thomas Vorherr and Ernesto Carafoli. (1992). Identification of two domains which mediate the binding of activating phospholipids to the plasma-membrane Ca2+pump. *Euro. J. Biochem, 204* 939-946.

Pfefferkorn, E. R. P. a. L. C. (1979). Quantitative studies of the mutagenesis of Toxoplasma gondii. *J. Parasitol., 65*, 364-370.

Phillip E. Scherer, G. Z. L., Suzanne Williams, Michael Fogliano, Giulia Baldini and Harvey F. Lodish. (1996). Cab45, a novel Ca2+-binding protein localized to the golgi lumen. *The Journal of Cell Biology, 133*, 257-268.

Ping Lin, H. L.-N., Robert Hofmeister, J. Michael McCaffery, Mingjie Jin, Hanjo Hennemann, Tammie McQuistan, Luc De Vries, and Marilyn Gist Farquhar. (1998). The Mammalian Calcium-binding Protein, Nucleobindin (CALNUC), Is a Golgi Resident Protein. *The Journal of Cell Biology, 141*, 1515-1527.

Prole, D. L., & Taylor, C. W. (2011). Identification of intracellular and plasma membrane calcium channel homologues in pathogenic parasites. *PLoS One, 6*(10), e26218. doi:10.1371/journal.pone.0026218

Que, X., Engel, J. C., Ferguson, D., Wunderlich, A., Tomavo, S., & Reed, S. L. (2007). Cathepsin Cs are key for the intracellular survival of the protozoan parasite, Toxoplasma gondii. *J Biol Chem, 282*(7), 4994-5003. doi:10.1074/jbc.M606764200

RA Bressan, P. H., JM Pardo. (1998). Plants use calcium to resolve salt stress. *Trends in plant science*.

Ramakrishnan, S., Unger, L. M., Baptista, R. P., Cruz-Bustos, T., & Docampo, R. (2021). Deletion of a Golgi protein in Trypanosoma cruzi reveals a critical role for Mn2+ in protein glycosylation needed for host cell invasion and intracellular replication. *PLoS Pathog, 17*(3), e1009399. doi:10.1371/journal.ppat.1009399

Rathore, S., Sinha, D., Asad, M., Bottcher, T., Afrin, F., Chauhan, V. S., . . . Mohmmed, A. (2010). A cyanobacterial serine protease of Plasmodium falciparum is targeted to the apicoplast and plays an important role in its growth and development. *Mol Microbiol, 77*(4), 873-890. doi:10.1111/j.1365-2958.2010.07251.x

Rodrigues, C. O., Ruiz, F. A., Rohloff, P., Scott, D. A., & Moreno, S. N. (2002). Characterization of isolated acidocalcisomes from Toxoplasma gondii tachyzoites reveals a novel pool of hydrolyzable polyphosphate. *J Biol Chem, 277*(50), 48650-48656. doi:10.1074/jbc.M208990200

Rohloff, P., Miranda, K., Rodrigues, J. C., Fang, J., Galizzi, M., Plattner, H., . . . Moreno, S. N. (2011). Calcium uptake and proton transport by acidocalcisomes of Toxoplasma gondii. *PLoS One, 6*(4), e18390. doi:10.1371/journal.pone.0018390

Roiko, M. S., Svezhova, N., & Carruthers, V. B. (2014). Acidification Activates Toxoplasma gondii Motility and Egress by Enhancing Protein Secretion and Cytolytic Activity. *PLoS Pathog, 10*(11), e1004488. doi:10.1371/journal.ppat.1004488

Roos, R. G. K. D. a. D. S. (1995). Insertional mutagenesis and marker rescue in a protozoan parasite: Cloning of the uracil phosphoribosyltransferase locus from Toxoplasma gondii. *Proc. Natl. Acad. Sci. USA, 92*, 5749-5753.

Rotmann, A., Sanchez, C., Guiguemde, A., Rohrbach, P., Dave, A., Bakouh, N., . . . Lanzer, M. (2010). PfCHA is a mitochondrial divalent cation/H+ antiporter in Plasmodium falciparum. *Mol Microbiol, 76*(6), 1591-1606. doi:10.1111/j.1365-2958.2010.07187.x

Rudella, A., Friso, G., Alonso, J. M., Ecker, J. R., & van Wijk, K. J. (2006). Downregulation of ClpR2 leads to reduced accumulation of the ClpPRS protease complex and defects in chloroplast biogenesis in Arabidopsis. *Plant Cell, 18*(7), 1704-1721. doi:10.1105/tpc.106.042861

S. Brogger Christensen, I. K. L., and Ulla Rasmussen. (1982). Thapsigargin and Thapsigargicin, Two Histamine Liberating Sesquiterpene Lactones from Thapsia garganiea. X-ray Analysis of the 7,11 Epoxide of Thapsigargin. *American Chemical Society, 47*, 649-652.

Schneider, C. A., Rasband, W. S., & Eliceiri, K. W. (2012). NIH Image to ImageJ: 25 years of image analysis. *Nat Methods, 9*(7), 671-675. doi:10.1038/nmeth.2089

Sheiner, L., Demerly, J. L., Poulsen, N., Beatty, W. L., Lucas, O., Behnke, M. S., . . . Striepen, B. (2011). A systematic screen to discover and analyze apicoplast proteins identifies a conserved and essential protein import factor. *PLoS Pathog, 7*(12), e1002392. doi:10.1371/journal.ppat.1002392

Shen, B., Brown, K. M., Lee, T. D., & Sibley, L. D. (2014). Efficient gene disruption in diverse strains of Toxoplasma gondii using CRISPR/CAS9. *mBio, 5*(3), e01114-01114. doi:10.1128/mBio.01114-14

Shigaki, T., Rees, I., Nakhleh, L., & Hirschi, K. D. (2006). Identification of three distinct phylogenetic groups of CAX cation/proton antiporters. *J Mol Evol, 63*(6), 815-825. doi:10.1007/s00239-006-0048-4

Shuhong Luo, M. V., Jessica Graves, Li Zhong and Silvia N.J.Moreno. (2001). A plasma membrane-type Ca2+-ATPase co-localizes with a vacuolar H+-pyrophosphatase to acidocalcisomes of Toxoplasma gondii. *The EMBO Jounrnal, 20*, 55-64.

Sibley, V. B. C. a. L. D. (1999). Mobilization of intracellular calcium stimulates microneme discharge in Toxoplasma gondii. *Molecular Microbiology, 31*, 421-428.

Sidik, S. M., Hackett, C. G., Tran, F., Westwood, N. J., & Lourido, S. (2014). Efficient genome engineering of Toxoplasma gondii using CRISPR/Cas9. *PLoS One, 9*(6), e100450. doi:10.1371/journal.pone.0100450

Sidik, S. M., Hortua Triana, M. A., Paul, A. S., El Bakkouri, M., Hackett, C. G., Tran, F., . . . Lourido, S. (2016). Using a Genetically Encoded Sensor to Identify Inhibitors

of Toxoplasma gondii Ca2+ Signaling. *J Biol Chem, 291*(18), 9566-9580. doi:10.1074/jbc.M115.703546
Sidik, S. M., Huet, D., Ganesan, S. M., Huynh, M. H., Wang, T., Nasamu, A. S., . . . Lourido, S. (2016). A Genome-wide CRISPR Screen in Toxoplasma Identifies Essential Apicomplexan Genes. *Cell, 166*(6), 1423-1435 e1412. doi:10.1016/j.cell.2016.08.019
Sievers, F., Wilm, A., Dineen, D., Gibson, T. J., Karplus, K., Li, W., . . . Higgins, D. G. (2011). Fast, scalable generation of high-quality protein multiple sequence alignments using Clustal Omega. *Mol Syst Biol, 7*, 539. doi:10.1038/msb.2011.75
Skou, J. c. (1957). The influence of some cations on an adenosine triphosphate from peripheral nerves. *Biochimica et biophysica, 23*.
Sloves, P. J., Delhaye, S., Mouveaux, T., Werkmeister, E., Slomianny, C., Hovasse, A., . . . Tomavo, S. (2012). Toxoplasma sortilin-like receptor regulates protein transport and is essential for apical secretory organelle biogenesis and host infection. *Cell Host Microbe, 11*(5), 515-527. doi:10.1016/j.chom.2012.03.006
Stasic, A. J., Chasen, N. M., Dykes, E. J., Vella, S. A., Asady, B., Starai, V. J., & Moreno, S. N. J. (2019). The Toxoplasma Vacuolar H(+)-ATPase Regulates Intracellular pH and Impacts the Maturation of Essential Secretory Proteins. *Cell Rep, 27*(7), 2132-2146 e2137. doi:10.1016/j.celrep.2019.04.038
Stasic, A. J., Dykes, E. J., Cordeiro, C. D., Vella, S. A., Fazli, M. S., Quinn, S., . . . Moreno, S. N. J. (2021). Ca(2+) entry at the plasma membrane and uptake by acidic stores is regulated by the activity of the V-H(+) -ATPase in Toxoplasma gondii. *Mol Microbiol*. doi:10.1111/mmi.14722
Stribny, J., Thines, L., Deschamps, A., Goffin, P., & Morsomme, P. (2020). The human Golgi protein TMEM165 transports calcium and manganese in yeast and bacterial cells. *J Biol Chem, 295*(12), 3865-3874. doi:10.1074/jbc.RA119.012249
Striepen, B. (2011). The apicoplast: a red alga in human parasites. *Essays Biochem, 51*, 111-125. doi:10.1042/bse0510111
Sullivan, W. J., Jr., & Jeffers, V. (2012). Mechanisms of Toxoplasma gondii persistence and latency. *FEMS Microbiol Rev, 36*(3), 717-733. doi:10.1111/j.1574-6976.2011.00305.x
Tadini-Buoninsegni, F., Bartolommei, G., Moncelli, M. R., Guidelli, R., & Inesi, G. (2006). Pre-steady state electrogenic events of Ca2+/H+ exchange and transport by the Ca2+-ATPase. *J Biol Chem, 281*(49), 37720-37727. doi:10.1074/jbc.M606040200
Takahara, A. (2009). Cilnidipine: a new generation Ca channel blocker with inhibitory action on sympathetic neurotransmitter release. *Cardiovasc Ther, 27*(2), 124-139. doi:10.1111/j.1755-5922.2009.00079.x
Tamura, K., Stecher, G., & Kumar, S. (2021). MEGA11: Molecular Evolutionary Genetics Analysis Version 11. *Mol Biol Evol, 38*(7), 3022-3027. doi:10.1093/molbev/msab120
Thines, L., Deschamps, A., Sengottaiyan, P., Savel, O., Stribny, J., & Morsomme, P. (2018). The yeast protein Gdt1p transports Mn(2+) ions and thereby regulates manganese homeostasis in the Golgi. *J Biol Chem, 293*(21), 8048-8055. doi:10.1074/jbc.RA118.002324

Ton, V. K., Mandal, D., Vahadji, C., & Rao, R. (2002). Functional expression in yeast of the human secretory pathway Ca(2+), Mn(2+)-ATPase defective in Hailey-Hailey disease. *J Biol Chem, 277*(8), 6422-6427. doi:10.1074/jbc.M110612200

Trond Olav BERG, P. E. S., Torunn LOVDAL, Per Ottar SEGLEN and Trond BERG. (1994). Use of glycyl-L-phenylalanine 2-naphthylamide, a lysosome-disrupting cathepsin C substrate, to distinguish between lysosomes and prelysosomal endocytic vacuoles. *Biochem J., 300*, 229-236.

Tu, V., Yakubu, R., & Weiss, L. M. (2018). Observations on bradyzoite biology. *Microbes Infect, 20*(9-10), 466-476. doi:10.1016/j.micinf.2017.12.003

Uboldi, A. D., Wilde, M. L., McRae, E. A., Stewart, R. J., Dagley, L. F., Yang, L., . . . Tonkin, C. J. (2018). Protein kinase A negatively regulates Ca2+ signalling in Toxoplasma gondii. *PLoS Biol, 16*(9), e2005642. doi:10.1371/journal.pbio.2005642

van Dooren, G. G., Tomova, C., Agrawal, S., Humbel, B. M., & Striepen, B. (2008). Toxoplasma gondii Tic20 is essential for apicoplast protein import. *Proc Natl Acad Sci U S A, 105*(36), 13574-13579. doi:10.1073/pnas.0803862105

Vanoevelen, J., Raeymaekers, L., Parys, J. B., De Smedt, H., Van Baelen, K., Callewaert, G., . . . Missiaen, L. (2004). Inositol trisphosphate producing agonists do not mobilize the thapsigargin-insensitive part of the endoplasmic-reticulum and Golgi Ca2+ store. *Cell Calcium, 35*(2), 115-121. doi:10.1016/j.ceca.2003.08.003

Vella, S. A., Calixto, A., Asady, B., Li, Z. H., & Moreno, S. N. J. (2020). Genetic Indicators for Calcium Signaling Studies in Toxoplasma gondii. *Methods Mol Biol, 2071*, 187-207. doi:10.1007/978-1-4939-9857-9_11

Vella, S. A., Moore, C. A., Li, Z. H., Hortua Triana, M. A., Potapenko, E., & Moreno, S. N. J. (2021). The role of potassium and host calcium signaling in Toxoplasma gondii egress. *Cell Calcium, 94*, 102337. doi:10.1016/j.ceca.2020.102337

Wang, C., Xu, W., Jin, H., Zhang, T., Lai, J., Zhou, X., . . . Yang, C. (2016). A Putative Chloroplast-Localized Ca(2+)/H(+) Antiporter CCHA1 Is Involved in Calcium and pH Homeostasis and Required for PSII Function in Arabidopsis. *Mol Plant, 9*(8), 1183-1196. doi:10.1016/j.molp.2016.05.015

Wei, H. X., Wei, S. S., Lindsay, D. S., & Peng, H. J. (2015). A Systematic Review and Meta-Analysis of the Efficacy of Anti-Toxoplasma gondii Medicines in Humans. *PLoS One, 10*(9), e0138204. doi:10.1371/journal.pone.0138204

Williams, M. J., Alonso, H., Enciso, M., Egarter, S., Sheiner, L., Meissner, M., . . . Tonkin, C. J. (2015). Two Essential Light Chains Regulate the MyoA Lever Arm To Promote Toxoplasma Gliding Motility. *mBio, 6*(5), e00845-00815. doi:10.1128/mBio.00845-15

Wu, N., Nishioka, W. K., Derecki, N. C., & Maher, M. P. (2019). High-throughput-compatible assays using a genetically-encoded calcium indicator. *Sci Rep, 9*(1), 12692. doi:10.1038/s41598-019-49070-8

Yu, A. Y., & Houry, W. A. (2007). ClpP: a distinctive family of cylindrical energy-dependent serine proteases. *FEBS Lett, 581*(19), 3749-3757. doi:10.1016/j.febslet.2007.04.076

Yu, X., Hao, L., & Inesi, G. (1994). A pK change of acidic residues contributes to cation countertransport in the Ca-ATPase of sarcoplasmic reticulum. Role of H+ in

Ca(2+)-ATPase countertransport. *Journal of Biological Chemistry, 269*(24), 16656-16661. doi:10.1016/s0021-9258(19)89440-1

Yuan, Y., Kilpatrick, B. S., Gerndt, S., Bracher, F., Grimm, C., Schapira, A. H., & Patel, S. (2021). The lysosomotrope GPN mobilises Ca(2+) from acidic organelles. *J Cell Sci, 134*(6). doi:10.1242/jcs.256578

Zalk, R., Lehnart, S. E., & Marks, A. R. (2007). Modulation of the ryanodine receptor and intracellular calcium. *Annu Rev Biochem, 76*, 367-385. doi:10.1146/annurev.biochem.76.053105.094237

Zhang, S. L., Yu, Y., Roos, J., Kozak, J. A., Deerinck, T. J., Ellisman, M. H., . . . Cahalan, M. D. (2005). STIM1 is a Ca2+ sensor that activates CRAC channels and migrates from the Ca2+ store to the plasma membrane. *Nature, 437*(7060), 902-905. doi:10.1038/nature04147

Zhang, Y. L., Moran, S. P., Allen, A., Baez-Nieto, D., Xu, Q., Wang, L. A., . . . Pan, J. Q. (2022). Novel Fluorescence-Based High-Throughput FLIPR Assay Utilizing Membrane-Tethered Genetic Calcium Sensors to Identify T-Type Calcium Channel Modulators. *ACS Pharmacol Transl Sci, 5*(3), 156-168. doi:10.1021/acsptsci.1c00233

Zheng, B., Halperin, T., Hruskova-Heidingsfeldova, O., Adam, Z., & Clarke, A. K. (2002). Characterization of chloroplast Clp proteins in Arabidopsis: Localization, tissue specificity and stress responses. *Physiologia Plantarum, 114*(1), 92-101.

Zhong, S. N. J. M. a. L. (1996). Acidsocalcisomes in Toxoplasma gondii tachyzoites. *Biochem J, 313*, 655-659.